University of Alberta

Characterization of Recombinant HSV-GFP Reporter Viruses

by

Xiaoqing Hou

A thesis submitted to the Faculty of Graduate Studies and Research
in partial fulfillment of the requirements for the degree of

Master of Science
in
Virology

Medical Microbiology and Immunology

Spring 2011
Edmonton, Alberta

Examing committee:

Dr. James R. Smiley, Medical Microbiology and Immunology

Dr. Edan Foley, Medical Microbiology and Immunology

Dr. Tom Hobman, Cell Biology

Dr. David Evans, Medical Microbiology and Immunology

Abstract

VP16 initiates the HSV replication cycle by activating immediate early (IE) gene expression. It recruits the RNA pol II through an acidic C-terminal domain. The defective VP16 encoded by the V422 mutant of HSV-1 possesses a truncated C-terminal domain. Therefore, V422 replication is suppressed in most cell-lines, except U2OS osteosarcoma cells. The permissive phenotype of U2OS cells stems from a failure to express one or more inhibitory factors that are produced in restrictive cells. The initial project was designed to identify these host inhibitory factors in restrictive cells of V422, using siRNA silencing technology. To facilitate the siRNA screen, a GFP reporter gene has been inserted into the thymindine kinase (TK) gene of the V422 genome and the wild-type KOS genome. This thesis provides information about characterizing the kinetics of GFP expression from recombinant viruses at both protein and mRNA levels, during different infection times in HeLa and Vero cells.

Table of Contents

List of Tables

List of Figures

List of Abbreviations

Aly/REF	RNA export factor
BAC	Bacterial artificial chromosome
CENP	Centromeric protein
ChIP	Chromatin Immunoprecipitaton
CTD	Carboxy-terminal domain
DMEM	Dulbecco's Modified Eagle Medium
DMSO	Dimethylsulphoxide
DNA	Deoxyribonucleic Acid
DOG	2-Deoxy-galactose
E	Early
EDTA	Ethylenediaminetetraacetic acid
EJC	Exon junction complex
FBS	Fetal bovine serum
GFP	Green fluorescent protein
HCMV	Human cytomegalovirus
HCF	Host cell factor
HDAC	Histone deacetylase
HEL	Human embryonic lung
HEXIM	Hexamethylene *bis*-acetimide inducible
HHV	Human herpesvirus
HIV	Human immunodeficiency virus
HMBA	Hexamethylene *bis*-acetimide
hpi	Hours post-infection
HSV	Herpes Simplex Virus
ICP	Infected cell protein
IE	Immediate early
IF	Immunofluorescence
IFN	Interferon
INHAT	Inhibitor of histone acetyltransferase
ISRE	Interferon stimulated response element
JNK	Jun kinase
kDa	kiloDalton
KSHV	Kaposi's sarcoma-associated herpesvirus
L	Late
LAT	Latency-associated transcript
LB	Luria Broth
MOI	Multiplicity of infection
ND10	Nuclear domain 10
NLS	Nuclear localization signal
Oct-1	Octamer transcription factor-1
ORF	Open reading frame
Ori	Origin
PAA	Phosphonoacetic acid

PBS	Phosphate buffered saline
PCR	Polymerase chain reaction
PFU	Plaque forming units
PI3K	Phosphoinositol-3 kinase
PKR	Protein kinase R
PML	Promyelocytic leukemia protein
REST	RE1 silencing transcription factor
RNA	Ribonucleic acid
RNA pol II	RNA polymerase II
RT PCR	Real-time PCR
SDS	Sodium dodecyl sulphate
SUMO	Small ubiquitin-like modifier
TAF	Template activating factor
TAP	Transporter associated with antigen processing
TBP	TATA-binding protein
TE	Tris-EDTA
TF	Transcription factor
TK	Thymidine kinase
UL	Unique long
US	Unique short
vhs	Virion host shutoff
VP	Virion protein

Chapter 1: Introduction

1.1 Overview of Herpesviridae:

The family *Herpesviridae* is a group of enveloped viruses with large DNA genomes that are highly dispersed in most animal species. A classic herpesvirion possesses a linear double-stranded DNA genome embedded in an icosadeltahedral capsid consisting of 162 capsomeres. The capsid is surrounded by an amorphous and protein filled space designated as the tegument, which is covered by a lipid bilayer envelope with viral glycoprotein spikes on its surface [1]. The herpesviruses share the following three distinct biological properties. Firstly, their genomes encode a large group of enzymes which participate in nucleic acid metabolism (such as thymidine kinase), DNA synthesis (e.g., DNA polymerase and helicase) and protein modification (e.g. protein kinase). Secondly, viral DNA replication and capsid assembly take place in the nucleus, whereas the tegument association and envelope acquisition occur in the cytoplasm, as viruses exit the host cell. Finally, infectious viruses can either go through a lytic lifecycle accompanied by destruction of the host cell or establish a latent state in the host cell. The latent genome can be reactivated by various stimuli, entering the lytic life cycle and causing disease upon reactivation [1].

To date, there have been approximate 200 herpesviruses identified in nature, and most of them are clustered into three subfamilies: Alphaherpesvirinae, Betaherpesvirinae and Gammaherpesvirinae [1]. The classification of each subfamily is based on host-cell range, length of replication cycle, and cell type

where latency is established. The herpes simplex virus type 1 and type 2 (HSV-1 and -2) and varicella zoster virus (VZV) are the classic examples of Alphaherpesvirinae. This subfamily is characterized by a broad host range, relatively short lytic lifecycle, rapid spread in culture, and efficient destruction of infected cells. Also, Alphaherpevirinae are able to establish the latency in sensory ganglia. The Betaherpevirinae have a narrow host range and long replication cycle in infected cells. They are able to establish latency in secretory glands, lymphoreticular cells, kidneys and other tissues. The Betaherpevirinae includes Human Cytomegalovirus (HCMV), Human Herpesvirus-6 (HHV-6) and HHV-7. Lastly, the gammaherpevirinae generally replicate in lymphoblastoid cells, especially in T or B lymphocytes, and also establish latency in lymphoid tissues. The best known members of this subfamily are Epstein-Barr virus (EBV) and Kaposi's Sacoma-associated Herpesvirus (KSHV) [1].

1.2 The Herpes Simplex Virus type-1 (HSV-1) structure:

The HSV-1 virion is composed of four elements: a linear double-stranded DNA encompassed in an electron-opaque core, an icosahedral capsid, a large proteinacous space referred as the tegument, and an envelope with glycoprotein spikes at the outermost layer of the virion [1].

1.2.1 HSV-1 DNA genome:

The DNA genome of HSV-1 in a mature virion is linear and double stranded. (H3) The genome consists of approximately 150 kilo base pair (kbp) (of which 68% are G/C), and it carries at least 84 protein-encoding open reading frames (ORF) [2].

The entire linear genome of HSV-1 is composed of two covalently linked components; the L (long) and S (short) units. It has been shown that the L and S units invert relative to each other, and the DNA genome produces four linear isomers of equal proportion in infected cells [3].

1.2.2 HSV-1 nucleocapsid:

The viral DNA genome is enclosed by an icosahedral protein shell, referred to as the nucleocapsid. The nucleocapsid of a complete virion is composed of an outer layer with T=16 icosahedral symmetry and an intermediate layer arranged in a T=4 symmetry [4]. The total molecular mass of the capsid shell is 0.2 billion daltons, and the outer layer of the nucleocapsid is composed of 4 viral proteins: VP5, VP26, VP23 and VP19C [5].

The nucleocapsid is not located in the center of the tegument. The proximal pole of the capsid is closer to the envelope than the distal pole, which is 30 to 35 nm away from the envelope [1]. Within the envelope, the nucleocapsid takes up about one third of the volume, while the tegument occupies the remaining rest two thirds of the volume [1].

1.2.3 HSV-1 tegument:

Inside of the HSV-1 virion, the space between the nucleocapsid and the envelope is called the tegument. It is an apparently amorphous matrix filled with viral proteins [6]. The tegument consists of at least 20 viral proteins [6]. Some of these proteins, such as VP16, are responsible for triggering the viral immediate early (IE) gene expression [7]. Others contribute to creating a more suitable

environment for viral replication in infected cells; examples include the virion-associated host shutoff protein (vhs) which degrades cellular mRNA to enhance the efficiency of viral protein translation [8], and the protein encoded by U_S11, an RNA binding protein which inhibits the activation of protein kinase R (PKR) induced cellular translation arrest in host cells [9, 10].

Cellular and selected viral RNAs are also detected in the tegument of highly purified HSV-1 virions. Detected by a human gene array, those cellular RNAs in the tegument are identified to be the most abundant species of cellular RNAs in the cytoplasm [9]. It has also been shown that there are nine viral gene transcripts present in the tegument; however, they are not sequence specific but simply the most abundant species of viral RNAs in infected cells [9, 10]. Moreover, these viral transcripts are not degradation products from infected cells; for example, packaged U_S 8.5 mRNAs are able to be translated into protein in newly infected cells [10]. Three viral tegument proteins are reported to be responsible for packaging these viral RNAs into the tegument. These are the protein products encoded by U_S11, U_L47, and U_L49 (VP22) [10]. The U_L47 gene product has been demonstrated to enhance the transactivating function of VP16 during the IE phase of viral infection [11]. VP22 has been shown to have the capability of intercellular transport [12], and the ability of VP22 to transport mRNA from cell to cell has been suggested to be important in creating a suitable environment for efficient viral production in infects cells [10].

1.2.4 HSV-1 envelope:

HSV-1 virions are visualized as pleiomorphic membrane-bound particles, and their envelopes are obtained from the cytoplasmic membranes of infected cells [13, 14]. Recent cryo-electron tomography studies have demonstrated that the average diameter of a spherical HSV-1 virion is 186 nm, which enlarges to 225 nm once spikes on the envelope surface are included. The lipid layer of the envelope is seen as a continuous silkily circular surface, around 5 nm thick [13].

There are at least 9 different viral glycoproteins embedded in the lipid membrane of the HSV-1 virion: gB, gC, gD, gE, gG, gH, gI, gL and gM. Also, the envelope contains at least 2 non-glycosylated intrinsic membrane proteins [1]. There are approximately 595-758 glycoprotein spikes on the surface of the membrane, and they vary in length, spacing and in the angles at which they stick out from the membrane [13]. The spikes are non-randomly distributed on the surface of the membrane; they are presented thinly at the proximal pole and compactly around the distal pole. The distribution of the spikes may be related to the receptor-recognizing function during cell entry [13, 15].

1.3 HSV-1 infections:

As with other members of the Herpesviridae, HSV-1 can establish either lytic or lantent infection within host cells. During lytic infection of HSV-1, the viral proteins and DNA genomes are expressed and replicate in a temporal order, as discussed in later sections. In contrast, only the latency-associated transcript (LAT) is actively produced in the latent infection of HSV-1 in sensory neuron cells [16]. The latent virus can be re-activated and then enter the lytic infection around the primary infection site in response to any of a number of stressors [17].

My project focuses on viral IE gene expression during HSV-1 lytic infection, so I will focus on the background of lytic cycle of HSV-1.

1.4 HSV-1 lytic infection:

1.4.1 Viral entry:

It is generally proposed that HSV enters host cells through direct fusion of the virion envelope with the outer plasma membrane [18]. Viral entry into cells requires at least four viral glycoproteins: gD, gB and the heterodimer gH/gL. Initially, gC and gB interact independently with heparan sulfate (HS) proteoglycans to promote the attachment of the virion to the host cell. In vitro, the interactions of gC/gB with HS are not essential for viral entry. A gC-deletion virus is still infectious, and a gB mutant virus (that is only defective in its interaction with HS) can still be infectious with reduced binding activity [19, 20].

Upon attachment to the cell surface, gD interacts with one of several cell surface receptors: herpes virus entry mediator (HVEM), nectin-1 or 3-O-sulfated heparan sulphate [21]. Then, gD may send a signal to gB and/or gH/gL which mediates cell fusion with the plasma membrane. This signalling was found to be triggered by a proline-rich region in the C-terminus of gD protein [22, 23].

The last stage of viral entry is fusion of the viral envelope of HSV-1 with the cell membrane. This process is the most complex and least understood stage in HSV-1 entry into host cells. It is proposed that the central fusion machinery involves gB and the heterodimer gH/gL. Mutant virus lacking gB, gH and gL cannot enter target cells [22-26]. The function of gH to assemble viral fusion

proteins requires the interaction with gL, which acts as a gH chaperone for proper processing and for leading gH to the viral envelope. gL is a short glycoprotein lacking a transmembrane domain [27-29]. In the absence of gH expression, gL does not stay at the viral envelope and is secreted from the infected cells [28]. It has been shown that virions lacking gL also lack gH, and while they are able to attach to the cell surface, they do not penetrate the cell membrane [29, 30]. After the virion successfully fuses to a cell, the nucleocapsid is released into the cytoplasm along with the surrounding tegument proteins.

1.4.2 HSV DNA genome enters the nucleus:

The nucleocapsid then migrates to the nucleus and injects the viral DNA genome into the nucleus through the nuclear pore [31, 32]. It has been shown that the migration of the nucleocapsid to the nuclear pore depends on the cellular microtubular network and the microtubule minus-end directed motors dynein and dynactin [33, 34]. In vitro experiments show that at the nuclear pore, DNA release from the capsid requires the assistance of cellular protein importin-β along with the Ran GTPase cycle [35]. In addition, inhibition of importin-β with antibody blocks viral DNA release *in vitro* [35]. In the nucleus, the released DNA genome then is prepared for IE gene expression, triggered by the tegument protein VP16.

The tegument proteins are also released into the cytoplasm along with the penetration of the nucleocapsid, in order to modify the cellular environment for viral replication. VP1-2 localizes to the nuclear pore along with the capsid, mediates DNA release into nucleus [31, 36]. One of the most studied tegument proteins, VP16, also migrates into the nucleus through interaction with a cellular

protein HCF-1. VP16 is essential for viral replication, and as described below it initiates the IE gene expression and turns on viral propagation in host cells [37]. Not all the tegument proteins target the nucleus. Vhs, encoded by UL41, localizes in the cytoplasm and functions to arrest the expression of cellular genes through degradation of the cellular mRNAs [38].

1.4.3 Chromatinization of viral input genomes:

Before the viral DNA genome is released into the nucleus, it is not associated with any cellular histone proteins inside the capsid [39-41]. Once the viral genome enters the nucleus as a linear DNA, it rapidly transforms to a circular form and is deposited with cellular nucleosomes [42, 43]. The order of these two events, assembly of chromatin or circularization, has not yet been determined. It has been reported that during lytic infection, mononucleosomes were detected from the HSV-1 genome using MNase assays [44-46]. To determine the location of the associated nucleosomes on viral genome, studies utilizing chromatin immunoprecipitation (CHIP) assay show that several genes in each gene class (IE, E and L) are associated with nucleosomes during lytic infection [40, 47, 48]. The location of nucleosomes on the HSV-1 genome and the temporal changes after chromatinization of viral genome are still under investigation. It has been reported that during lytic infection, the chromatinization of HSV-1 genome occurred within 3-6 hpi [49].

The structure of the newly assembled HSV-1 chromatin is different from the cellular chromatin structure in the host cell [47]. Associated histone protein content relative to DNA is much lower on the HSV-1 genome compared to the

cellular genome, and nucleosomes associate disorderly with viral DNA, not in a regularly repeating pattern [47, 48, 50]. The nucleosomes associated with viral DNA have also been analyzed for histone modifications. Post-translational modifications of histone proteins, such as methylation and acetylation, play critical roles in determining the activation or repression of gene transcription. For instance, active transcription sites on the cellular genome are marked by acetylation of the lysine residues within the N-terminal tail of histone 3 (H3) proteins [51]. Methylation of histones on different residues can produce the opposite effect, either activation or repression of gene transcription. For example, methylation of H3K4 has been shown to promote transcription, whereas H3K9 methylation has been detected in heterochromatin of cellular genome, which are the sites of silenced transcription (reviewed in [51]).

Histone modification is also important for regulating the viral gene expression during HSV-1 infection. Studies have shown that during lytic infection, the nucleosomes bound to the HSV-1 viral genome contained "active" euchromatin markers, such as H3K9/K14 acetylation (ac) and H3K4 methylation [49, 50]. In contrast, the histones bound to the silent region of latent or quiescent genome show modifications typical of heterochromatin. Moreover, the latency-associated transcript (LAT) gene (which is expressed during latency) shows the H3K9/K14ac markers on associated H3 histones during latency, but upon reactivation from latency, these markers are depleted from the LAT region. Another experiment using a general inhibitor of protein methylation, MTA, resulted in a great reduction in viral nucleosome methylation and the replication

of HSV-1 [52]. Together, these observations demonstrate that modification of chromatin might be an important mechanism for viral gene expression, during HSV-1 infection.

The post-translational modification on viral associated histones is mediated through both viral and cellular factors. It has reported that depletion of A-type lamin in the host nucleus results in increased heterochromatin formation on viral promoters during the lytic infection of HSV-1 [53]. Studies using CHIP assay have indicated that during HSV-1 lytic infection, several IE promoters are associated with H3 and the chromatin modifiying coactivator proteins CBP, p300, BRG-1 and BRM [47]. CBP and p300 could promote the active chromatin and activate transcription through their histone acetyl transferase (HAT) activities. BRM and BRG-1 also play important roles in promoting the remodelling of chromatin and in turn, activating gene transcription. However, previous studies from Triezenberg group showed that disruption of these coactivators mentioned above did not affect the IE gene expression of HSV-1 *in vitro* [54].

Viral proteins of HSV-1, such as VP22, VP16 and ICP0, also play critical roles in promoting the active form of chromatin on the viral genome. The tegument protein VP22 has been shown to prevent histone binding to the viral genome through inhibiting the template-activating factor 1(TAF-1) [55]. VP22 interacts with TAF-1, evidenced by an affinity chromatography experiment [55]. TAF-1 is involved in facilitating the assembly of histones on naked DNA. It is found in the multi-subunit complex INHAT that associates with histones and blocks their acetylation [56].

Another tegument protein, VP16, has been reported to play critical roles in targeting the viral genome to the nuclear lamina (unpublished results from L. Silva), and mediating histone post-translational modifications. It has been shown that VP16 interacts and recruits some transcription factors and chromatin modifiers, including p300, CBP, BRG-1 and BRM to the IE gene promoters [47]. Moreover, VP16 functions to reduce the amount of the histone protein H3 on IE promoters early in infection, but it shows fewer effects on E and L promoters [47]. In contrast, previous study from Smiley group showed that VP16 had a global effect of chromatin modification on the viral genome, which is not only restricted to the IE promoters [57].

ICP0, the first expressed IE protein in HSV-1 lytic infection, also plays significant roles in promoting the active form of chromatin on the viral genome. ICP0 has been shown to reduce the amount of H3 on the viral genome 3-8 hpi [58]. Also, ICP0 has been proposed to function as a histone deacetylase inhibitor [59]. It has been reported that ICP0 interacts and interferes with class II histone deacetylase in transfected cells [60]. Furthermore, it has been shown that ICP0 interacts with the REST/CO-REST/HDAC1 complex, resulting in the displacement of HDAC1 from the complex, which would indirectly promote acetylation of the viral chromatin [48, 61, 62]. Abundant studies have been developed around the mechanism of ICP0 counteracting the cellular repression of viral gene expression from ND10 domains, which will be discussed in more details in later sections.

1.4.4 IE gene expression:

The remodelling of viral chromatin by host factors and viral proteins promotes the transcription of viral genes. The first class of genes expressed during HSV-1 lytic infection are the IE genes, named by the phase of viral replication. The tegument protein VP16 initiates the transcription of IE genes soon after the DNA genome entering the nucleus. As mentioned above, VP16 activates the IE gene transcription through at least two pathways – recruiting the RNA II polymerase to the IE promoters and promoting the active form of viral chromatin. Upon uncoating, VP16 and other tegument proteins are released into the cytoplasm. VP16 then interacts with HCF-1 and localizes to the nucleus along with HCF-1 [63]. Inside of the nucleus, VP16-HCF-1 associates with a cellular transcription factor, Oct-1, to form a protein complex. Oct-1 recognizes a specific sequence-5'GyATGnTAATGArATTCyTTGnGGG3'on IE promoters. Thus, through Oct-1, this protein complex localizes to the IE promoters and recruits the RNA polymerase II to start the transcription of IE genes [64, 65]. The four major IE proteins (ICP0, ICP4, ICP22 and ICP27) are described below.

1.4.4.1 ICP0

ICP0 is encoded by the gene α0, located in the inverted repeat sequences flanking the unique long sequence (UL) of the viral genome [1]. ICP0 is a 100 kDa protein, containing 775 amino acids [66]. The regions most important for ICP0 function are the C3HC4 RING finger domain near the N-terminus and a nuclear localization signal [66, 67]. At the C-terminus, ICP0 also contains sequences required for binding to the ubiquitin specific protease 7 (USP7), which

is important for localizing to the cellular ND10 domains [66, 67]. These structural domains accomplish the many functions of ICP0 in the viral replication cycle.

ICP0 is extensively processed after translation. It gets phosphorylated by the viral protein kinase UL13 and the cell-cycle kinase cdc2 [68-70]. ICP0 is also nucleotidylylated by casein kinase II [71]. Due to its nuclear localization signal (NLS) domain, ICP0 localizes to the nucleus early during viral replication. The newly expressed ICP0 accumulates initially at or near nuclear structure-ND10 domains, and causes degradation of ND10 components at early phase of infection [72]. As the amount of protein increases, ICP0 spreads out and fills the nucleus. After viral DNA synthesis, ICP0 is found in the cytoplasm [73, 74], and this translocation is assisted by interaction with the cell cycle regulator cyclin D3 [75]. Late after infection, ICP0 seems to shuttle between the nucleus and cytoplasm, and it may linger in the nucleus rather than reside in the cytoplasm. The proteasome inhibitor, MG132, blocks the exit of ICP0 from nucleus to cytoplasm [74, 76].

Although ICP0 is not essential for viral replication in host cells, the ICP0-deletion mutant virus results in a 10-100 fold decrease in viral titer compared to the wild type [1] at low multiplicity of infection in the same cell line. ICP0 is a multifunctional protein involved in inhibiting the host antiviral system, promoting the viral replication and reactivation of latency.

Due to its C3HC4 RING finger domain, ICP0 possesses ubiquitin E3 ligase activity [77, 78]. Causing the degradation of cellular proteins through the

ubiquitin-proteasome pathway may accomplish the viral defense function of ICP0. ICP0 has been shown to interact with proteasomes, and it enhances the interactions between cdc34 (an E2 ubiquitin-conjugating enzyme) and proteasomes [76, 79, 80]. The most extensively studied targets of ICP0-induced degradation are the ND10 components, including ProMyelocytic Leukaemia (PML) and Sp100. ND10, also referred to as PML nuclear bodies (NBs) has been linked to a large number of diverse cellular processes, including oncogenesis, the DNA damage response, the stress response, apoptosis, the ubiquitin pathway, and the interferon (IFN) response. In the absence of IFN stimulation, PML is expressed at low level in the nucleus. However, type I and II IFNs largely increase PML expression through an "IFN stimulated response element" (ISRE) and an "IFN-gamma activation site" (GAS) that are present in the promoter of its gene. Sp100 is also directly induced by IFNs, and its promoter also contains ISRE and GAS elements [81-83]. Besides the IFN antiviral pathway, PML and other NB components, including hDaxx, HIRA and the Bloom's Syndrome DNA helicase BLM, are also involved in the regulation of chromatin structure, transcription and DNA repair processes [84-87]. Previous studies have shown that PML-/- mouse fibroblasts exhibit defective sister chromatid exchange during mitosis [88]. Some studies also show that ND10 undergoes changes in response to agents that block transcription or lead to chromatin damage [89, 90]. Previous studies have shown that PML, Sp100, hDaxx and ATRX were involved in repression of HSV-1 gene expression, in the absence of a functional ICP0 [91-93]. The importance of ND10 domain in antiviral defense and chromatin metabolism

and remodeling gives ICP0 a good reason for targeting and causing their degradation. ICP0 specifically targets the SUMOylated isoforms of PML and Sp100, and USP7 contributes to this function of ICP0. USP7 can cleave the SUMO-1 subunits from PML and Sp100, then they could be ubiquinatedby ICP0 and targeted to the proteasome for degradation [79]. Moreover, USP enzymes also clear the ubiquitin subunits from the targeted protein, in order to protect it from proteasome-dependent degradation [94]. Thus, by binding to USP7, ICP0 could target proteins for degradation without itself becoming a target for cellular E3 ligase. ICP0 also has been reported to cause the degradation of other cellular proteins, such as centromeric proteins C and A (CENP-C & A), and the catalytic subunit of the DNA-dependent protein kinase (DNA-PK) [95, 96]. ICP0 also has been demonstrated to inhibit the interferon regulatory factor 3 (IRF3) phosphorylation, dimerization and localization to the nucleus, but it had no apparent inhibition on IRF3 when it was already localized to the nucleus [97].

Another important function of ICP0 contributing to the HSV-1 life cycle is promotion of viral gene expression and viral replication. ICP0 does not possess a DNA binding domain, so its activation of viral gene expression may be linked to cellular or viral transcription factors. ICP0 has been shown to be an inhibitor of the class II histone deacetylase (HDAC) , and this indirectly promotes the acetylation of viral chromatin [98]. Also, current studies showed that the circadian CLOCK histone acetyl transferase was recruited to ND10 domain through the interaction of ICP0 and Bmal1, which is a transcription factor that forms a heterodimer with CLOCK [99, 100]. ICP0 also interacts with the translation

elongation factor EF-1δ [73], which is found to be phosphorylated by the HSV protein kinase UL13 [101, 102]. Therefore, hyperphosporylation of EF-1δ may enhance the translation efficiency of viral mRNAs. It also has been shown that ICP0 interacts with and recruits cyclin D3 to ND10 structures to activate cdk4. Additionally, assisted by other viral proteins including ICP4 and ICP8, ICP0 recruits active cdk4 to ND10 structures and ultimately to replication compartments for enhanced expression of viral genes and viral DNA synthesis [103]. The function of ICP0 on the activation of viral gene expression may be related to the viral transcription factor ICP4. ICP0 has been shown to be over 20-fold more potent at driving mRNA synthesis when combined with ICP4, than either itself or ICP4 alone [104, 105]. Residues 617 to 775 of ICP0 interact with ICP4, including the domain involved in synergy with ICP4 (residues 680-767). However, some studies have also demonstrated that by interacting with ICP4, ICP0 antagonizes the repression function of ICP4 on its own transcription [106].

Transition from latency to the lytic life cycle of HSV-1 in neuronal cells is another well studied function of ICP0. Previous studies provide evidence that the quiescent genomes of HSV could be reactivated by later expression of ICP0 from another source [107]. Moreover, silent viral genomes could be produced from infection with ICP0-deficient viruses at low MOI, and they could be reactivated later by the presence of ICP0 [108-110]. However, the Preston group suggested that ICP0 was not essential to reactivate the silent viral genome, and reactivation in the absence of ICP0 was dependent on the MOI as well as the trans-acting factors [111].

1.4.4.2 ICP4

ICP4 of HSV-1 is a large protein with a molecular mass of 175 kDa [112]. ICP4 exists as a 350-kDa homodimer in the host nucleus [113, 114]. There are two copies of the α4 gene encoding ICP4; they are located in the inverted repeat region flanking the short segment (Us) of HSV-1 genome [1]. During IE infection, ICP4 is localized to the nucleus and is rapidly recruited to the viral genome [115]. Later during viral DNA replication, ICP4 is found in the replication compartments inside the nucleus.

ICP4 functions as a regulatory protein for activating E and L gene expression and repressing IE gene expression. The structure of ICP4 consists of a DNA binding domain, a nuclear localization domain and two transactivation regions [116]. Previous studies have shown that the N-terminal region of ICP4 is required for efficient cooperativity in TBP-TFIIB-DNA and ICP4 complex (transcription complex) formation and repression in vitro, while the C-terminal domain was dispensable for these two function [117, 118]. However, another study showed that the C-terminal 542 amino acids were essential for forming the transcription complex on a gC promoter at early times post-infection or when DNA synthesis was inhibited [119]. The C-terminal domain of ICP4 is required for DNA binding oligomerization [120]. In addition to the DNA binding domain of ICP4, the 274 amino acids at the N-terminus are essential for repression activity [117]. This region and one between amino acid 774 and 1298 are essential for the transcription activation function of ICP4 [121-124]. Mutant viruses lacking one of these two regions express reduced levels of E and L genes, and they

demonstrate impaired growth in vitro [122, 125]. The double deletion of these two regions severely impairs viral growth and E gene expression in culture [114, 118].

The function of ICP4 during viral gene expression is still not fully understood. Most current studies concentrate on two aspects of ICP4 biology: its DNA binding activity and its interaction with cellular transcription factors. ICP4 binds DNA non-specifically, but it also shows a preference for the DNA sequence-ATCGTCNNNNYCGRC (R=purine, Y=pyrimidine and N=any base). When the mRNA synthesis start site overlaps this sequence, ICP4 inhibits the transcription in trans [126-128]. However, deletion of this binding site does not affect the activation function of ICP4 on E or L genes [129]. ICP4 can induce the transcription from promoters that minimally contain the recognizable cis-acting element of ICP4, which is a TATA homology sequence [130-132]. Independent of how DNA binding assists the regulatory function of ICP4, it suggests that ICP4 operates through the transcriptional machinery acting at the TATA box [118]. ICP4 has been demonstrated to form complexes with TBP, TFIIB and TAF250 in vitro. ICP4 can form tripartite complexes on viral promoters with the general transcription factors TFIID and TFIIB. The interaction with TFIID is through the TBP-associated factor (TAF) 250 subunit [116]. Binding of TFIID to the promoter region in conjunction with ICP4 triggers the formation of transcription pre-initiation complexes, and eventually recruits RNA polymerase II to start viral mRNA transcription [133].

ICP4 also has been shown to repress the transcription of IE genes. This auto-repression of ICP4's own transcription has been clearly demonstrated in the

literature [126, 128, 134]. ICP4 has been shown to physically interact with ICP0, and repress the mRNA synthesis of ICP0 through the ICP4-DNA-binding site upstream of the TATA box [106]. Previous studies have also demonstrated that ICP4 could inhibit both SP1-activated transcription and USF-activated transcription without affecting basal transcription [135, 136]. Furthermore, it has been shown that ICP4 interferes with the viral transcription factors VP16 in vitro [117]. The detailed mechanism of ICP4 repression on transcription is still unclear. The DNA binding activity of ICP4 is essential for this regulation, but it is not sufficient [117]. An ICP4-DNA-binding site located in one orientation within approximately 45 bp 3'to the TATA box is required for ICP4 to block the transcription factor functions [117]. In addition, the repression activity of ICP4 was most strongly observed when the ICP4 binding site was in a position that resulted in the formation of tripartite complexes with TBP and TFIIB [117]. Therefore, by binding to specific DNA sites, ICP4 may repress the transcription through interfering with the basal transcription complex formation at the TATA box of target promoter [117].

1.4.4.3 ICP22

ICP22 is encoded by the α22 gene in the unique short region of the viral genome. ICP22 is a 68 kDa protein, containing two nuclear localization signals within its structure [137]. After translation, it is phosphorylated by the viral protein kinase UL13 or US3 [138, 139], and nucleotidylylated by casein kinase II (CKII) [71, 140]. ICP22 is found in discrete nuclear bodies along with ICP4 and RNA polymerase II after the initiation of viral DNA replication [141, 142].

The function of ICP22 in HSV-1 replication in host cell has not been fully demonstrated. ICP22 has been reported to be involved in modification of the carboxy-terminal domain (CTD) of RNA polymerase II. During active transcription, in normal cells, the CTD of RNA polymerase II is phosphorylated on both serine 2 and 5. During HSV-1 infection, CTD has been shown to be only phosphorylated at serine 5 not serine 2. In addition, ICP22 mediates degradation of the serine 2-phosphorylated form of RNA polymerase II by the proteasome [143-145]. Moreover, it has been reported that ICP22 and UL13 are both required for mediating phosphorylation of the large subunit of RNA polymerase II [146]. The N-terminal segment of ICP22 (residue 1 to 146) is critical for its effect on RNA polymerase II phorsphorylation, and this region is also required for inducing virus-induced chaperone-enriched (VICE) domain formation in HSV-1 infected vero cells [147]. VICE domains contain cellular chaperone proteins, proteasomal components and ubquinated proteins inside the nucleus, and they are proposed to function in protein turn over and nuclear remodelling in HSV-1 infected cells [147].

ICP22 mutant viruses are restricted to replication in some rodent cell lines and human fibroblasts. This host-range phenotype is not MOI-dependent and is caused by reduction of late gene expression [148]. ICP22 has been shown to be essential for the optimal accumulation of some true late ($\gamma 2$) viral proteins, including US11, UL38 and UL41 proteins [138, 149, 150]. In conjunction with UL13, ICP22 mediates the activation and post-translational modification of cdc2, and the degradation of cyclins A and B [69, 151, 152]. Furthermore, ICP22 is

required for switching the binding partner of cdc2 from cyclin B to a viral protein UL42, which is the viral DNA polymerase processivity factor [152]. The cdc2-UL42 complex has been proposed to recruit topoisomerase IIα to induce late gene expression in an ICP22-dependent manner [153].

1.4.4.4 ICP27

ICP27 is a 63 kDa IE regulatory phosphoprotein, encoded by the UL54 gene in the unique long region of the HSV-1 genome. ICP27 is comprised of several domains, including a nuclear localization signal, an RGG-box RNA binding domain, and the protein-protein interaction region at the C-terminus (reviewed in [154]). At early times post-infection, ICP27 is detected diffusely throughout the nucleus; but it then moves to replication compartments, and finally shuttles between the nucleus and cytoplasm at late times post-infection [155-157].

ICP27 is essential for HSV-1 lytic replication, and it is highly conserved among all mammalian and avian herpesviruses [154]. ICP27-deletion mutant viruses show over-expression of some E genes, a great reduction of viral DNA synthesis, a low level of leaky-L gene expression and no production of true late proteins [158-160]. ICP27 plays a critical role in the efficient expression of some E genes, especially the less abundant viral DNA replication proteins [161]. By increasing the mRNA level of E gene products which are required for DNA replication, ICP27 indirectly regulates viral DNA synthesis.

It has been suggested that the effect of ICP27 on inducing L gene expression may be different to its function in regulating viral DNA synthesis

[160]. Cells infected with the mutant virus-n504, which produces a defective ICP27 truncated at the carboxyl terminus, results in a normal level of viral DNA synthesis and leaky-late proteins, but they are unable to efficiently express true late mRNA or proteins [160]. Experiments with n504 further demonstrate that the regulatory function of ICP27 on E gene expression and DNA replication is independent of its activation of L gene expression [162]. ICP27 may induce some L gene expression, which has the weak poly-adenylation signals, through altering the specificity of the poly-adenylation machinery. In this way, ICP27 could activate the 3'-ends of viral mRNA processing by cellular proteins [163-166]. In addition, ICP27 has been shown to associate with the RNA polymerase II holoenzyme [167]. The C-terminal domain of ICP27 interacts with the large subunit of RNA polymerase II, in order to enhance initiation or termination of transcription [143]. Moreover, ICP27 is involved in degradation of the serine 2-phosphorylated RNA polymerase CTD through interacting with the charperon protein Hsc70 [168]. ICP27 has also been reported to play roles in promoting nuclear export of viral mRNA and translation of viral mRNA. ICP27 utilizes the cellular export receptor TAP/NFX1 to export the viral mRNAs into cytoplasm [169]. During infection, ICP27 directly interacts with a cellular protein complex Aly/REF to recruit the TAP [170]. In uninfected cells, Aly/REF interacts directly with TAP [171], and is recruited to pre-mRNA sites near exon junctions [172, 173], as part of a multi-protein exon-junction complex (EJC). Aly/REF then becomes bound to the spliced mRNP [174]. Previous studies showed that excess Aly/REF increased the rate and efficiency of cellular mRNA export in vitro [174,

175]. During infection, Aly/REF is recruited by ICP27 from splicesomes to viral intronless RNAs, and facilitates the export of viral mRNAs. Since Aly/REF cannot bind to intronless mRNAs, ICP27 bridges the viral mRNA and Aly/REF to export these transcripts into cytoplasm through the TAP/NFX1 pathway [170]. In contrast, knockdown of Aly/REF by siRNA has been shown to have minor effect on ICP27 exporting, but a decrease in TAP/NFX1 levels severely impairs the ICP27 exporting in host cells [169].

ICP27 also plays a critical role in subverting the antiviral defence system of host cells. ICP27 has been shown to be involved in disrupting the host cell mRNA splicing and exporting at early times post infection through preventing splicesome assembly and redistributes splicing factors [170, 176, 177]. ICP27 has also been proposed to alter several cellular signalling pathways. It has been reported to induce the p38 and JNK protein kinase pathways [178]. ICP27 also interferes with the IFN response through reducing Stat1 phosphorylation and blocking its translocation to the nucleus [179].

1.4.5 Replication compartment formation:

Viral DNA replication initiates at nuclear structure ND10 domains (or PML nuclear bodies). It has been shown that the ND10-like structures migrate to the incoming viral genome located at the nuclear envelope, forming the viral nucleoprotein complexes [180]. The authors also suggested that the assembly of these viral nucleoprotein complexes is enhanced by the initial transcription of IE genes on the viral genome [180]. Moreover, previous studies demonstrated that the transcriptional activity on HSV-1 genomes increases their association with

ND10 components [115, 181]. As mentioned above, the IE protein ICP0 causes the degradation of ND10 components through the ubiquitin-proteaosome pathway. Then, later during the infection, the E proteins involved in DNA replication localize to ND10 domain to initiate viral DNA synthesis [182, 183]. During DNA replication, the pre-replicative sites enlarge to form viral replication compartments. These replication compartments contain viral gene regulatory proteins, such as ICP4, and proteins required for DNA replication, such as ICP8 and UL9. In addition, cellular proteins involved in DNA repair and replication, including p53, Rb, DNA polymerase δ, DNA ligase, and the DNA damage response proteins Mre11 and ATM are all found in those viral replication compartments [184, 185].

Not only viral DNA replication takes place in the replication compartment; L gene expression and encapsidation of progeny DNA also occur there. As replication progresses, the replication compartments enlarge and eventually fill the entire nucleus [1].

1.4.6 Expression of E genes:

The expression of E genes are induced by IE proteins, and the production of E genes reaches maximal levels at approximately 5-7 hours post-infection [186]. The transcription of E genes is triggered by the viral transcription factor ICP4 along with other cellular proteins. The other three major IE proteins-ICP0, ICP22, and ICP27 also play critical roles in the production of E proteins. Temporally, E proteins are produced after IE proteins, and they are separated into two categories, E1 and E2. E1 proteins are expressed at a short time after, or

almost concurrently with, the onset of synthesis of IE proteins. The ssDNA binding protein ICP8 and the large subunit of ribonucleotide reductase ICP6 are examples of E1 proteins. E2 genes are expressed at later time then E1 genes, and E2 proteins include the viral thymidine kinase (encoded by UL23) and the viral DNA polymerase (UL39). After expression, E proteins then stimulate viral DNA synthesis, and they are also involved in the nucleotide metabolism of viral replication [186].

1.4.7 Viral DNA replication:

Once E proteins are expressed, they travel into the nucleus and localize to viral replication compartments [1]. There are seven viral proteins essential for mediating viral DNA replication: the viral DNA polymerase catalytic subunit (encoded by UL30), its processivity factor (UL42), origin binding protein (UL9), ICP8-ssDNA binding protein (UL29), and a helicase-primase complex made up of 3 proteins (UL5, 8 and 52) [1, 187].

There are three origins of viral DNA synthesis identified on the HSV-1 genome [188, 189]. OriS is present in two copies in the viral genome, and each copy is located in the c sequence of the inverted repeat region flanking the unique short region. The last origin, oriL is located between genes UL29 and UL30, which encode for ICP8 and viral DNA polymerase. Both oriL and oriS are palindromic sequences. The reason for having the 3 origins is not yet known, since neither of the origins is specially required for viral replication. It has been reported that an oriL-deletion mutant virus produced normal amount of viral progeny with titers comparable to the wild type virus [190]. In addition, oriL

mutant virus shows decreased viral replication in mouse tissue, and they produce a phenotype of reduced reactivation from latency [191]. Another study showed that a mutant virus without any oriS sequence had a fourfold reduction in viral yield, and slightly delayed viral DNA synthesis [192].

In general, viral DNA synthesis starts according to the θ replication model, and soon after it switches to a rolling circle mechanism, resulting in concatemeric DNA progeny molecules (reviewed in [1]). Initially, after entry into the host nucleus, the linear viral genome transforms to a circular DNA form. After expression, the origin binding protein, encoded by UL9, localizes to the nucleus and binds to specific elements in the replication origin (either oriS or oriL); then, it starts to unwind the DNA double helix. UL9 also recruits ICP8 which binds to the unwound single-strand DNA (ssDNA). UL9 and ICP8 then recruit five other essential viral proteins of DNA synthesis to the replication fork, including the viral DNA polymerase and the helicase-primase complex. The helicase-primase complex and DNA polymerase initiate the first round of θ form replication. The replication mechanism soon after initiation is then switched to the rolling circle mode, and it remains unclear how the switch occurs in the nucleus. Rolling circle replication generates long head-to-tail concatamers of viral DNA, which then get cleaved into monomeric molecules during viral assembly [1]. During viral DNA replication, cellular proteins are also recruited to the viral replication fork to assist the DNA synthesis. Proteomic studies have demonstrated that cellular factors involved in DNA repair, the DNA damage response and DNA recombination were associated with ICP8 and localized to replication compartments in the

nucleus [193]. Furthermore, cells lacking WRN helicase or Mre II produce less viral progeny compared to normal cells, potentially suggesting a function for these proteins in viral DNA replication [184].

1.4.8 L gene expression:

As L genes are heterogeneous with respect to their time of peak synthesis, they have been divided into two groups. L1, or leak-late genes, are expressed before DNA replication, and their expression is enhanced by viral DNA synthesis [1]. The expression of L2, or true-late genes is dependent on, and occurs after, DNA replication. In addition, the expression of L2 genes could be restricted by the presence of effective concentration of viral DNA synthesis inhibitors, such as PAA; however, these inhibitors cannot block the production of L1 proteins.

The transcription of late genes occurs in replication compartments within the infected cell nucleus. ICP4 and RNA polymerase II have been shown to localize to replication compartments at late time post infection [194-196]. IE proteins-ICP4, ICP22, ICP27 and E protein ICP8 play essential roles in mediating L gene expression. ICP27 and ICP8 have been proposed to activate the transcription of late genes by recruiting RNA polymerase II to the progeny viral DNA through a direct interaction [197]. ICP8 affects L gene expression either by making the promoters of the input genome more accessible to transcription factors or by promoting transcription off progeny genomes after viral DNA replication [198]. As the viral transcription activator, ICP4 facilitates the assembly of the preinitiation complex and RNA polymerase II on late gene promoters, thereby activating their transcription [199].

1.4.9 Virion assembly and egress:

At late time post infection, after the capsid proteins are synthesized in the cytoplasm, they transit to the nucleus, where the viral capsid is assembled. Electron microscopy has revealed that viral capsids are assembled inside of the nucleus, not in the cytoplasm. During early times of infection, the capsid is assembled within the replication compartments, where the viral DNA replication occurs [200, 201] at late time of infection, the assembly also occurs in nuclear structures called asssemblons in certain cell types [202, 203].

Three types of capsids (as known as A-, B- and C-capsid) have been detected by sucrose density gradient ultracentrifugation of nuclear extracts from the infected cell. A-capsids lack viral DNA and scaffold proteins. B-capsids also lacks viral genome DNA, but they are filled with VP22a and VP21 (the cleaved forms of the scaffold protein, pre-VP22a) and a viral protease VP24. C-capsids, which contain viral DNA and other tegument proteins, can mature into infectious virions by budding through the nuclear membrane [1].

The three major primary structural components of the HSV-1 capsid are a major capsid protein, VP5 and two minor proteins, VP19C and VP23. Assembly of the capsid involves the participation of two additional proteins: a scaffold protein encoded by UL26 and a viral protease (VP24) encoded by UL26.5. VP5 forms 150 hexons and 11 pentons within the capsid, and six copies of VP26 interact with the tip of VP5 hexons. VP5 is transported to the nucleus through its interaction with the C-terminal tail of the scaffold protein pre-VP22a [204]. Then, the VP5-pre-VP22a complex comes together as a result of self-interactions of pre-

VP22a molecules, in order to from a partial capsid. As hexons and pentons are added, the partial capsid assembles into a round pro-capsid [205, 206]. By interacting with the scaffold protein, a portal complex of twelve UL6 protein molecules is assembled onto the pro-capsid [207]. In vitro, the pro-capsid can be assembled only with the purified viral components VP5, VP19C, VP23 and a scaffold protein, and cellular factors are not required for this process [208]. After assembly, the round pro-capsid undergoes a structural transformation to become angular and polyhedral, and then it is ready for DNA encapsidation.

The mechanism of DNA encapsidation is still not fully understood. The concatemer of viral DNA is speculated to be cleaved to a certain length of DNA that fills the capsid, during DNA packaging into the pro-capsid. There are two packaging sequences mapped on viral genome: *pac*1 and *pac2* [209].

DNA encapsidation is mediated by several viral gene products, including UL6, UL15, UL17, UL25, UL28, UL32 and UL33 proteins. The complex made by twelve UL6 proteins serves as the portal at one capsid vertex for the entry of viral progeny DNA [210]. The concatmeric DNA is then cleaved into monomers by a complex of UL15, UL28 and UL23, when a monomer is packaged into the capsid [211]. UL25 may be involved in retaining the DNA in the capsid [212].

After virion assembly, the viral capsid exits from the nucleus through budding. Viral proteins encoded by UL31, UL43 and US3 have been reported to mediate capsid travel to the nuclear inner membrane by altering the nuclear lamins [213, 214]. Once the capsid buds through the inner nuclear membrane into

to the perinuclear space, it acquires a nuclear envelope, and the capsid is released into the cytoplasm by membrane-membrane fusion with the outer nuclear membrane. This membrane fusion has been proposed to be mediated by gB protein [215]. The naked capsid then acquires a tegument layer when traveling through the cytoplasm [216]. It also acquires an envelope by budding through the post-ER cytoplasmic compartment [217, 218], and eventually, the mature virion exits the host cell with a cellular envelope.

1.5 VP16

VP16 is a 65 kDa phosphoprotein, encoded by the L gene UL48. It is a tegument protein which contains a core region and a C-terminal transcriptional activation domain enriched in acidic residues [37]. This core region is conserved in many α-herpesviruses, such as the human varicella-zoster virus (VZV), the chicken Marek's disease virus (MDV) and bovine (BHV-1) herpesviruses. In contrast, the acidic activation domain of VP16 is not conserved among these viruses. VP16 has been under enormous study, due to its multiple functions in HSV-1 replication, such as inducing IE gene expression, promoting viral chromatin remodelling, and facilitating the viral egress.

1.5.1 VP16 as a transcription factor:

As mentioned above, VP16 forms an inducing-complex with cellular protein HCF-1 and Oct-1 to recruit the RNA polymerase II and its associated transcription factors to initiate the viral IE gene expression. Upon cell entry, VP16 is transported into the nucleus by the cellular protein HCF-1, which is also known as C1, VCAF or CFF. HCF-1 is a large protein of 2035 amino acids. It is

translated into a 300 kDa precursor protein and then is subsequently cleaved to produce a family of polypeptides ranging from 110 to 150 kDa [219, 220]. HCF-1 has been shown to play important roles in both cell growth and division [221]. It has been reported that HCF-1 interacts with two cellular protein complexes which are involved in histone modification: the Sin3 histone deacetylase (HDAC) complex and the trithorax-related Set1/Ash2 lysine 4 histone H3 methyltransferase (HMT) [58]. Therefore, by binding to the two complexes, HCF-1 could promote or repress active chromatin formation, leading to the induction or inhibition of transcription. During HSV-1 infection, VP16 selectively interacts with HCF-1that is bound to the Set1/Ash2 HMT complex, thereby promoting viral chromatin remodelling and activating viral gene expression [58].

Another cellular protein associated with the VP16-induced complex is Oct-1. Oct-1 is a broadly expressed transcription factor, and its target genes are involved in basic cellular processes, such as chromatin remodelling, RNA processing and transcriptional elongation. However, it also has been shown to repress gene transcription by several mechanisms; for instance, by binding to the target site, Oct-1 obstructs adjacent NFAT binding to the IL-4 promoter, resulting in repression of IL-4 gene transcription [222]. Oct-1 recognizes DNA through its POU domain, a bipartite DNA-binding domain [223]. The POU domain of Oct-1 has a high affinity for an octamer DNA sequence-ATGCAAAT. In addition, Oct-1 interacts with VP16 through its POU domain [223]. Within the target DNA site, the GARAT element of the VP16-targeting sequence (TAATGARAT) is not essential for binding of Oct-1, but it plays an essential role in recognizing Oct-1

by VP16 [224]. After being bound by Oct-1, the GARAT element induces a conformational change in the POU domain, and this change facilitates the efficient interaction of VP16 and Oct-1 [225]. VP16 selectively interacts with Oct-1 in host cells. VP16 has been reported to be unable to activate transcription via the B-cell POU-domain transcription factor Oct-2, which has identical DNA-contacting surfaces to Oct-1 [226-228].

VP16 has been shown in many studies to interact with general transcription factors through its C-terminal activation domain, in order to recruit RNA polymerase II to initiate IE gene transcription. Accurate transcription requires assembly of the RNA polymerase II holoenzyme at the promoter, which consists of RNA polymerase II, a subset of general transcription factors (TFIIA, B, C, D, E, F, H, and J) and regulatory proteins, known as SRB proteins. TFIID recognizes the TATA box on the promoter, and the subunit of TFIID which binds to this region is referred as TBP. The TBP associated factors (TAFs) in the TFIID complex, such as the cellular protein Sp1 and VP16 of HSV-1, are also essential for transcription activation [229]. Moreover, mutational analysis of the C-terminal activation domain of VP16 demonstrates that this domain is essential for the DA-complex (TFIID and TFIIA) formation at the TATA box and start site of transcription [230]. It has been reported that VP16 interacts with a subunit of human TFIID-TAFII32 through its acidic activation domain [231]. VP16 also has been shown to bind TFIIB and TFIIH directly [229]. Recent studies have also shown that VP16 is able to interact with positive transcription elongation factor b (P-TEFb) through its acidic activation domain [232]. P-TEFb is a cycline

dependent kinase, containing cdk9 and a c-type cyclin (CycT1, CycT2 or CycK) [233]. It regulates mRNA transcription at the level of elongation by releasing RNA polymerase II from the negative elongation factors DSIF and NELF [234].

Another tegument protein, encoded by UL14, has been reported to enhance the nuclear localization of VP16 [235]. In addition, UL14 has been shown to facilitate transportation of the nucleocapsid to the nuclear pore [235]. Previous studies on HSV-1 infection have suggested that another two tegument proteins, VP11/12 (UL46) and VP13/14 (UL47), might also facilitate VP16-activated IE gene expression through direct interactions [11, 236, 237].

1.5.2 VP16 as a repressor of vhs activity

The virion host shutoff (vhs) protein is a tegument protein of HSV-1, encoded by gene UL41. It is an endoribonuclease, and it mediates the degradation of pre-existing and newly transcribed mRNAs during the first few hours after infection (reviewed in [238]). Previous studies have demonstrated that vhs could not differentiate between viral IE mRNAs and host mRNA based on their nucleotide sequences. It has been shown that vhs caused the degradation of viral IE mRNAs in the presence of inhibitors of protein synthesis in the infected cells [239-241]. Later in infection, the RNase acitivity of vhs stops after the L gene expression; and this activity of newly synthesized vhs is proposed to be hindered by its interaction with VP16 [242]. Experiments using co-immunoprecipitation, in vitro pulldown assays and yeast two-hybrid assays have shown that the newly synthesized vhs directly interacts with VP16, and that this interaction may inhibit vhs activity but facilitate the incorporation of vhs into the tegument [242, 243].

Furthermore, cells infected with the VP16 null mutant HSV-1 virus (8MA) display enhanced early host-shutoff and greatly reduced viral protein synthesis, compared to a wild-type infection. However, this phenotype could be partially rescued by a mutant VP16 protein, which still binds vhs but lacks any transcription activation function [242]. Moreover, constitutive expression of mutant VP16 in cells was able to inhibit host shutoff activity during superinfection of HSV-1 [242]. Another group of studies suggested that the interactions of vhs with VP16 and VP22 may facilitate the accumulation of viral proteins, but it does not affect the stability of viral mRNA [244].

1.5.3 VP16 and viral assembly:

Due to its role in viral assembly, VP16 is essential for HSV-1 replication. Previous studies have shown that Vero cells infected with a VP16-deletion mutant virus produced nearly normal levels of viral DNA and capsids, but DNA encapsidation was reduced. As well, the later steps of virion maturation were shown to be defective using transmission electron microscopy [245]. Moreover, this virus replicated similar to a wild-type virus in a VP16-expressing cell line [245]. Therefore, the lack of VP16 leads to the termination of the lytic infection of HSV-1 at late times, during HSV-1 particle assembly. Recent studies have demonstrated that the absence of VP16 blocks the secondary envelopment of HSV-1 virion assembly, which involves the interaction between the capsid and the tegument structure [246].

VP16 has been proposed to have a structural role during virion assembly, due to its role in linking the capsid/inner tegument and outer

tegument/glycoprotein complexes [247]. Experiments with yeast two-hybrid assays, in vitro pull-down and co-immunoprecipitation assays have shown that VP16 interacts with the outer tegument proteins, encoded by UL41, UL46, UL47 and UL49. In addition, interactions between VP16 and the cytoplasmic tails of glycoproteins gB, gD and gH have been identified by chemical cross-linking studies, as well as co-immunoprecipitation and in vitro pull-down assay [247].

1.6 The phenotype of VP16 mutant viruses:

1.6.1 VP16-null mutant virus (8MA):

The VP16-deletion mutant virus (8MA) has been reported to be only able to grow and propagate in a wild-type VP16-expressing cell line [245]. Non-complementing cells infected with 8MA produced normal IE expression, nearly normal levels of DNA replication and capsid formation, and slightly reduced levels of DNA encapsidation. Consistent with these observations, a very low level of dense-coded capsids was detected in cells infected with 8MA using transmission electron microscopy. Furthermore, the production of infectious 8MA virions could not be detected by either plaque assay or single-step replication assay [245]. These observations demonstrate that VP16 is essential for the secondary envelopment of viral assembly in the cytoplasm.

1.6.2 VP16 mutant virus-In1814:

The mutant virus In1814 of HSV-1 (strain 17) was constructed by inserting a 12 nt-linker sequence encoding four amino acids at the 397th codon of VP16 gene. This mutation disables the abilities of VP16 to associate with OCT-

1/HCF-1 and to bind to the TAAGAGRAT sequence of the IE promoters. Cells infected with In1814 produce a high particle-to-PFU ratio in plaque assays and reduced levels of some IE mRNAs at relatively high MOIs. Moreover, in vivo experiments show that infection with In1814 is essentially avirulent in mice [248].

1.6.3 VP16 mutant virus-V422:

The mutant virus V422 of HSV-1 (strain KOS) carries a defective VP16 protein with a truncated C-terminal acidic activation domain. V422 is constructed by inserting a 12-linker sequence bearing the amber stop codons in all three reading frames at the 422nd codon of VP16 ORF [242]. Previous studies showed that V422 could replicate in non-complementing Vero cells, and its viral titer was detected >100-fold less than the wild-type virus in Vero cells. Compared to In1814, in the presence of a protein synthesis inhibitor-cycloheximide, V422 displayed a more severe defect in the accumulation of ICP4 and ICP0 mRNAs in infected Vero cells. Both of V422 and In1814 produced substantially more plaques on U2OS osteosarcoma cells than Vero cells [249]. Another common observation of V422 and In1814 infection is that hexamethylene bisacetamide (HMBA) treatment (3mM) could increase the viral titers of these two viruses approximately 100-fold in Vero cells. In addition, HMBA partially increase (3-5 folds) the accumulation of ICP4 and ICP0 mRNA produced in V422 infected cells, in the presence of cycloheximide (200 μg/mL). During In1814 infection, HMBA enhances the IE mRNA production to approximate the level of wild-type infection in the absence of HMBA [226].

HMBA, the prototype hybrid polar compound, is known to be an effective inducer of differentiation and apoptosis in transformed cells in culture [250-252]. Referring to the virus-cell interaction, HMBA has been reported to promote the reactivation of latent HSV-1 and HSV-2 in vitro [253, 254]. HMBA also has been shown to stimulate the major IE (MIE) gene expression and consequentially viral replication of HCMV in the human thyroid papillary carcinoma cell line TPC-1 [255]. This stimulation by HMBA may contribute to the induction of the NF-κB pathway in host cells. The enhancer of the MIE promoter of HCMV contains binding sites for cellular transcription activators, such as NF-κB, AP-1, SP-1 and CREB/ATF [256]. Mutations of the NF-κB binding sites at the MIE promoter diminished the ability of HMBA to induce MIE gene transcription in transfected cells [255].

HMBA also has been shown to reactivate HIV replication from latency [257]. It has been shown that the activation of HIV replication by HMBA is independent of the NF-kβ pathway, but the SP-1 binding site at the promoter is essential for this activation [258]. The effect of HMBA on HIV reactivation is predicted to involve the PI3K/AKT pathway and the release of p-TEFb [257]. P-TEFb enhances the transcription at the elongation step, through phosphorylating the C-terminal domain of RNA polymerase II and the negative transcription elongation factors. These phosphorylations recruit RNA polymerase II and release it from the binding of the negative transcription elongation factors [259, 260]. After expression, p-TEFb is inhibited and restrained by HEXIM1 and 7SK snRNA in the cytoplasm. Phosphorylation of HEXIM1 could lead to the release of

p-TEFb from its transcriptionally inactive complex. In HMBA-treated cells, the PI3K/AKT pathway is found to be upregulated resulting in the release of p-TEFb from the phosphorylated HEXIM1; p-TEFb is then proposed to be recruited to the HIV promoter to enhance transcription. This is suggested by the fact that inhibitation of the PI3K/AKT pathway or expression of a mutant HEXIM1 (that cannot be phosphorylated by AKT) in chronically infected cells, disables the activation of HIV transcription from HMBA [257]. With respect to HSV infection, the mechanism by which HMBA reactivating HSV latency and promoting the replication of VP16-mutant virus in restrictive cell lines is still unknown.

1.7 Rational of this project:

HSV-1 mutants lacking the activation function of ICP0 or VP16 display low levels of IE gene expression upon low multiplicity infection in many cell types. The most restrictive host cell types of these ICP0 or VP16 mutants appear to be the primary human fibroblasts [261, 262]. In contrast, U2OS osteosarcoma cells have been shown to complement the replication of these mutant viruses [249, 263]. This observation suggests that U2OS cells either express an endogenous activator that can complement the defective VP16 or ICP0, or they lack inhibitory mechanisms that are blocked by wild-type VP16 or ICP0 in other cells [264]. To distinguish between these two possibilities, Hancock, et al., [264] performed a somatic cell fusion experiment with U2OS and HEL, mediated by the p14 fusion protein of HIV. It also has been proved that expression of p14 did not alter the permissive or restrictive phenotype of U2OS and HEL cells to a VP16/ICP0-double mutant virus (KM110). The U2OS-HEL heterkarya were shown to be as

restrictive as HEL cells. In addition, expressing VP16 or ICP0 *in trans* could rescue the replication of KM110 in this heterokarya. Together, these results demonstrated that U2OS cells are lacking an inhibitory mechanism that can be silenced by either VP16 or ICP0 during wild-type infection in other restrictive cells, such as HEL [265]. Furthermore, PI3 kinase inhibitor-LY294002 has been shown to render the HEL permissive to V422 and KM110, but its effect on HSV gene expression did not stem from inhibition of PI3 kinase [266]. This result raises the possibility that cellular protein kinases may be involved in this inhibitory mechanism, which is missing in the U2OS cells.

Therefore, this project was originally designed to identify cellular proteins involved in repressing the replication of the VP16 mutant virus, V422, in HeLa cells by performing a global small RNA interference (siRNA) screen on the cellular genome.

RNA interference (RNAi) is a fundamental regulation system for gene expression in eukaryotic cells in which the sequence-specific siRNA is able to bind and cause the cleavage of complementary mRNA. In in vitro experiments, double-stranded (ds) siRNA (21-23 nts) is synthetically produced and then directly transfected into cells using specific reagents. Once the siRNA enters the cytoplasm, it is assembled into the RNA induced silencing complex, RISC. Argonaute 2, a major component of RISC, causes cleavage of the sense strand of the ds siRNA. Therefore, the active form of RISC, containing the anti-sense strand of siRNA, selectively targets and degrades mRNA that is complementary to this siRNA. In this way, expression of the target gene is captured and shut

down before translation occurs (reviewed in [267]. Genomic-wide siRNA screens have been shown to be a powerful tool to identify novel cellular factors involved in viral-host interactions, and as such, it has been used to identify cellular proteins facilitating infections of HIV, HCV, WNV etc. [268-270] Thus, we plan to employ a global siRNA screen to investigate the interaction between the HSV-1 mutant V422 (as well as the wild-type KOS) and host HeLa cells.

A successful screen requires an assay to allow quantitation of a cellular phenotype after the siRNA treatment; and in this case, this assay needs to show the differences between V422 infection in restrictive and permissive cells. To this end, I constructed V422-and KOS-based green fluorescent protein (GFP) reporter viruses using BAC recombineering technology [271], in which GFP expression was expected to be an indicator of viral replication following siRNA treatment. However, while optimizing the infections of the KOS- and V422-derived GFP reporter viruses, I observed unexpectedly low levels of GFP expression in HeLa cells. Furthermore, the kinetics of GFP expression driven by the HSV IE promoter did not appear to be comparable to other IE proteins of HSV-1. These two observations have made it difficult for us to continue pursuing the siRNA screening project. Thus, to this end, the goal of this project is to better understand why an exogenous gene (GFP) under the control of an IE promoter inserted into the viral thymidine kinase locus is unable to undergo efficient and regulated expression following infection.

Chapter 2: Materials and Methods:

2.1 Mammalian cell culture:

Human U2OS osteosarcoma, HeLa cervical carcinoma, and African green monkey kidney epithelial (Vero) cells were obtained from the American Type Culture Collection. Cells were maintained in 150 cm^2 tissue culture flasks (Corning) containing 25 mL Dulbecco's Modified Eagle Medium (DMEM) supplemented with10% fetal bovine serum (FBS), 50 units/mL penicillin and 5 µg/mL streptomycin (complete DMEM). Cells were incubated at 37 ℃ in a humidified atmosphere in the presence of 5% CO_2.

Cells were passaged when they reached confluency by washing once with phosphate buffered saline (PBS-10 mg/mL NaCl, 0.25 mg/mL KCl, 1.8 mg/mL Na_2HPO_4, 0.3 mg/mL, pH7.5), then trypsinizing the cells until they no longer attached to the flask (Trypsin, Gibco), resuspending them in complete DMEM, and reseeding to approximately 20% confluency. U2OS, HeLa and Vero cells were passaged up to 50 times before a new vial of cells was thawed.

Monolayers of confluent cells were prepared by seeding to 65% confluency in tissue culture plates (Corning) the day before use. The exact number of cells was determined before seeding with a hemocytometer.

To start cell cultures from a liquid nitrogen stock, each cryovial was thawed at room temperature (RT), and diluted in 10 mL complete DMEM. Then the cells were pelleted at low speed and resuspended into 25 mL growth medium in a 150 cm^2 flask.

2.2 Virus Strains:

The following viruses have been used in this project:

KOS: wild type virus HSV-1

V422: a VP16 mutant virus of HSV-1; it was generated by inserting a 12 nt linker sequence (bearing an amber stop codon-UAG in all three reading frames) into the VP16 gene of KOS, resulting in truncation of the protein after amino acid residue 422 [242]

KOS-HSV-GFP: an EGFP expression cassette driven by the HSV ICP22 promoter is inserted into the thymidine kinase gene (UL23) of KOS

V422-HSV-GFP: an EGFP expression cassette driven by the HSV ICP22 promoter is inserted into the thymidine kinase gene (UL23) of V422

KOS-CMV-GFP: an EGFP expression cassette driven by the IE promoter of HCMV inserted to the thymidine kinase gene (UL23) of KOS [272]

V422-CMV-GFP: an EGFP expression cassette driven by the IE promoter of HCMV inserted into the thymidine kinase gene (UL23) of V422

Note: HSV IE promoter-driven EGPF expression cassette is inserted between the 429^{th} and 451^{th} bp of the TK open reading frame (ORF) in V422 and KOS37 BACs. The HCMV promoter-driven EGFP gene is inserted into an *SstI* site (downstream of 442^{nd} bp) within the TK ORF.

2.3 Amplification of virus stocks:

All HSV strains listed above were propagated on U2OS cells, which complement the VP16 mutation of V422 [249]. To prepare viral stocks, confluent monolayers of U2OS cells grown in 150 cm^2 flasks were infected with virus at a multiplicity of infection (MOI) of 0.05 in 5 mL serum-free DMEM. After one hour of infection at 37 ℃, rocking every 15 minutes, 20 mL complete DMEM was added. To increase the production of V422 and V422-GFP viruses, cells were treated with 3mM hexamethylene-bis-acetimide (HMBA) during and after the one hour infection. When a majority of cells exhibited extensive cytopathic effect (approximately 3 days for KOS & KOS-GFP infections, and 5 days for V422 & V422-GFP infections), cells were collected and pelleted at 2000rpm (BECKMAN GS-6R) for 5 minutes at 4 ℃ in a bench top centrifuge. Cell pellets were resuspended in 1 mL serum-free DMEM per 150 cm^2 flask. Virus was then released by three cycles of freezing the cells at -80 ℃ for 15 minutes and thawing at 37 ℃ for 5 minutes, followed by three cycles of sonication (Model 550 Fisher Scientific Sonic Dismembrator) at level 7 using pulses of 20 seconds, followed by 20 seconds on ice. Large cellular debris was removed by centrifugation at 2000rpm (BECKMAN GS-6R) for 15 minutes in a bench top centrifuge at 4 ℃. Supernatants were then aliquoted and stored at -80 ℃.

2.4 Titration of HSV stocks:

Viral stocks were titrated by ten-fold dilutions from 10^{-2} to 10^{-7} in serum-free DMEM. 0.25mL of each dilution was used to infect each well of confluent U2OS cells in 12-well plates (Corning). The infections were incubated for one

hour at 37 ℃, with rocking every 15 minutes. Then, the inoculum was replaced with 1mL DMEM containing 1% human serum. In the case of V422 (or V422-GFP) infection, the medium was additionally supplemented with 3mM hexamethylene-bis-acetimide (HMBA) during and after the one hour infection. After 2-3 days, plaques in each well were counted under a light microscope. For improved accuracy, wells with plaque numbers >20 and <200 were used to calculate the plaque forming units per mL of virus stock solution.

2.5 Infection of mammalian cells with HSV:

Cells were infected in a confluent monolayer at the appropriate MOI in serum-free medium. Infections were carried out at 37 ℃ in a humidified incubator in the presence of 5% CO_2. During the one hour infection, cells were rocked every 15 minutes to provide the full adsorption of virus to cells. Then the infecting medium was replaced with complete DMEM. Cells were incubated in a humidified incubator at 37 ℃ for the appropriate length of time.

2.6 Plasmids and cloning:

2.6.1 Production of pUC19-HSV-GFP:

The plasmid pA-EUA1 which contains the EGFP gene driven by the ICP22 promoter and utilizing the bovine growth hormone (BGH) poly A signal was kindly provided by Dr. Luis Schang (University of Alberta) [273]. Since the entire sequence of the plasmid pA-EUA1 is not known, cloning the EGFP expression cassette into a well-known vector (i.e. pUC19) allowed us to further analyze and utilize this DNA.

The EGFP expression cassette was excised from 10 µg pA-EUA1 using the restriction enzyme SphI at 37 ℃ for 1 hour. DNA was separated on a 1% agarose gel and purified using a gel extraction kit (QIAGEN). 10 µg of pUC19 (Invitrogen) was also digested with SphI using the same conditions, followed by dephosphorylation of the 5' ends using Antarctic phosphatase (New England Biolabs) at 37 ℃ for 30 minutes. The EGFP expression cassette was then inserted into pUC19 using T4 DNA ligase (Invitrogen) overnight at 14 ℃, creating pUC19-HSV-GFP (Figure 3.1.1-A).

2.6.2 Transformation of competent bacteria

Plasmids were transformed and amplified in *Escherichia coli* (*E.coli*) strain DH5α. Electro-competent DH5α (40 µL) were mixed with 50ng of plasmid DNA in an eppendorf tube, on ice. The mixture was pulsed in a pre-chilled electrocuvette using a BIORAD Gene Pulser II with the resistance set at 200 ohms, the capacitance at 25 µfaraday and the voltage at 1.8 volts. Then the transformed bacteria were immediately added to 1 mL super optimal broth with catabolite repression (SOC) medium (0.02g/mL Bacto-tryptone, 5 µg/mL yeast extract, 5mM NaCl, 25mM KCl, 10mM $MgCl_2$ and 20mM glucose), and incubated at 37 ℃ for 1 hour while shaking at 225 rpm. 50-100 µL of these bacterial cells were spread onto LB (Luria Broth-1% w/v bactotryptone, 0.5% w/v yeast extract, 1% w/v NaCl) agarose plates containing the proper antibiotic, and incubated at 37 ℃ overnight (12-16 hours).

2.7 BAC recombineering:

HSV viruses carrying the EGFP expression cassettes from pUC19-HSV-GFP or pEGFP-C1 were synthesized by using a bacterial artificial chromosome (BAC) recombineering system that has been described previously [271]. This BAC recombineering strategy is based on homologous DNA recombination, utilizing a *galK* (galactokinase) positive/counter-selection cassette, and a modified bacterial strain SW102 which lacks the galK gene of the galactose operon. The EGFP expression cassette was inserted into the thymindine kinase (gene U_L23) open reading frame (ORF) in the HSV-1 genome. A TK-galK DNA construct containing the galK gene surrounded by DNA homologous to that which flanks the inserting region of the HSV-1 TK ORF (50 bp 5' and 3' of the TK ORF) was generated by polymerase chain reaction (PCR) using TK-galK primers (Table 1) on pgalK plasmid [271], with Pfx DNA polymerase (Invitrogen), and a program of 94 ℃ for 15 seconds, 55 ℃ for 30 seconds, and 68 ℃ for 3 minutes, repeated for 25 cycles. Before use in recombineering the construct was gel purified.

The EGFP recombinant viruses were constructed by inserting the EGFP expression cassettes into a BAC carrying either the wild-type HSV-1 KOS genome or the mutant V422 genome, named KOS37 BAC [274] or V422 BAC. The BAC sequence (CCBAC1B from Epicentre Inc., Madison, WI) flanked by two LoxP sites on either end was inserted between U_L37 and U_L 38 in the KOS genome by homologous recombination [274]. The HSV-1 KOS37 BAC was introduced into SW102 cells [275]. The mutant V422 BAC was constructed by insertion of a 12 linker sequence containing a NheI site right after the 1266^{th} bp

(i.e. 422nd codon) of the VP16 ORF in the KOS37 BAC through BAC recombineering (constructed by Candace Haarsma). The TK-galK expression cassette was introduced into the HSV-1 KOS37 or V422 TK ORF using recombineering as outlined in the online protocol (www.recombineering.ncifcrf.gov/Protocol.asp). After overnight incubation at 32 ℃ in LB with 12.5 μg/mL chloramphenicol, expression of the DNA recombination machinary in SW102 cells containing the KOS37 BAC was induced by heatshock at 42 ℃ for 30 minutes in a shaking incubator. The cells were then washed three times in double distilled H_2O (ddH_2O) and collected by centrifugation at 5000 rpm at 0 ℃ for 5 minutes using Avanti^{TM} J-25 centrifuge (Beckman). TK-galK (400 ng) was introduced into the SW102 cells by electroporation in a 0.1cm cuvette (BioRad) at 25 μF, 1.75 kV and 200 ohms, followed by recovery in 1 mL LB at 32 ℃ for 1 hour. After recovery, 1 mL of transformed bacteria was washed twice in 1XM9 medium, plated on M63 minimal media plates, and incubated at 32 ℃ for 3 days. Colonies were purified by 4 rounds of selections on MacConkey plates with chloramphenicol and galactose (as the only sugar source). The insertion of the galk gene was tested by PCR with primer 1 and 2 (Table 1) designed to amplify across the insertion region.

Secondly, the inserted galK expression cassette was removed and replaced with the EGFP cassette through a negative selection against the galK gene. Similarly to the first step, the replacement of galK gene was also accomplished by the homologous DNA recombination with a DNA fragment carrying the EGFP cassette flanked by the homology sequence of TK.

The TK-CMV-GFP (the EGFP gene driven by the CMV IE promoter) DNA fragment was amplified by PCR on plasmid pTK-green [272] with TK-CMV-GFP primers (Table 1). pTK-green was constructed by inserting the EGFP cassette from pEGFP-C1at the 442nd bp of the TK coding sequence (CDS) carried by pTK173 plasmid [272]. The TK-HSV-GFP DNA fragment containing the EGFP gene driven by the HSV-1 IE promoter was amplified by PCR from the vector pUC19-HSV-GFP using TK-pUC-GFP primers (Table 1), which contained the same TK homology sequence as TK-galK primers. The SW102 cells containing the BAC-HSV-galK construct were transformed with 400 ng TK-GFP (TK-HSV-GFP or TK-CMV-GFP) DNA by electroporation as described above for TK-galK. For negative selection of *galK*, cells were plated onto M63 minimal media plates containing 2-deoxygalactose and chloramphenicol, incubated at 32 ℃ for 3 days. The substitution of *galK* by the GFP expression cassette was tested by PCR with primer 2 and 3 (Table 1) and Southern analysis with an EGFP probe (Described in Section 2.12).

The HSV-BACs containing the EGFP cassette driven by either HSV IE promoter or CMV IE promoter were the purified using a large-construct kit (QIAGEN) and transferred into U2OS cells using Lipofectamine^{TM} 2000 to make HSV-GFP viruses.

Table 1: Primers used in this project.

TK-galK forward	5’CAATGGGCATGCCTTCTGCCGTGACCG ACGCCGTTCTGGCTCCTCATATC-cctgttgacaattaatcatcggca-3’
TK-galK reverse	5’CGATGGGATGGCGGTCGAAGATGACC CTGAGGGCCGGGGGCGGGGCATGT-tcagcactgtcctgctcctt-3
TK-CMV-GFP forward	5’CAATGGGCATGCCTTATGCCG-3’
TK-CMV-GFP reverse	5’CGATGGGATGGCGGTCGAAG-3’
TK-pUC-GFP forward	5’CAATGGGCATGCCTTCTGCCGTGACCG ACGCCGTTCTGGCTCCTCATATC-agtcgactgcaggcatg-3’
TK-pUC-GFP reverse	5’CGATGGGATGGCGGTCGAAGATGACC CTGAGGGCCGGGGGCGGGGCATGT-ccatgattacgccaagcttg 3’
Primer 1	5’TACCCGAGCCGATGACTTAC- 3’
Primer 2	5’GAAAGCTGTCCCCAATCCTC-3’
Primer 3	5’ATGGTGAGCAAGGGCGA-3’
Primer 4	5’TGTTTGACTGCCTCTGTTGC-3’
Primer 5	5’AGGGCATCGGTAAACATCTG- 3’
Primer 6	5’CGTCGCCGTCCAGCTCGACCAG- 3’
Primer 7	5’ATGACAAGCGCCCAGATAAC- 3’
M13-F	5’GTTTTCCCAGTCACGAC- 3’

TK-primers listed above were used to construct the EGFP recombinant viruses using BAC recombinneering. For TK-galK and TK-pUC-GFP primers, capital letters represent the sequence of TK homology (the same sequences for both sets of primers) and lowercase letters represent sequence of the galK gene or pUC19 plasmid. Primers 1 to 3 were used to confirm the insertion of EGFP. Primers 4 and 5 were used to confirm the V422 mutation of VP16. Primers 6, 7 and M13-F were used to confirm the EGFP insertions in sequencing analysis.

2.8 DNA transfection:

Plasmid DNA (or HSV-BAC DNA) (1.6 µg) and 4 µL Lipofectamine™ 2000 (Invitrogen) were each diluted in 100 µL of Opti-MEM I medium and incubated at RT for 5 minutes. The diluted Lipofectamine™ 2000 was then mixed with the diluted DNA, and incubation continued at RT for 20 minutes. The entire mixture was added to a monolayer of confluent cells grown in 800 µL antibiotic-free DMEM (10% FBS) in a 12-well plate, and the plate was incubated at 37 ℃ for 4 hours. The medium was then replaced with complete DMEM and incubated for the length of time (indicated in the figure legends of the results section (Chapter 3).

2.9 Western blot analysis:

Non-infected (Mock) or virally infected cells were harvested at various time points, according to the experiment. Cells were lysed in 1X RIPA buffer (50 mM Tris-HCl pH 7.4, 150mM NaCl, 1mM EDTA, 1% Triton X-100, 0.1% SDS, with 1X complete protease inhibitor (Roche)) or 2X SDS-PAGE lysis buffer (125mM Tris-HCL pH 6.8, 2% SDS, 20% glycerol, 2% bromophenol blue, with 0.031g DTT/1mL). Samples in 1X SDS-PAGE buffer (125mM Tris, 1M glycine and 0.5% SDS) were resolved on a 10% SDS-PAGE gel (Stacking gel-4% Acrylamide, 250mM Tris-HCl pH 6.8, 0.1% SDS, 0.1% TEMED and 1% Ammonium persulfate Resolving gel-10% Acrylamide, 375mM Tris-HCL pH8.8, 0.1% SDS, 0.05% TEMED and 0.5% Ammonium persulfate) in 1X SDS-PAGE buffer (125mM Tris, 1M glycine and 0.5% SDS), at 120 volts for 1 and 1/2 hours. The sample proteins were then transferred from the gel to the nitrocellulose

membrane (GE Healthcare) in the transfer buffer (16.8mM Tris, 192mM Glycine and 20% Methanol) at 100 volts for one hour. The transferred membrane was blocked in 5% skim milk in TBST (1.5M NaCl, 250mM Tris-HCl pH 8, and 0.1% Tween) overnight at 4 ℃. The appropriate primary antibody was then applied to the blot diluted 1:1000 in 5% milk-TBST (except anti-β- actin which was used at a dilution of 1:10,000), and incubated at RT for 1 hour. Secondary antibody (conjugated to horseradish peroxidase-HRP**)** was used at a dilution of 1:10,000, incubated for 1 hour at RT. The blot was then washed three times for 5 minutes each in TBST. Target proteins were visualized on X-RAY film (FUJI) with the ECL Plus Western Blotting Detection kit (GE Healthcare), and a M35A X-OMAT processor (KODAK).

2.10 Indirect immunofluorescence assay

Confluent monolayers of mock-infected or virally-infected cells grown on coverslips in 24 well-plates were washed with 1 mL PBS. The cells were then fixed using 300 µL 3.6% formaldehyde at RT for 15 minutes, and permeabilized in 0.2% Triton- X100 for 10 minutes at RT. The cells were washed 3 times in PBS, and blocked in 5% FBS in PBS for 30 minutes at RT. Primary antibody was applied at a dilution of 1:1000 in PBS containing 5% FBS at RT for 1 hour, and washed 3 times in PBS. The secondary antibody was added at a dilution of 1:10,000 at RT for 45 minutes, followed by 3 washes in PBS. The coverslip carrying the cells was dipped into distilled H_2O and inverted onto 6.5 µL of 1 mg/mL DAPI dye in Mounting media (Vector) on a microscope slide, and sealed with nail polish. The EGFP production was detected using the Zeiss Axiovert 200

fluorescence microscope with the X-Cite 120 Fluroresence illumination system as a light source.

2.11 Northern Analysis:

2.11.1 Total RNA isolation

A 60mm plate of mock-infected or viral-infected monolayer cells was collected and then lysed in 1mL TRI_{ZOL} Reagent (Invitrogen) by incubation for 5 minutes at RT. Then, these cells were collected using a cell scraper into a 1.5mL eppendorf tube. Chloroform (200 µL) was added to each tube, and the mixture was shaken for 2-3 minutes and centrifuged (Eppendorf centrifuge 5417C) at 14000 rpm for 10 minutes at 4 ℃. The upper aqueous layer was transferred to a fresh tube, and samples were re-extracted with 600 µL of chloroform. The aqueous phase was again transferred to a new tube, and the total RNA was precipitated in 600 µL of isopropanol for 15 minutes at RT. Following centrifugation (20817 xg), the RNA pellet was washed with 1mL 70% ethanol and centrifuged again for 5 minutes. The supernatant was aspirated and the pellet was allowed to dry for 10 minutes before resuspension in 40 µL Diethylpyrocarbonate (DEPC)-treated water. The concentration of RNA was determined using a Nano Drop spectrophotometer (ThermoScentific). RNA samples were stored at -80 ℃.

2.11.2 Northern Analysis:

For each sample, 10 µg of total RNA (or 5 µg 0.5-10 kb RNA ladder (Invitrogen) was mixed with 3 µL 10X MOPS pH 7 (200mM 3-(N-Morpholino) propanesulfonic Acid, 50mM Na-Acetate Trihydrate, 10nM EDTA and DEPC , 5

μL formaldehyde, and 15 μL formamide. Samples were denatured at 60 ℃ for 15 minutes and placed on ice for 2 minutes followed by a quick spin at RT. RNA samples were loaded onto a 1.2% agarose, 2% formaldehyde, 1X MOPS and 0.005% ethidium bromide gel, and separated at 120 V for 2 hours. RNA was transferred to a GeneScreen Plus nylon membrane (PerkinElmer) in 10X SSC buffer (1.5M NaCl, 150mM Na citrate). The RNAs was then fixed on the membrane using a UV Stratalinker 2400 (Stratagene).

2.11.3 Hybridization with ^{32}P-labelled probes

Membranes with RNA samples were pre-hybridized in 5 mL pre-warmed ExpressHyb Hybridization Solution (Clontech) at 68 ℃ for 30 minutes while being rotated in a H1 16000 hybridization incubator (Tyler Research Instruments). The ^{32}P-labelled probe was denatured at 95 ℃ for 3-5 minutes before addition to the membrane. Hybridization of the probe ($1X10^7$ counts/blot) for 1 hour at 68 ℃ was followed by two washes in buffer #1 (10X SSC and 0.05% SDS) for 20 minutes at RT, and two washes in buffer #2 (10% SSC and 0.1% SDS) for 20 minutes at 50 ℃. Finally, the membrane was exposed by a FUJI imaging plate at RT or BioMax XAR film (Kodak) at -80 ℃. The image was processed by phosphoimager FLA-5100 (FUJI) or M35A X-OMAT processor (Kodak). Some blots were stripped and re-probed by two washes in stripping buffer (0.5%SDS and 10mM Tris-HCl pH8) for 15 minutes at 95 ℃. The cleanness of the blot after striping was ensured by a FUJI imaging plate exposure of 1-3 hours.

2.12 Southern Analysis:

2.12.1 DNA isolation from infected cells

Monolayers of mock-infected or HSV-infected cells grown on 60 mm plates were harvested at 24 hours post infection. Cells were then collected by spinning at 1400 rpm (GH-3.8 rotor) for 5 minutes in a Beckman GS-6R swinging bucket centrifuge, and supernatants were aspirated. The pellets were resuspended in 500 µL urea/SDS lysis buffer (7M urea, 350mM NaCl, 10mM Tris pH 7.8, 10mM EDTA and 1% SDS). Samples were centrifuged through a QIAshedder column (Qiagen) by centrifuging at 14000 rpm for 2 minutes. Samples were incubated with 5 µL Proteinase K (Invitrogen) at 37 ℃ for 45 minutes. The viral genomic DNA was extracted with 500 µL phenol/chloroform, and centrifuging at 14000 rpm for 5 minutes at RT. The aqueous phase was saved and transferred to a new tube. The extraction was repeated three times. DNA was precipitated with 1 mL 95% ethanol at -80 ℃ for 15 minutes, and collected by centrifugation at 20817 g for 15 minutes at 4 ℃. The DNA pellet was then resuspended in 250 µL 0.3M NaOAc, and incubated with 2 µL RNase for 45 minutes at 37 ℃. The DNA was then precipitated with 750 µL 95% ethanol at -80 ℃ for 15 minutes, and was pelleted at 14000 rpm for 15 minutes at 4 ℃. The DNA pellet was washed with 1 mL 70% ethanol and then with 1 mL 95% ethanol, and was finally dissolved in 40 µL H_2O.

2.12.2 Southern analysis:

DNA was digested with NheI/BamHI for 1 hour. Following the digestion, samples (or 10 µL of 1kb DNA ladder (GeneRuler)) were run on a 1% agarose gel

containing 0.005% ethidium bromide in Tris-acetate EDTA (TAE) for 2 hours at 100V in TAE buffer. The gel was then sequentially washed with the following solutions for 15 minutes each: 0.25 M HCl, 0.5 M NaOH, 1 M Tris/1.5 M NaCl, and 10X SSC. DNA was transferred from the gel to a GeneScreen Plus nylon membrane in 300 mL 10X SSC overnight. The blot was UV-cross-linked using a Stratalinker 2400 (Stratagene). Hybridization of ^{32}P-labelled probes was carried out at 60 ℃. The remaining hybridization procedures and conditions were the same as for Northern Blot Analysis, described above.

2.12.3 ^{32}P-labelled probes:

Template DNA was isolated from the following plasmids by digestion with the indicated restriction enzymes or by PCR with primers:

ICP22 probe: plasmid: pICP22 [276]

Restriction enzymes: *SacI/XhoI*

1278 bp probe fragment

ICP8 probe: plasmid: pE/3583 [194]

Restriction enzymes: *EcoRI/BamHI*

1857 bp probe fragment

VP16 probe: KOS genomic DNA

Primer 4 and 5 (Table 1)

EGFP probe: plasmid: pEGFP-C1 (Clontech)

Restriction enzymes: *AgeI/SacI*

750 bp probe fragment

Template DNA (250 ng) was mixed with random primers (2 µg) in 26 µL H_2O, denatured at 95 ℃ for 4 minutes and cooled on ice for 2 minutes. Random priming was proceeded with the addition of 7 µL oligo labelling buffer (2M Tris pH 8.0, 1M $MgCl_2$, 2-mercaptoethanol, 100mM dGTP, 100mM dATP, 100m dTTP, 2M HEPES pH 6.6), 2 µL BSA (10mg/mL), 50 µCi [α-32P] dCTP, and 6 U Large Fragment DNA Polymerase I (Invitrogen) at 37 ℃ for 30 minutes. The total volume of the reactions was adjusted to 100 µL through the addition of 50 µL TE (10mM Tris, pH 7.0, 1mM EDTA), and DNA was then extracted with 100 µL phenol/chloroform (centrifuging: 20817 g for 5 minutes). The aqueous phase was passed through a NICK column (GE Healthcare) to remove any unincorporated nucleotides. The probe was eluted in 500 µL TE, and its radioactivity was counted with a Beckman LS 6500 scintillation detector.

2.13 siRNA transfection optimization

In a single well of 96-well plate, 10 µL of 200nM GAPDH siRNA or non-silencing siRNA were mixed with 0.25 µL DharmaFECT 1 transfection reagent (Thermo Scientific Dharmacon) in 14.75 µL Opti-MEM I medium, incubated at RT for 20 minutes. 6000-6500 HeLa cells per well in a volume of 75 µL antibiotic-free DMEM (10% FBS) were adding to the siRNA mixture. The siRNA transfection was incubated at 37 ℃ for 4 hours, followed by replacing the medium

with complete DMEM. The knockdown of GAPDH by siRNA silencing was halted at 72 hours post-transfection for analysis.

The conditions of siRNA transfection were optimized by measuring GAPDH knockdown using the KDalert™ GAPDH Assay (Ambion). At 72 hour post-transfection, the culture medium was replaced with 200 µL KDalert lysis buffer. After incubation at 4 ℃ for 20 minutes, the cells were homogenized by pipetting lysates, and 10 µL of homogenate was added to 90 µL of KDalert Master Mix. The kinetics of fluorescence was measured by using Envison 2104 Multilabel Plate Reader (PerkinElmer) at RT.

Chapter 3: Results

3.1 Construction of derivatives of HSV-1 bearing reporter EGFP expression cassettes

In this project, I made three fluorescent EGFP recombinant viruses derived from the wild type HSV-1 KOS stain. These viruses were designed for use in a siRNA intereference-base experimental system to identify cellular proteins regulating IE gene expression. To make these reporter viruses, I introduced two EGFP expression cassettes into the TK gene, in a wild-type KOS and V422 (VP16 mutant) background. The EGFP gene in the two cassettes is either driven by the HCMV IE promoter or an HSV IE promoter (from ICP22 gene). The viruses carrying the HSV-EGFP cassette are designated KOS-HSV-GFP and V422-HSV-GFP, and the ones bearing the HCMV-EGFP cassette are referred to as KOS-CMV-GFP and V422-CMV-GFP. KOS/V422-HSV-GFP and V422-CMV-GFP were constructed by me. KOS-CMV-GFP (also referred to as KOS-Green) was constructed by Rebecca Minaker [272].

The EGFP recombinant viruses were constructed by using lambda (λ) Red-mediated homologous recombination of infectious BAC clones of HSV-1. The BAC carrying the wild-type KOS genome, referred to as KOS37 BAC, was kindly provided by David Leib's lab [274], and the V422 BAC was made by Candace Haarsma. These BAC constructs were introduced into *E.coli* SW102, which is a bacterial strain suitable for recombineering [271]. Mutagenesis was accomplished by two steps of BAC recombineering involving sequential positive

and negative selections for the galactokinase gene (*galK*), in the SW102 cells lacking a functional *galK* protein. First, the sequence from 429th to 451st nt of the TK ORF (both KOS37 and V422 BACs) was replaced with a *galK* expression cassette, and the recombinants were selected on the medium containing galactose as the only carbon source. Second, the inserted *galK* cassette was then replaced with either one of the EGFP expression cassettes, yielding BAC clones of KOS/V422-HSV-GFP and V422-CMV-GFP (Figure 3.1.1).

Both steps of recombineering involve introducing linear DNA bearing 5' and 3' homology to the target BAC into cells, in which the lambda red recombination system has been induced. For all the EGFP viruses, the linear DNA fragment carrying the *galK* gene (termed TK-*galK*) was made by PCR using the primers (TK-*galK* primers) containing TK homology, in the first step of recombineering. The linear DNA involved in the second step of recombineering of V422-CMV-GFP BAC construction (termed TK-CMV-GFP) was also synthesized by PCR on the plasmid pTK-green [272]. The EGFP expression cassette on TK-CMV-GFP fragment is located between the 422nd and 423rd nt on the TK ORF. Thus, after recombineering, the EGFP gene driven by the HCMV IE promoter was inserted at the 442nd nt of the TK ORF of V422-CMV-GFP BAC (Figure 3.1.2).

The linear DNA (TK-HSV-GFP) containing the EGFP gene driven by the ICP22 promoter used in the second step of recombineering (negative selection for *galK*) was constructed by PCR from the plasmid pUC19-HSV-GFP. The primers used to generate the TK-pUC-GFP fragment have the same TK homology

sequence as the primers for TK-*galK*. At the 3' end, each of the TK-pUC-GFP primers has a sequence of 20 nts specific for the pUC19 residues that flank the EGFP cassette. As a result, after recombineering, the region between 430th and 450th nts of the TK ORF of the KOS/V422-HSV-GFP BACs is replaced with the EGFP cassette bearing 20 nts of pUC19 sequences at either end (Figure 3.1.3).

The BACs bearing the desired modifications were identified as described in section 3.1.1-3.1.2. Then, the BAC clones of EGFP viruses were transfected into U2OS cells to produce the corresponding infectious viruses. The V422-CMV-GFP virus was then passaged three times through Cre-Vero cells, in order to delete the BAC sequence in its genome. The Cre enzyme from Cre-Vero cells removed the BAC from the viral genome through the recombination with LoxP sites flanking at the either end of the BAC sequence. Since the BAC was originally inserted between U_L37 and U_L38 of the viral genome, after Cre-mediated excision of the BAC vector sequence, there is supposed to be only one LoxP site left at that location in V422-CMV-GFP genome. The KOS/V422-HSV-GFP viruses were not passaged in Cre-Vero cells, so their genome still carried the BAC sequence.

After generation of these EGFP recombinant viruses, I confirmed their structures by PCR screening, southern blot and western blot analysis. The results of each analysis are shown in the following sections (3.1.1-3.1.4).

Figure 3.1.1-Summary of BAC recombineering.

The acquisition of EGFP expression cassettes by KOS and V422 viruses was accomplished using BAC recombineering and a *galK* positive/counterselection cassette. A. In the first step, the *galK* gene was inserted into the TK ORF of the KOS37 (or V422) BAC by homologous DNA recombination. Recombinants were selected on medium containing galactose as the only carbon source, which requires galactokinase function. B. In the second step, the *galK* gene was replaced with the EGFP cassette using medium containing DOG to select against the *galK* gene. The *galK* gene, BAC sequence, and EGFP gene are indicated by a solid rectangle, a black circle and a five-point star, respectively.

A) Step 1: *galK* insertion

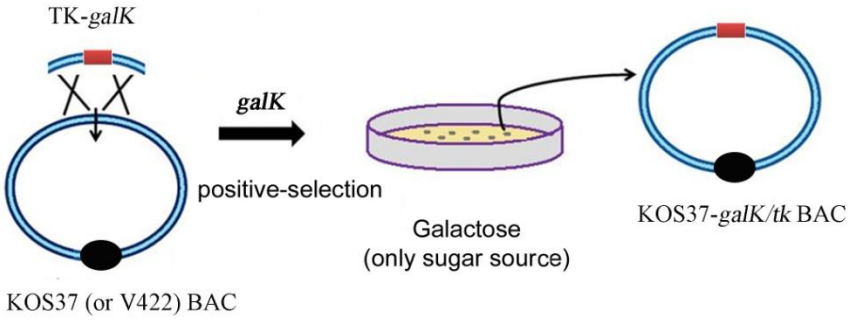

B) Step 2: *galK* replacement

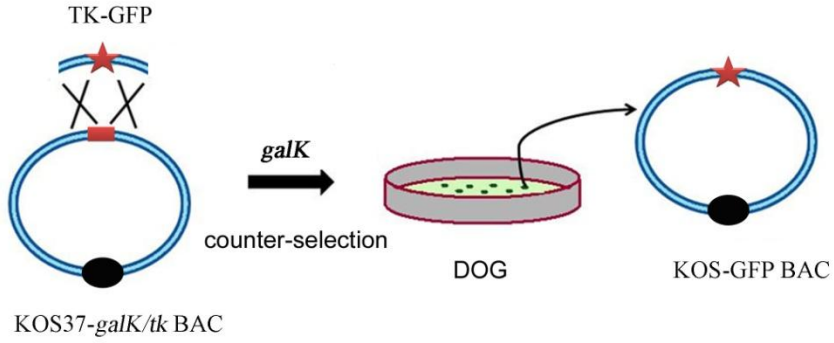

Figure 3.1.2-Construction of the V422-CMV-GFP virus

A) Construction of TK-*galK* DNA and the V422-*galK/tk* BAC. The TK-*galK* DNA was made by PCR using the indicated TK-*galK* primers and plasmid p*galK* as the template (shown in pink). The TK-*galK* primers have the *galK* sequences (pink arrows) at their 3' end and TK homology sequences (black lines) at the 5' end. In the first step of BAC recombineering, the *galK* gene was inserted into the TK locus of the V422 BAC. The TK gene is shown in blue, with the region homologous to the TK-galK fragment in black, and the region deleted from TK in yellow (429^{th}-451^{st} nt of the TK ORF).

B) Construction of the TK-CMV-GFP DNA fragment. The TK-CMV-GFP DNA fragment was constructed by PCR using the indicated TK-CMV-GFP primers (black arrows) and the plasmid pTK-green as the template. Driven by the HCMV IE promoter (shown in red), the EGFP ORF followed by a SV40 poly A signal (shown in green) is inserted at the SstI site of the TK ORF on the pTK-green plasmid. The region within TK-CMV-GFP DNA homologous to the TK gene is shown in black, with the region between the 429^{th}-451^{st} nt of TK ORF in yellow, the HCMV IE promoter in red, and the EGFP ORF followed by the SV40 poly A signal in green.

C) In the second step of recombineering, the *galK* gene (shown in pink) of the V422-*galK*/tk BAC was replaced with the EGFP cassette (red and green) to construct the V422-CMV-GFP BAC. The EGFP cassette was inserted at the SstI site (442^{nd} nt) inside the yellow region of the TK ORF. There was no sequence deletion from the TK ORF of the V422-CMV-GFP BAC. The final BAC clone of V422-CMV-GFP was then transfected into Cre-Vero cells to produce the infectious virus, shown in C.

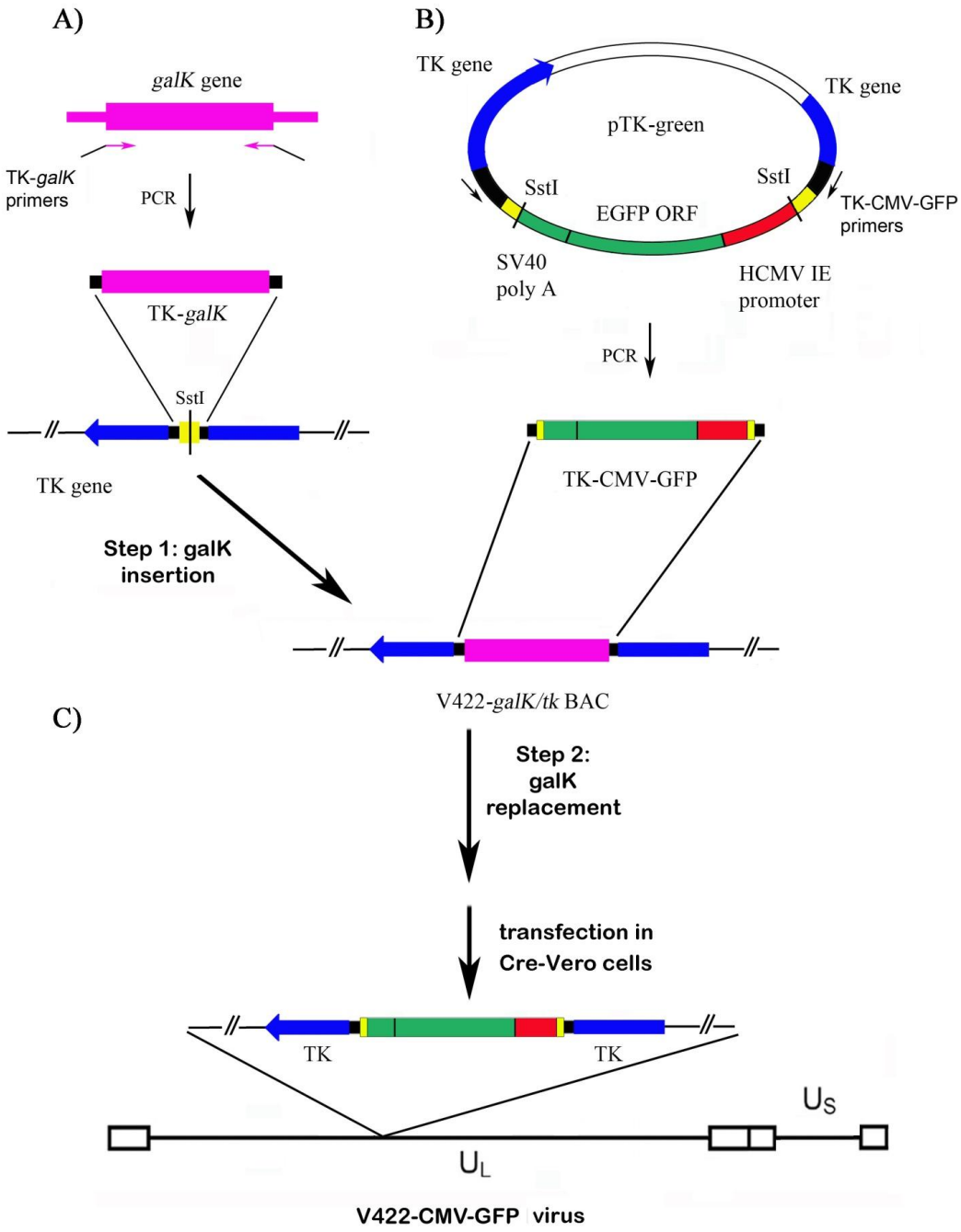
A)
galK gene
TK-galK primers
PCR
TK-galK
SstI
TK gene
Step 1: galK insertion
B)
TK gene
TK gene
pTK-green
SstI
SstI
EGFP ORF
TK-CMV-GFP primers
SV40 poly A
HCMV IE promoter
PCR
TK-CMV-GFP
V422-galK/tk BAC
C)
Step 2: galK replacement
transfection in Cre-Vero cells
TK
TK
US
UL
V422-CMV-GFP virus

Figure 3.1.3-Structural diagrams of DNAs used in construction of KOS/V422-HSV-GFP virues

A) Construction of TK-galK DNA and KOS37/V422-galK/tk BAC (the same procedure as Figure 3.1.3-A).

B) Construction of the TK-HSV-GFP DNA fragment. The TK-HSV-GFP DNA was made by PCR using the indicated TK-pUC-GFP primers (red arrows with black lines) and the plasmid pUC19-HSV-GFP as the template. The TK-pUC-GFP primers contain the sequence of pUC19 (red arrows) at the 3' ends and TK homology sequences (black lines, the identical TK sequences of the TK-galK primers in A) at the 5' ends. The TK-CMV-GFP DNA is shown with the region homologous to the TK-galK in black, the pUC19 sequences in red, the HSV IE promoter in yellow and the EGFP ORF followed by the BGH poly A signal in green.

C) In the second step of recombineering, the *galK* gene (pink) in KOS37/V422-*galK*/tk BAC was replaced with the EGFP cassette (red, yellow, and green) to construct the KOS/V422-HSV-GFP BAC. There is a TK sequence deletion (the yellow region of the TK gene in A) and a pU19 sequence insertion (40 nts in red) along with the EGFP cassette (shown in green) in the final KOS/V422-HSV-GFP BAC. The final BAC clones of KOS/V422-HSV-GFP were then transfected into U2OS cells to produce the infection virus, shown in C.

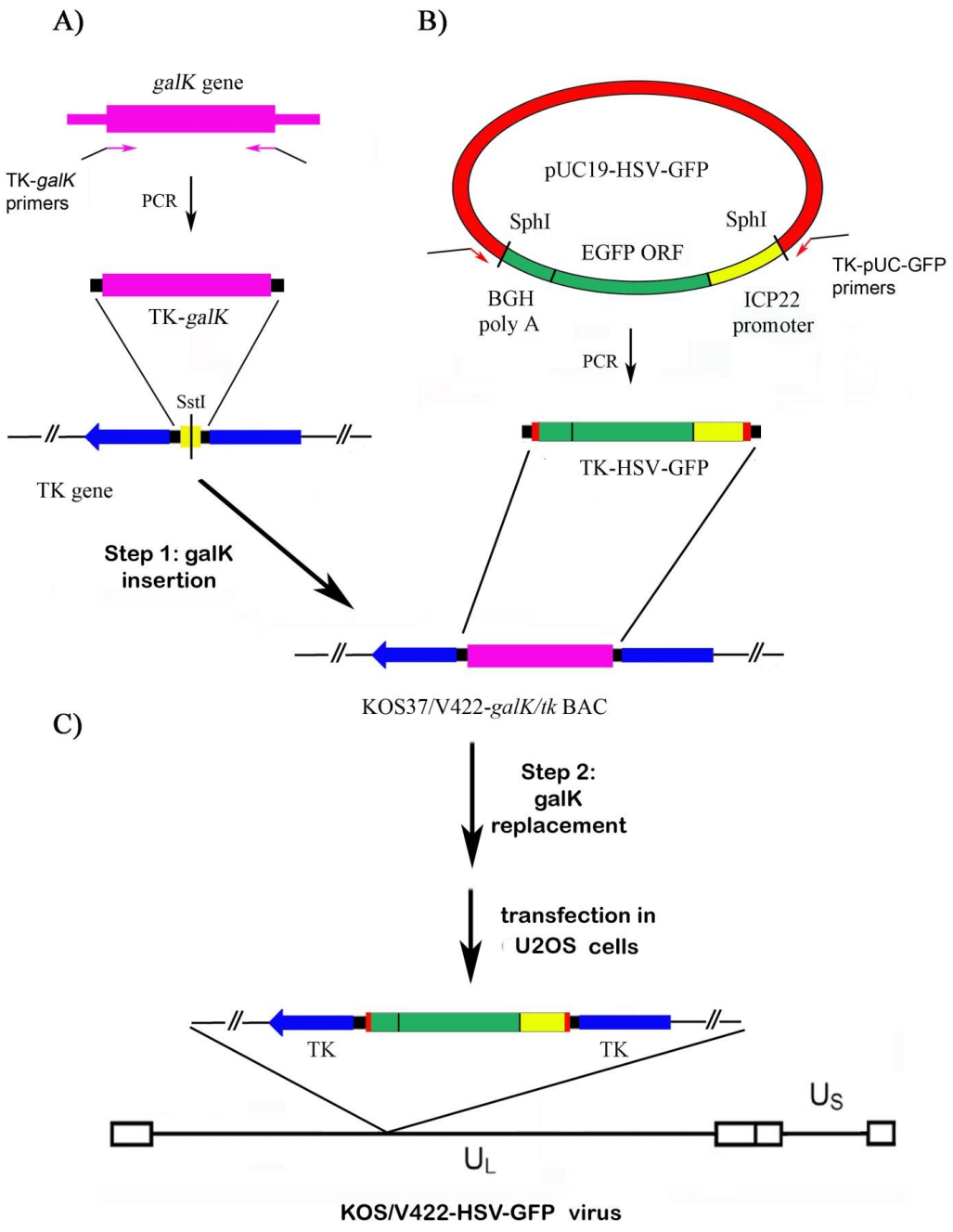
A)
B)
galK gene
TK-galK primers
PCR
TK-galK
SstI
TK gene
pUC19-HSV-GFP
SphI
SphI
EGFP ORF
TK-pUC-GFP primers
BGH poly A
ICP22 promoter
PCR
TK-HSV-GFP
Step 1: galK insertion
KOS37/V422-galK/tk BAC
C)
Step 2: galK replacement
transfection in U2OS cells
TK
TK
US
UL
KOS/V422-HSV-GFP virus

3.1.1 Identification of candidate BAC clones by PCR

DNA isolated from colonies grown on galactose plates in the first step of the BAC recombineering (Figure 3.1.1-A) was purified and screened for *galK* insertion by PCR (Figure 3.1.4). Primers 1 and 2 (Table 1) were used to amplify the targeted region of the TK gene. The predicted sizes of the PCR products arising from the wild-type and mutant TK genes are 547 bp and 1.8 kb respectively (Figure 3.1.4-A). As expected, all of the screened samples (lane 2-12 in B.) originating from the V422 BAC were shown to have the *galK*-insertion at the TK locus, evidenced by the 1.8 kb PCR product. Also, the PCR product from the parental KOS37 BAC (lane 1 in B) had the predicted size of 547 bp characteristic of the the wild-type TK gene. The four candidate colonies (lane 2-5 in C.) derived from KOS37 BACs were also confirmed to have the mutant TK by showing the predicted 1.8 kb bands. A *galK*-positive sample of the V422 (lane 3 in B.) and KOS37 BACs (lane 2 in C.) were selected and used in the second step of BAC recombineering, which involved the replacement of *galK* by EGFP cassette.

Candidate BACs isolated from the DOG-resistant colonies isolated in the second step of BAC recombineering (Figure 3.1.1-B) were screened for replacement of the *galK* gene with the EGFP expression cassettes at the TK locus by PCR (Figure 3.1.5). Primers 1 and 2 (Table 1) were used to determine if the EGFP gene driven by the CMV IE promoter at the TK locus was successfully inserted into the V422 BACs (Figure 3.1.5-A). This insertion produced a DNA fragment with an expected size of 2.2 kb. The PCR products from the four

candidate V422 BACs (lane 1-4 in B.) all had the predicted size of 2.2 kb, which confirmed the successful replacement of the EGFP gene driven by the HCMV IE promoter in these V422 BACs.

Primers 2 and 3 (Table 1) were used to detect whether the EGFP gene driven by the HSV IE (ICP22) promoter was inserted into the KOS37 and V422 BACs. The predicted size of this PCR product is 1.5 kb. Primer 3 binds to the N-terminal part of the EGFP ORF, so primers 2 and 3 only amplify templates containing the EGFP gene at the TK locus (Figure 3.1.5-A). Two out of the five candidate KOS37 BACs (lane 1 and 5 in C.) and two out of the four candidate V422 BACs (lane 6 and 9 in C) were shown to have the HSV-IE promoter driving the EGFP cassette, in that PCR produced amplimers with the predicted size of 1.5 kb. The negative ones (lane 2, 3, 4, 7, and 8 in C) might still have the *galK* gene at the TK locus, but these genes may contain mutations and produce defective *galK* proteins. Plasmid pTK-green was used as the positive DNA template for EGFP insertion in these PCR reactions. In this way, the KOS37 and V422 BACs bearing the desired EGFP cassettes were identified. A representative EGFP-positive BAC (lane 2 in B., lane 1 and 6 in C.) was then selected and used to make infectious V422-CMV-GFP, KOS-HSV-GFP and V422-HSV-GFP viruses.

The VP16 mutation in the candidate V422-CMV-GFP BAC (same samples as lane 1-4 in Figure 3.1.5-B.) was also verified by PCR followed by NheI digestion (Figure 3.1.6). Primers 4 and 5 (Table 1) were used in the PCR reaction. PCR products of BACs bearing the wild-type or mutant VP16 could not be differentiated by mere visualization on gel electrophoresis, since the wild-type

and mutant VP16 gene only have a difference of 12 nts in size. In addition, the V422 mutant bears a novel NheI site, this enzyme can be used to identify the mutation. In theory, after NheI digestion, the PCR product derived from the wild-type VP16 gene should generate a single band of 700 bp, while that derived from the mutant VP16 gene should produce two bands with a size of 520 and 180 bp (Figure 3.1.6-A). The parental V422 and KOS37 BACs were used as the controls of the mutant and wild-type VP16 genes. All the EGFP-positive V422 BACs (lane 1-4 in B.) produced two bands with the predicted sizes of 520 and 180 bp, which co-migrated with those arising from the parental V422 BAC. In contrast, the KOS37 BAC generated a single band of around 700 bp, which indicated the wild-type VP16 gene (lane 6 in B.). Therefore, this PCR experiment confirmed the VP16 mutation in the V422-CMV-GFP BAC.

Figure 3.1.4-PCR screen for *galK* insertion into the TK locus of the KOS37 and V422 BACs.

Candidate BACs derived from the KOS37 and V422 BACs were screened by PCR for the insertion of the *galK* gene at the TK locus. A. DNA structure of the TK locus from *galK*-positive derivatives is compared to that of the native TK locus. TK and *galK* sequences are labelled on the diagram. B. Identification of *galK*-positive V422 BACs. BACs from candidate colonies (lane 2-12) were analyzed by PCR using primer 1 and 2. KOS37 BAC was used as a control. (lane 1) C. Identification of KOS37 BACs containing the *galK* gene. PCR with the same primers as B. were used to select for *galK*+ derivatives from candidate colonies (Lane 2-5). Lane L is the DNA ladder (Fermentas).

A)

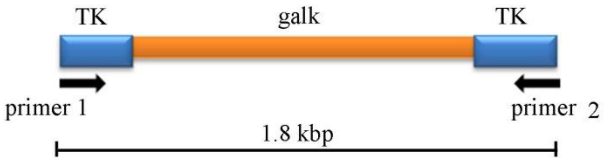
TK
galk
TK
primer 1
primer 2
1.8 kbp

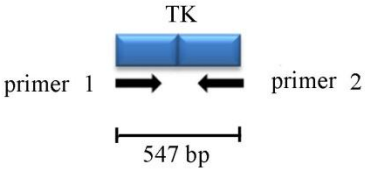
TK
primer 1
primer 2
547 bp

B)

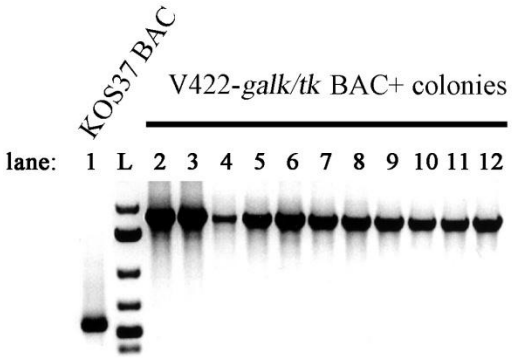
KOS37 BAC
V422-galk/tk BAC+ colonies
lane: 1 L 2 3 4 5 6 7 8 9 10 11 12

C)

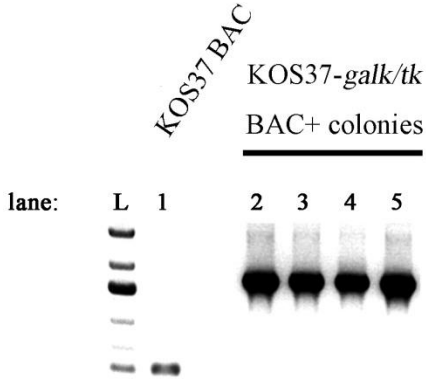
KOS37 BAC
KOS37-galk/tk
BAC+ colonies
lane: L 1 2 3 4 5

Figure 3.1.5-PCR screen for EGFP insertions into the TK locus of the KOS37 and V422 BACs.

Candidate BACs derived from KOS37-*galK*/*tk* (lane-3 in Figure 3.1.3-C) and V422-*galK*/*tk* (lane-3 in Figure 3.1.3-B) were screened for acquisition of the desired EGFP cassette at the TK locus by PCR.

A). The structure of the TK locus of the EGFP-positive BACs is compared to that of the parental *galK*-positive derivatives. TK, *galK*, and EGFP sequences are labelled in the diagram.

B). Identification of V422 derivatives containing the CMV-GFP expression cassette. Candidate BACs from four *galK*-negative colonies were analyzed by PCR using primers 1 and 2. (lane 1-4) The parental V422-*galK*/*tk* BAC was used as a control. (lane 5) The BAC DNA labelled as lane-2 was used to make the V422-CMV-GFP virus.

C). Identification of KOS and V422 derivatives bearing the HSV-GFP cassette. Candidate BACs (lane 1-5, KOS derivatives; lane 6-9, V422 derivatives) from individual *galK*-negative colonies were analyzed by PCR with primers 2 and 3. PCR amplimers from pTK-green were used as a positive control. The BAC DNAs labelled as lane-1 and lane-6 were used to make the KOS-HSV-GFP and V422-HSV-GFP viruses.

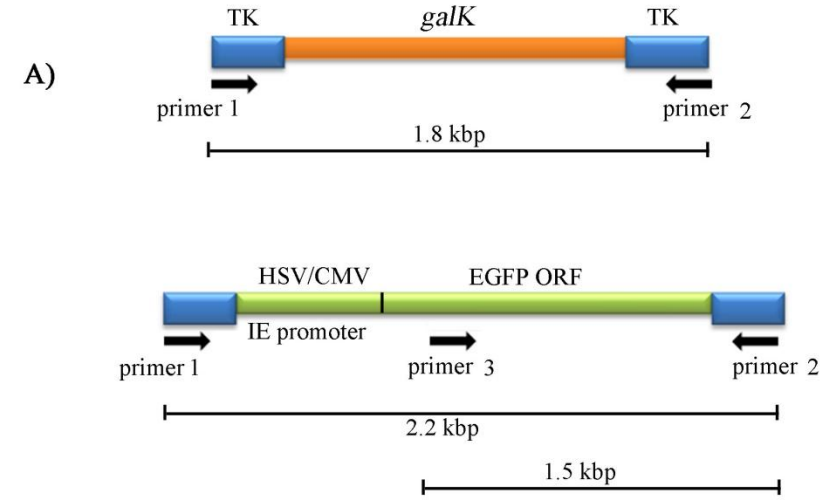
A)
TK
galK
TK
primer 1
primer 2
1.8 kbp
HSV/CMV
EGFP ORF
IE promoter
primer 1
primer 3
primer 2
2.2 kbp
1.5 kbp

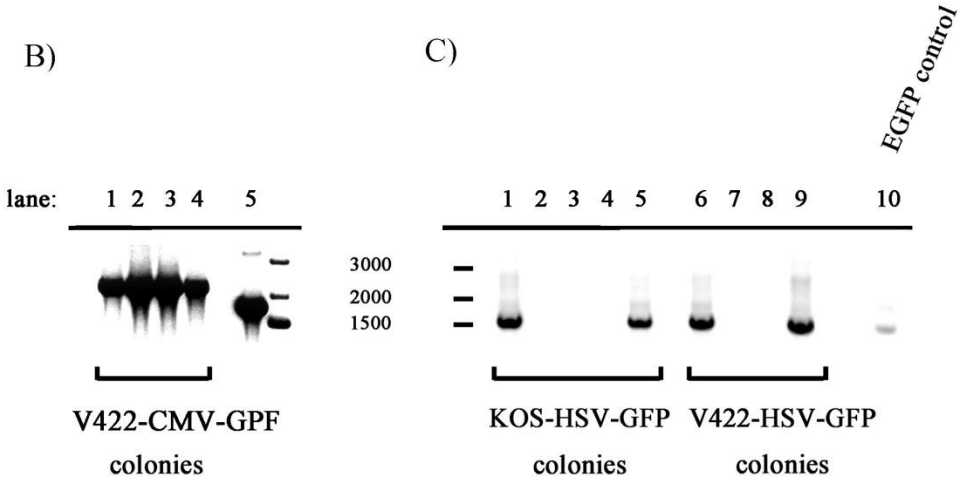
B)
C)
EGFP control
lane: 1 2 3 4 5
1 2 3 4 5 6 7 8 9 10
3000
2000
1500
V422-CMV-GPF
colonies
KOS-HSV-GFP
colonies
V422-HSV-GFP
colonies

Figure 3.1.6-Identification of VP16 mutations in V422-CMV-BACs by PCR.

The VP16 mutation of V422 derivatives bearing an EGFP cassette at the TK locus (the same BACs as lane 1-4 in Figure 3.1.4-B) was verified by PCR using primers 4 and 5, followed by NheI digestion of the PCR products. A. DNA structures of the wild-type and mutant VP16 genes. Construction of the V422 mutation resulted in a novel NheI site, which is not present in the PCR product from wild-type VP16 gene. B. Identification of the VP16 mutation in EGFP-positive V422 BACs (lane 1-4). V422 (lane 5) and KOS37 BAC (lane 6) were used as the positive and negative controls.

A)

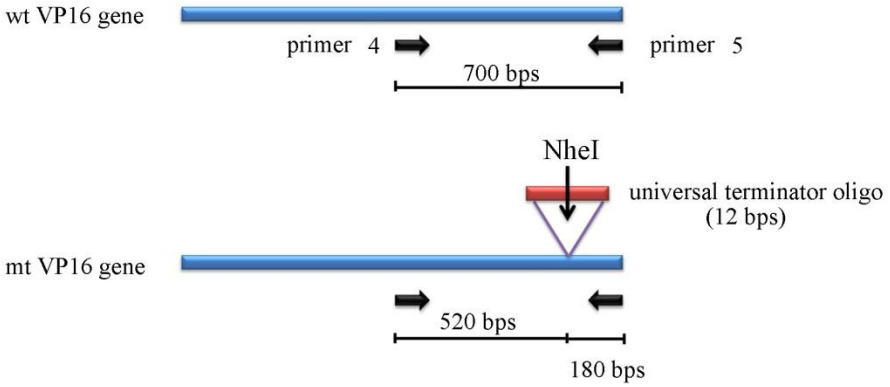
wt VP16 gene
primer 4
primer 5
700 bps
NheI
universal terminator oligo
(12 bps)
mt VP16 gene
520 bps
180 bps

B)

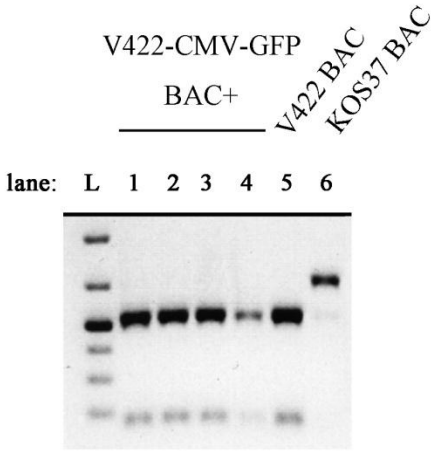
V422-CMV-GFP
BAC+
V422 BAC
KOS37 BAC
lane: L 1 2 3 4 5 6

3.1.2 Southern blot analysis of candidate recombinant BACs

The insertion of the EGFP cassettes into KOS37 or V422 BACs was further verified by Southern blot analysis (Figure 3.1.7). BAC DNAs (lane 2 in Figure 3.1.5-B., lane 1 and 6 in Figure 3.1.5-C.) were purified from SW102 cells using the Large-Construct kit (Qiagen), and digested with NheI and BamHI. Each sample was then electrophoresed through 1% agarose gels, tranferred to nylon membranes, and hybridized with the ^{32}P-labelled probes for EGFP and VP16. (as described in Chapter 2).

The EGFP probe was made by excising the entire EGFP ORF from the pEGFP-C1 plasmid. The EGFP cassette driven by the HCMV promoter was originally excised from the pEGFP-C1 plasmid with the SstI enzyme, and then inserted into the TK ORF at the SstI site of the pTK173 plasmid to construct the pTK-green plasmid [272]. The KOS- (or V422)-HSV-GFP BACs contain two BamHI sites around the inserted EGFP ORF: one located between the ICP22 promoter and the EGFP ORF, and one 2.3 kb downstream of the EGFP-insert region. There is no NheI site between these two BamHI sites. A double digestion with BamHI/NheI on KOS- (or V422)-HSV-GFP should produce a 3.3 kb band, which hybridizes to the EGFP probe. In the case of the V422-CMV-GFP BAC, a NheI site and a BamHI site flank either end of the EGFP ORF. Thus, digestion with BamHI/NheI should produce an 800 bp band which hybridizes to the EGFP probe (Figure 3.1.7-A). The results shown in Figure 3.1.7-B indicate the bands with the predicted sizes derived from the corresponding BACs. Also, the insertion of the EGFP cassette into the recombinant viruses was verified by Southern blot

analysis, and the same results as from their parental BACs were shown in figure 3.1.7-C. Thus, the insertion of the EGFP gene driven by the CMV or HSV IE promoter in KOS or V422 BACs was confirmed by Southern blot analysis.

The VP16 mutation in the V422-HSV-GFP and V422-CMV-GFP BACs was verified by Southern blot analysis using a VP16 probe (Figure 3.1.8). The probe DNA was synthesized by PCR amplification of the KOS DNA with primers 4 and 5. After a double digestion with BamHI/NheI, the KOS derived BACs should produce a single band of 8.1 kb, since there is no NheI site between the two BamHI sites (Figure 3.1.8-A). The result of the Southern blot analysis (Figure 3.1.8-B) shows that, as predicted, KOS-HSV-GFP and parental KOS37 BACs have an approximately 8.1 kb band indicating a wild-type VP16 gene. In contrast, the mutant VP16 gene of V422 bears a NheI site within the 12 bp linker located between the two BamHI sites. Therefore, a BamHI/NheI double digestion should produce two bands with sizes of 4.9 and 3.2 kb from the V422 derived BACs (Figure 3.1.8-A). As a result, the V422-HSV-GFP and parental V422 BACs have two bands with sizes of 4.9 and 3.2 kb (Figure 3.1.8-B), indicating the mutated VP16 gene bearing the NheI site, as does the V422-CMV-GFP BAC (Figure 3.1.8-C). The the identity of the VP16 gene of the recombinant viruses was also confirmed by Southern blot analysis, and the same results as from their parental BACs were shown in Figure 3.1.8-D.

The above results confirmed the successful insertion of the EGFP cassette driven by either HSV or HCMV IE promoter into the TK locus of the corresponding V422 and KOS37 derived recombinant viruses. The VP16

mutation of V422-derived viruses was also verified by Southern blot analysis with expected band motilities on gel electrophoresis.

Figure 3.1.7-Confirmation of the identity of EGFP insertions in the TK locus of the KOS37 and V422 BACs.

Acquisition of the EGPF expression cassette was verified using Southern blotting on the EGFP-positive BAC DNAs selected for making the viruses (lane-2 in Figure 3.1.5-B, and lane-1&6 in Figure 3.1.5-C). The BAC DNAs were digested with BamHI/NheI, followed by hybridization with a ^{32}P-labelled EGFP probe.

A). The location of restriction enzyme sites (BamHI/NheI) in the EGFP-inserted TK locus of KOS/V422-HSV-GFP BAC is compared to that of KOS/V422-CMV-GFP BAC. The EGFP probe is indicated by the thick black bar.

B). The result of Southern blot analysis shows that the KOS- and V422-HSV-GFP BACs have the expected product of about 3 kb, whereas V422-CMV-GFP BAC has a band with the predicted size of 800 bp.

C). The results of Southern blot analysis of the corresponding viruses from B).

A)

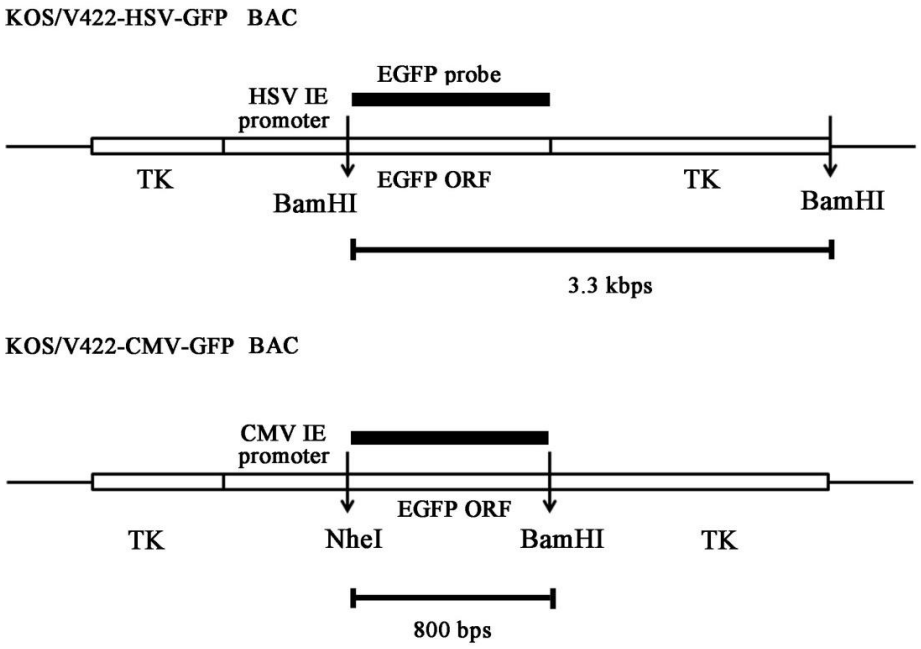
KOS/V422-HSV-GFP BAC
EGFP probe
HSV IE promoter
TK
BamHI
EGFP ORF
TK
BamHI
3.3 kbps
KOS/V422-CMV-GFP BAC
CMV IE promoter
EGFP ORF
TK
NheI
BamHI
TK
800 bps

B)

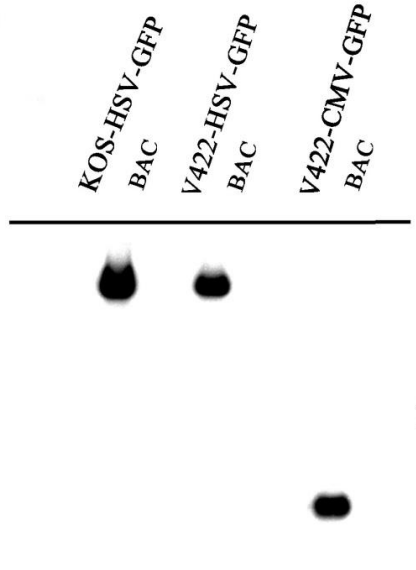
KOS-HSV-GFP BAC
V422-HSV-GFP BAC
V422-CMV-GFP BAC

C)

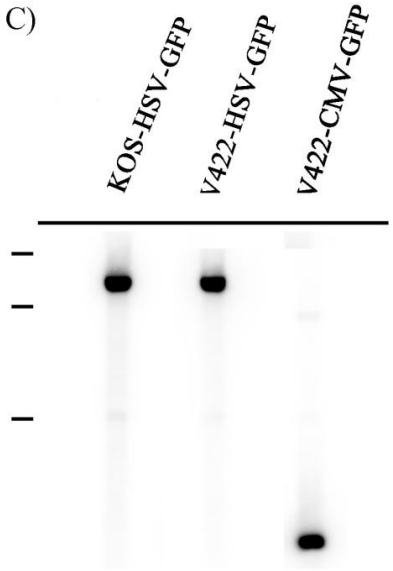
KOS-HSV-GFP
V422-HSV-GFP
V422-CMV-GFP
4 kb
3
1.5

Figure 3.1.8-Confirmation of the identity of the VP16 genes in the EGFP-positive V422 and KOS37 BACs.

A). DNA structure of the mutant VP16 gene (mut VP16) from V422 derivatives is compared with that of the native VP16 gene (wt VP16) of KOS37 derivatives. BAC DNA was digested with BamHI/NheI, followed by hybridization with a ^{32}P-labelled VP16-specific probe. The location of the VP16 probe hybridized to the VP16 gene is indicated by the thick black bar. Due to the presence of an NheI site in the mut VP16 gene, the VP16 probe was predicted to hybridize to two bands of DNA fromV422 derivatives, but one band from KOS37 derivatives, which do not contain the NheI site.

B). Southern blot analysis of the VP16 genes of V422-HSV-GFP and KOS-HSV-GFP BACs. The parental KOS37 and V422 BACs were used as controls.

C). Southern blot analysis of the mutant VP16 gene of V422-CMV-GFP BAC. The V422- and KOS-HSV-GFP BACs from B were used as the positive and negative control. The V422-, KOS-HSV-GFP and V422-CMV-GFP BACs were the same samples shown in Figure 3.1.7-B.

D). Southern blot analysis of the VP16 gene of KOS-, V422-HSV-GFP and V422-CMV-GFP viruses. The indicated viruses from D (the same viruses as in Figure 3.1.7-C) were originally produced from the BAC DNAs on C.

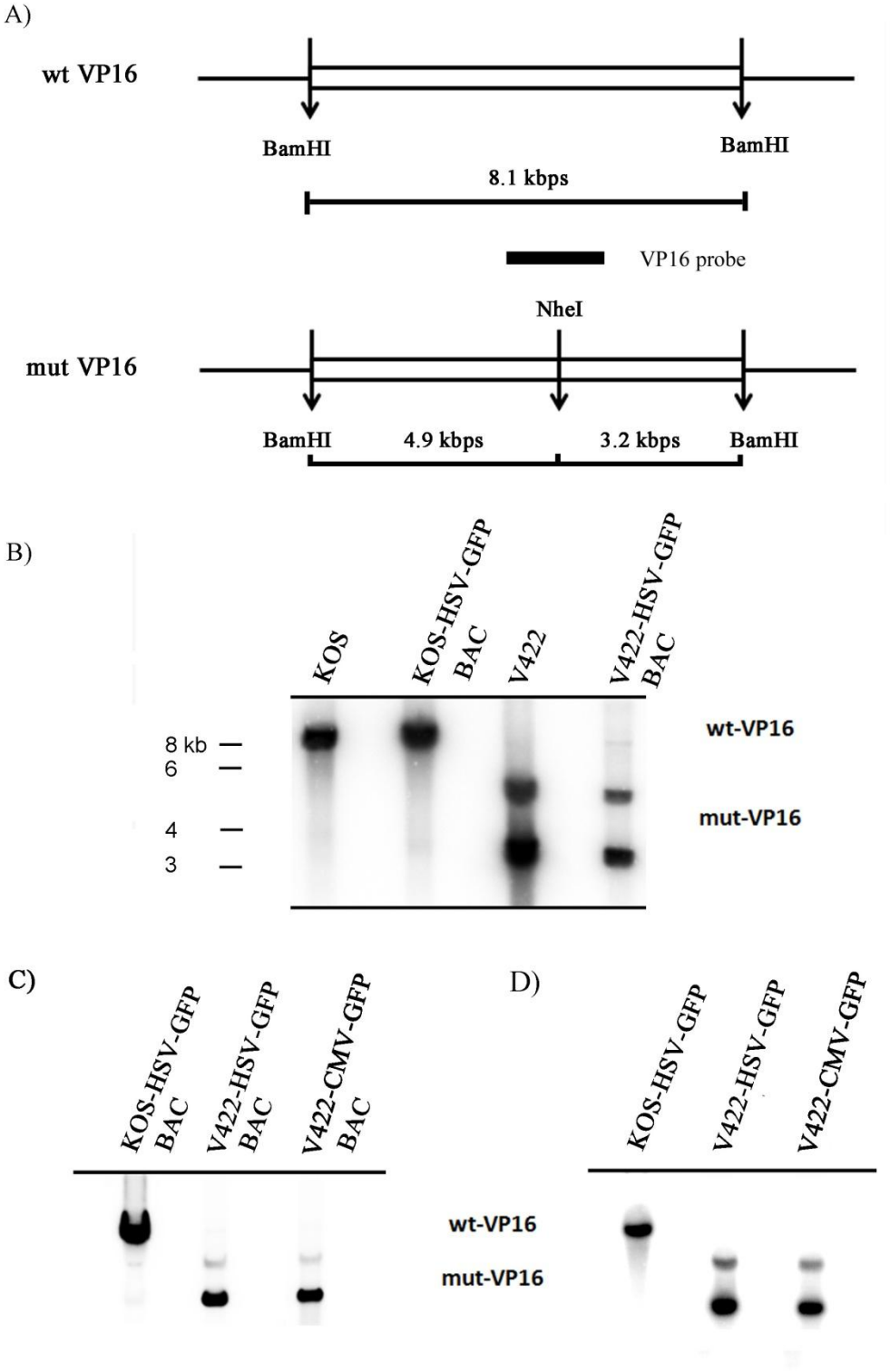
A)
wt VP16
BamHI
BamHI
8.1 kbps
VP16 probe
NheI
mut VP16
BamHI
4.9 kbps
3.2 kbps
BamHI
B)
KOS
KOS-HSV-GFP BAC
V422
V422-HSV-GFP BAC
8 kb
6
4
3
wt-VP16
mut-VP16
C)
KOS-HSV-GFP BAC
V422-HSV-GFP BAC
V422-CMV-GFP BAC
wt-VP16
mut-VP16
D)
KOS-HSV-GFP
V422-HSV-GFP
V422-CMV-GFP

3.1.3 Western blot analysis of recombinant viruses

We tested whether these recombinant viruses expressed EGFP and the intended form of VP16 (wild-type or mutant V422) by western blot analysis. Confluent monolayers of U2OS cells were infected with each recombinant HSV-1 virus at an MOI of 5, and incubated for 16 hours. The KOS and V422 parental viruses were used as positive controls for VP16 expression and negative controls for EGFP production. HMBA was supplied to the infections with the V422-derived viruses bearing the EGFP gene, in order to facilitate the mutant infections [249]. Extracts of infected cells were separated through a SDS-PAGE gel, transferred to a nylon membrane and assayed for VP16 and EGFP using anti-VP16 and anti-EGFP antibodies.

The V422 mutation of the VP16 gene was constructed via insertion of a chain terminating oligonucleotide (12 bp linker) in the VP16 ORF, leading to a truncated VP16 upon translation [242]. The results of the Western analysis with the KOS/V422-CMV-GFP viruses show that the KOS derivatives produce a wild type 65kDa VP16 protein, while the V422 derivatives express a truncated VP16 derivative with an apparent size of 47kDa (Figure 3.1.9-A). VP16 proteins of the appropriate size were also seen from the control infections with parental KOS and V422. In contrast, the EGFP protein (approximately 30 kDa) could only be detected from the recombinant viral infections, but not from the KOS or V422 infections (Figure 3.1.9-A). Figure 3.1.9-A also shows the results obtained with samples prepared from cells infected at a MOI of 1. The VP16 and EGFP proteins

were detected from V422- and KOS-HSV-GFP infections (Figure 3.1.9-B), which show similar results as V422- and KOS-CMV-GFP infections.

According to the sequencing data (Appendix, Figure A-1), the EGFP gene driven by the CMV promoter (in pEGFP-C1) contains 78 extra bps (equal to 26 additional amino acids) at the C-terminus compared to the EGFP gene driven by the ICP22 promoter (in pUC19-HSV-GFP). Therefore, the size difference between the two EGFP genes can be used to distinguish the recombinant viruses bearing the EGFP gene driven by the CMV or HSV IE promoter. As shown in Figure 3.1.9-C, EGFP from KOS- and V422-HSV-GFP infections has the same size as the one produced from pUC19-HSV-GFP transfection. As predicted, the HSV-GFP was smaller than the EGFP from KOS- (or V422-)-CMV-GFP infections, which ran at the same level on the blot as did EGFP from a pEGFP-C1 transfection (Figure 3.1.9-C). The slight difference in amino acid sequence did not affect EGFP fluorescence during infection, as evidenced by fluorescence microscopy (Figure 3.2.1).

In summary, the identities of the EGFP and VP16 genes of each recombinant virus were verified by Western blot analysis.

Figure 3.1.9- Analysis of VP16 and EGFP expression by the recombinant viruses.

Western blot analysis.

A). Identification of the VP16 gene and acquisition of the EGFP gene of KOS- and V422-CMV-GFP viruses. HeLa cells were infected with KOS, KOS-CMV-GFP, V422 and V422-CMV-GFP at an MOI of 5 or 1, as indicated in the brackets following the name of the virus. KOS and V422 were used as controls. Infections using V422-derived viruses were supplemented with 3mM HMBA. VP16 and EGFP proteins are labelled to the right of the Figure, and the protein size ladder is shown on the left.

B). Identification of the VP16 and the EGFP proteins in KOS- and V422-HSV-GFP infected HeLa cells (MOI=5). HMBA (3mM) was added to the V422 infections.

C). Comparison of the sizes of EGFP proteins expressed from the EGFP gene driven by the HSV or CMV IE promoters. The size of the EGFP protein produced from V422- or KOS-HSV-GFP infections is compared to that produced from V422- or KOS-CMV-GFP infections. HMBA (3mM) was added to the V422 related infections. HeLa cells tranfected with pUC19-HSV-GFP and pEGFP-C1 were used as the positive controls. Actin was included as a loading control.

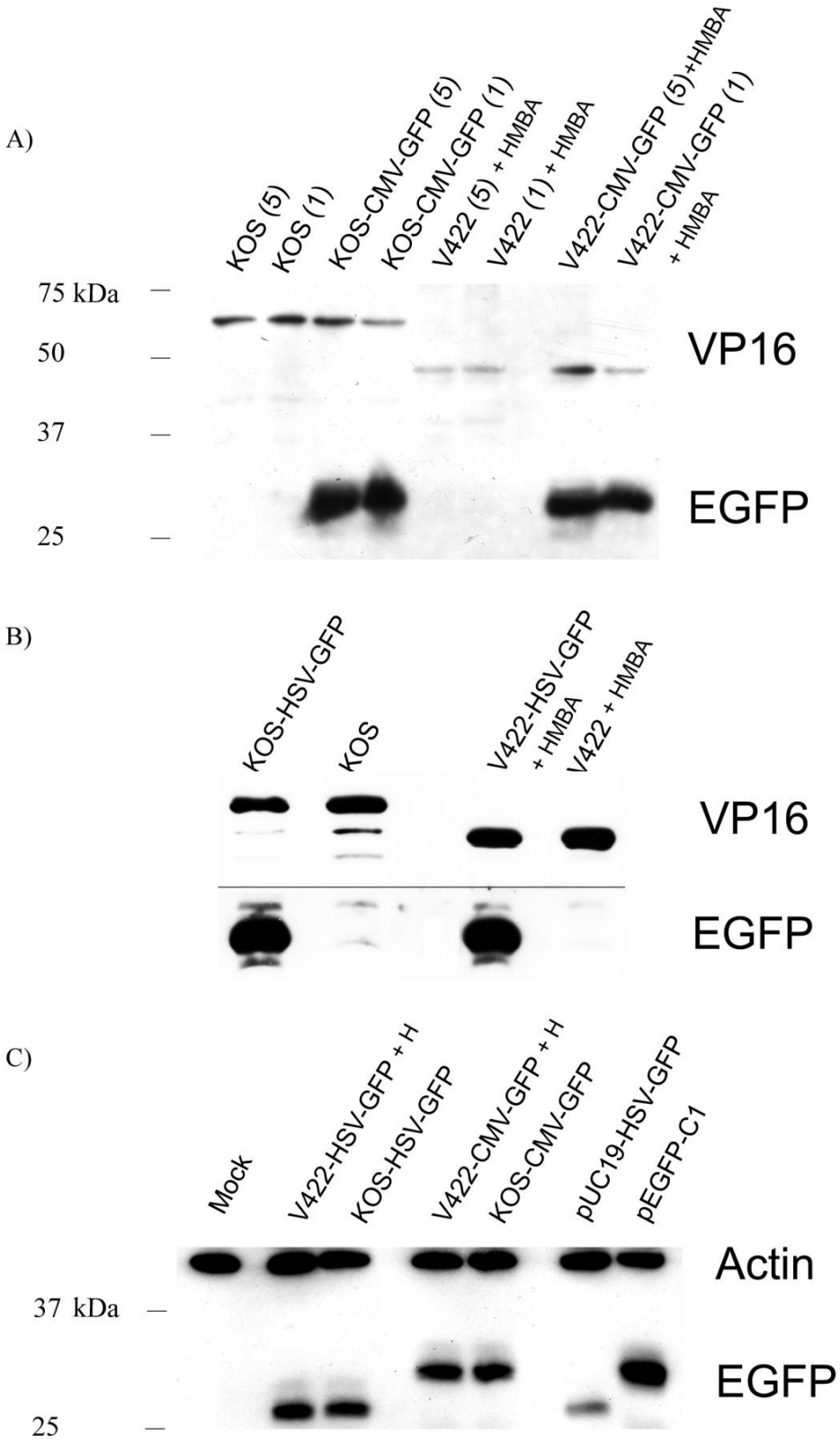
A)
KOS (5)
KOS (1)
KOS-CMV-GFP (5)
KOS-CMV-GFP (1)
V422 (5) + HMBA
V422 (1) + HMBA
V422-CMV-GFP (5)+HMBA
V422-CMV-GFP (1) + HMBA
75 kDa
50
37
25
VP16
EGFP
B)
KOS-HSV-GFP
KOS
V422-HSV-GFP + HMBA
V422 + HMBA
VP16
EGFP
C)
Mock
V422-HSV-GFP + H
KOS-HSV-GFP
V422-CMV-GFP + H
KOS-CMV-GFP
pUC19-HSV-GFP
pEGFP-C1
Actin
37 kDa
25
EGFP

3.1.4 Sequence analysis:

In order to determine if the promoters (HSV, HCMV) driving the EGFP gene in the recombinant HSV-1 strains had the same DNA sequences as the ones carried by the original plasmids used to construct the viruses (pUC19-HSV-GFP, pEGFP-C1), total DNA containing viral genomic DNA was isolated from infected cells as described in Chapter 2. The entire EGFP expression cassette was amplified by PCR of the genomic DNA of each virus with primers 1 and 2 (Figure 3.1.5-A). The 2.2 kb amplimers from KOS- and V422-CMV-GFP viruses were then sequenced with the primer 6, which binds to the N-terminal region of the EGFP ORF (Figure 3.1.10-A). Figure 3.1.11 shows the sequences obtained for the entire HCMV-IE promoter of V422- and KOS-CMV-GFP viruses compared with that of the plasmid pEGFP-C1. The sequence is shown in the orientation of primer 6, which is the opposite direction of EGFP transcription. The NheI site (separating the EGFP gene and the HCMV IE promoter) and the upstream TK sequence are labeled at the ends of the sequences. The results demonstrate that the sequences of HCMV-IE promoters from the viral genome are identical to that of the plasmid pEGFP-C1 (Figure3.1.11).

Due to the high GC content of the HSV-IE (ICP22) promoter, sequencing with primer 6 alone from V422- and KOS-HSV-GFP viral DNAs could only obtain part of the promoter sequences. Therefore, the sequences of the HSV-IE promoter were also obtained by using primer 7, which binds to the TK sequence upstream of the ICP22 promoter (Figure 3.1.10-B). Sequencing with primer 7 from the other end of the promoter would help to identify the rest of the ICP22

promoter sequence. As a control, the HSV-IE promoter from the parental vector pUC19-HSV-GFP was also sequenced using a commercial primer M13-F and the primer 6 (Figure 3.1.10-C). The sequence of the HSV-IE promoter (shown in Figure 3.1.12) is presented with a *BamHI* and *SphI* site at either end of the promoter. As in Figure 3.1.11, the sequence is also shown in the processing direction of the primer 6. Comparison between the KOS-HSV-GFP virus and the pUC19-HSV-GFP plasmid shows a 95.8% identity (ie. 21 bps). As shown in Figure 3.1.12, two mismatches are C-to-G and T-to-A changes, and the other 19 positions were due to unclear results from sequencing facility. The V422-HSV-GFP virus had a 98.8% identity to the pUC19-HSV-GFP plasmid, and all 6 positions were unclear nucleotides-"N". The blast result showed that the sequence of the ICP22 promoter in the pUC19-HSV-GFP plasmid was identical to that of the one from the strain 17 of HSV-1 as expected. The homologous DNA recombination between the external ICP22 promoter of the inserted EGFP cassette and the native ICP22 promoter of HSV-1 KOS strain may have caused the generation of the two base-changes in KOS-HSV-GFP viral genome.

In summary, the sequence results verified the identity of the desired EGFP and VP16 mutations in the corresponding recombinant viruses. In addition, the orientation of EGFP insertion in the TK gene of viral genomes was also determined by sequence analysis (Appendix, Figure A-2); results indicate that the mRNA of the EGFP gene from the recombinant viruses would be transcribed in the same direction as that of the TK gene, as shown in Figure 3.1.2 and 3.1.3.

Taken in combination, the above data obtained from the PCR screen, Southern and western analyses, and sequence analysis establish that the desired reporter viruses of HSV-1were successfully generated.

Figure 3.1.10-Summary of the primers used for sequencing the HCMV and HSV (ICP22) IE promoters of the EGFP expression cassettes in the EGPF-positive HSV-1 viruses.

A). Primer 6 was used to sequence the HCMV IE promoter from the KOS- and V422-CMV-GFP genomic DNAs in a reverse direction, which is indicated as a short arrow on the diagram.

B). Primers 7 and 6 were used to sequence the HSV IE promoter from the genomic DNAs of KOS- and V422-HSV-GFP viruses in directions indicated on the diagram. The EGFP cassette bearing the HSV IE promoter was placed at the same location of TK locus of KOS or V422 as A.

C). As a control, the HSV IE promoter in vector pUC19-HSV-GFP was also sequenced using primers M13-F and 6. The long thin arrows in each section indicate the sequence acquired by each primer.

A)

V422/KOS-CMV-GFP:

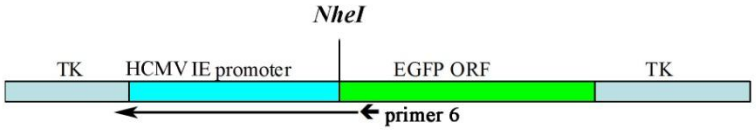

B)

V422/KOS-HSV-GFP:

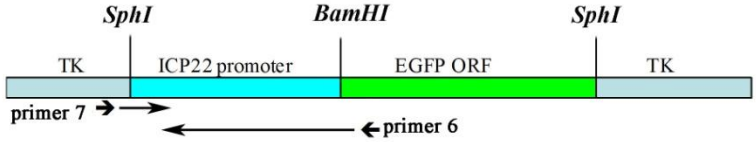

C)

pUC19-HSV-GFP:

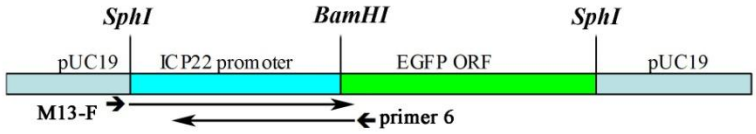

Figure 3.1.11- Confirmation of the authenticity of the HCMV-IE promoter in the V422- and KOS-CMV-GFP viruses.

The sequences of HCMV IE promoters acquired from V422- and KOS-CMV-GFP viruses were compared with that of the vector pEGFP-C1, which was used to construct the EGFP viruses. The sequence of pEGFP-C1 was obtained from the LabLife™ website-
https://www.lablife.org/g?a=seqa&id=vdb%5fg2%2ejhM75AFSGnfZ8WtEeOcS2bUKY8I%2d%5fsequence%5fcd4135a17d9390e26198566f44b6e4a08e381e57%5f10. The *NheI* site between the EGFP gene and HCMV promoter and the TK gene upstream of the promoter is labeled on the diagram. Stars indicate identical nucleotides between the three sequences.

HCMV IE promoter sequence comparison

```
pEGFP-C1          TAGTTATTAATAGTAATCAATTACGGGGTCATTAGTTCATAGCCCATATATGGAGTTCCG 60
KOS-CMV-GFP       GGCTGGGTAATAGTAATCAATTACGGGGTCATTAGTTCATAGCCCATATATGGAGTTCCG 60
V422-CMV-GFP      GGCTGGGTAATAGTAATCAATTACGGGGTCATTAGTTCATAGCCCATATATGGAGTTCCG 60
                     *  **************************************************

                  TK sequence
pEGFP-C1          CGTTACATAACTTACGGTAAATGGCCCGCCTGGCTGACCGCCCAACGACCCCCGCCCATT 120
KOS-CMV-GFP       CGTTACATAACTTACGGTAAATGGCCCGCCTGGCTGACCGCCCAACGACCCCCGCCCATT 120
V422-CMV-GFP      CGTTACATAACTTACGGTAAATGGCCCGCCTGGCTGACCGCCCAACGACCCCCGCCCATT 120
                  ************************************************************

pEGFP-C1          GACGTCAATAATGACGTATGTTCCCATAGTAACGCCAATAGGGACTTTCCATTGACGTCA 180
KOS-CMV-GFP       GACGTCAATAATGACGTATGTTCCCATAGTAACGCCAATAGGGACTTTCCATTGACGTCA 180
V422-CMV-GFP      GACGTCAATAATGACGTATGTTCCCATAGTAACGCCAATAGGGACTTTCCATTGACGTCA 180
                  ************************************************************

pEGFP-C1          ATGGGTGGAGTATTTACGGTAAACTGCCCACTTGGCAGTACATCAAGTGTATCATATGCC 240
KOS-CMV-GFP       ATGGGTGGAGTATTTACGGTAAACTGCCCACTTGGCAGTACATCAAGTGTATCATATGCC 240
V422-CMV-GFP      ATGGGTGGAGTATTTACGGTAAACTGCCCACTTGGCAGTACATCAAGTGTATCATATGCC 240
                  ************************************************************

pEGFP-C1          AAGTACGCCCCCTATTGACGTCAATGACGGTAAATGGCCCGCCTGGCATTATGCCCAGTA 300
KOS-CMV-GFP       AAGTACGCCCCCTATTGACGTCAATGACGGTAAATGGCCCGCCTGGCATTATGCCCAGTA 300
V422-CMV-GFP      AAGTACGCCCCCTATTGACGTCAATGACGGTAAATGGCCCGCCTGGCATTATGCCCAGTA 300
                  ************************************************************

pEGFP-C1          CATGACCTTATGGGACTTTCCTACTTGGCAGTACATCTACGTATTAGTCATCGCTATTAC 360
KOS-CMV-GFP       CATGACCTTATGGGACTTTCCTACTTGGCAGTACATCTACGTATTAGTCATCGCTATTAC 360
V422-CMV-GFP      CATGACCTTATGGGACTTTCCTACTTGGCAGTACATCTACGTATTAGTCATCGCTATTAC 360
                  ************************************************************

pEGFP-C1          CATGGTGATGCGGTTTTGGCAGTACATCAATGGGCGTGGATAGCGGTTTGACTCACGGGG 420
KOS-CMV-GFP       CATGGTGATGCGGTTTTGGCAGTACATCAATGGGCGTGGATAGCGGTTTGACTCACGGGG 420
V422-CMV-GFP      CATGGTGATGCGGTTTTGGCAGTACATCAATGGGCGTGGATAGCGGTTTGACTCACGGGG 420
                  ************************************************************

pEGFP-C1          ATTTCCAAGTCTCCACCCCATTGACGTCAATGGGAGTTTGTTTTGGCACCAAAATCAACG 480
KOS-CMV-GFP       ATTTCCAAGTCTCCACCCCATTGACGTCAATGGGAGTTTGTTTTGGCACCAAAATCAACG 480
V422-CMV-GFP      ATTTCCAAGTCTCCACCCCATTGACGTCAATGGGAGTTTGTTTTGGCACCAAAATCAACG 480
                  ************************************************************

pEGFP-C1          GGACTTTCCAAAATGTCGTAACAACTCCGCCCCATTGACGCAAATGGGCGGTAGGCGTGT 540
KOS-CMV-GFP       GGACTTTCCAAAATGTCGTAACAACTCCGCCCCATTGACGCAAATGGGCGGTAGGCGTGT 540
V422-CMV-GFP      GGACTTTCCAAAATGTCGTAACAACTCCGCCCCATTGACGCAAATGGGCGGTAGGCGTGT 540
                  ************************************************************

pEGFP-C1          ACGGTGGGAGGTCTATATAAGCAGAGCTGGTTTAGTGAACCGTCAGATCCGCTAGC 596
KOS-CMV-GFP       ACGGTGGGAGGTCTATATAAGCAGAGCTGGTTTAGTGAACCGTCAGATCCGCTAGC 596
V422-CMV-GFP      ACGGTGGGAGGTCTATATAAGCAGAGCTGGTTTAGTGAACCGTCAGATCCGCTAGC 596
                  ************************************************************ NheI
```

Figure 3.1.12- Sequence identification of the HSV-IE promoter borne in the EGPF gene of the V422- and KOS-HSV-GFP viruses.

The sequence of the HSV-IE (ICP22) promoter from parental vector pUC19-HSV-GFP was compared with the ones acquired from V422- and KOS-HSV-GFP viruses. The *SphI* and *BamHI* sites on the either end of the promoter are labeled on the diagram. The unique nucleotides of the sequences from V422- and KOS-HSV-GFP are bolded in the diagram, and the identical sequences of the three subjects are shown as stars.

ICP22 promoter sequence comparison

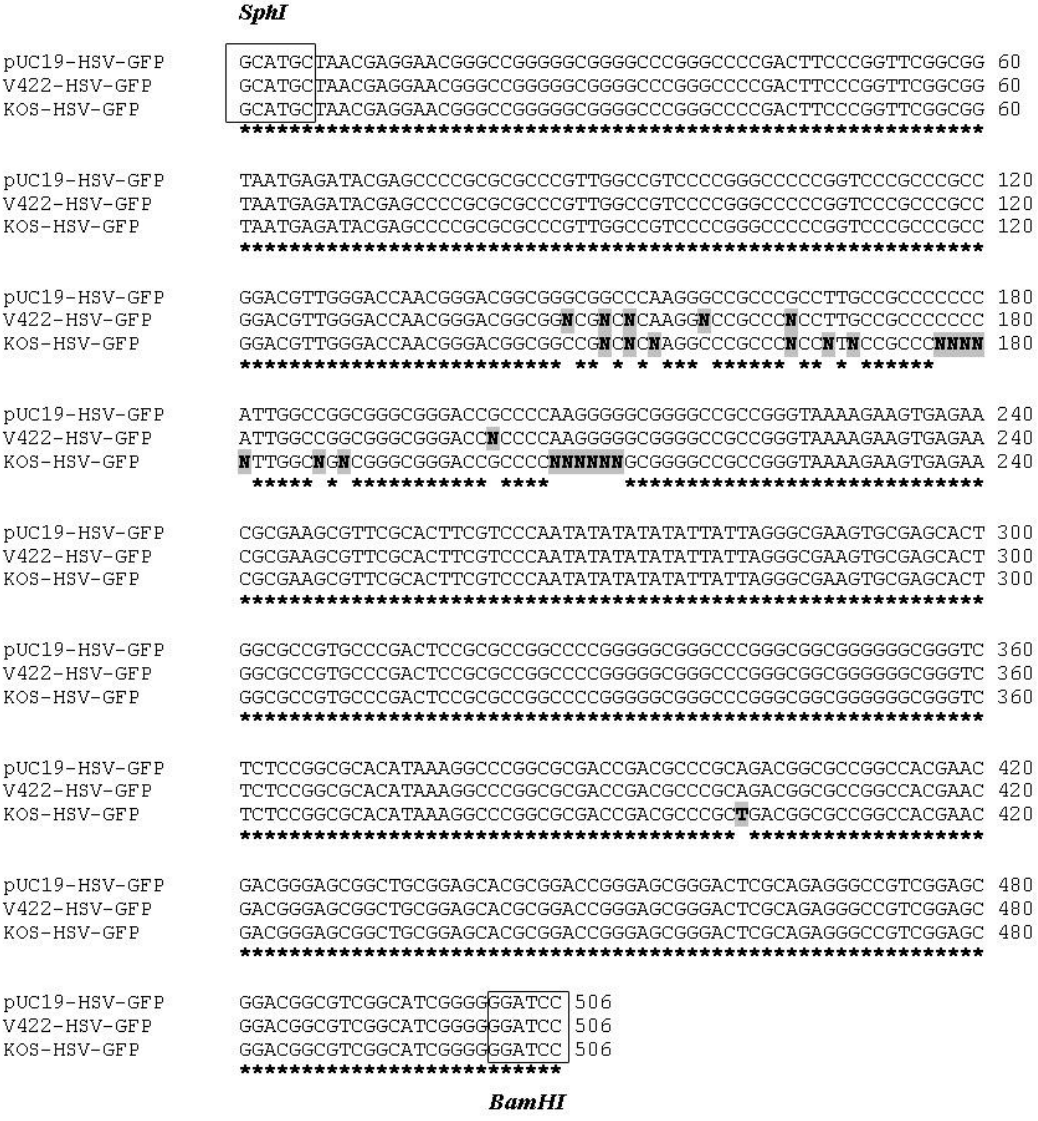

3.2 Detection of EGFP expression by plate reader and fluorescence microscopy:

The EGFP recombinant viruses were designed to be used in a screen with siRNAs against the human genome, in order to study the host-viral relationship. The EGFP fluorescence from these viruses would be quantified using an Envision plate reader (PerkinElmer) as an indication of viral activity. However, preliminary data obtained from both non-silencing siRNA or pure viral infection showed that the EGFP fluorescence from the KOS-(and V422-)-HSV-GFP infection could not be distinguished from background readings (non-infected HeLa cells or KOS infection). In the case of KOS-(or V422-)-CMV-GFP infection, EGFP fluorescence readout was three times higher (on average) than the background reading, but this difference could not be detected until 12 hpi.

In order to find out whether the recombinant viruses express EGFP, and when fluorescence could be detected, HeLa cells infected by each recombinant virus were examined using fluorescence microscopy. Monolayers of HeLa cells were infected with each virus at an MOI of 1, and the infections were halted at 4, 8 and 12 hpi, followed by washing with PBS. Expressed EGFP was detected in cells using fluorescence microscopy. KOS and V422 were used as the negative controls for detecting EGFP fluorescence. These results suggested that expression from the HSV ICP22 promoter was delayed and reduced relative to that driven from the HCMV IE promoter.

EGFP fluorescence could be detected from KOS-CMV-GFP infected cells and from cells infected with V422-CMV-GFP in the presence of HMBA as early

as 4 hpi. In contrast, EGFP regulated by the ICP22 promoter in KOS-HSV-GFP and HMBA-treated V422-HSV-GFP infections could not be detected until 12 hpi.

Figure 3.2.1 shows the EGFP expression from HeLa cells infected with recombinant viruses, detected at 12 hpi. In V422-HSV-GFP and V422-CMV-GFP infected cells HMBA treatment increased the green fluorescence, confirming the successful insertion of EGFP expression cassette into the recombinant genome of these viruses. The green cells shown in KOS-HSV-GFP and KOS-CMV-GFP infections also confirmed the successful construction of these recombinant viruses. However, it was surprising that only a minority of cells infected with KOS-HSV-GFP scored positive of EGFP, given the MOI used (1 pfu/cell).

Interestingly, the number of green cells and the signal intensity of each green cell were shown to be increased in V422- and KOS-CMV-GFP infections, compared to cells from the corresponding viruses expressing EGFP from the ICP22 promoter (KOS- and V422-HSV-GFP) (Figure 3.2.1-B & C). However, even at very high MOIs, not every cell infected by KOS-HSV-GFP showed green fluorescence. These observations lead us to further analyze the EGFP expression of the recombinant viruses.

Figure 3.2.1-Detection of the green fluorescent EGFP protein in HeLa cells infected by V422 and KOS derived viruses.

The expression of the EGFP gene of indicated V422 and KOS-derived viruses was observed using fluorescent microscopy on infected HeLa cells. (infections with an MOI of 1 and 12 hrs incubation). HeLa cells infected with KOS or V422 were used as negative controls.

A)

V422 + HMBA

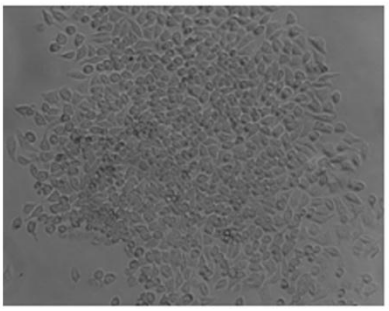

KOS

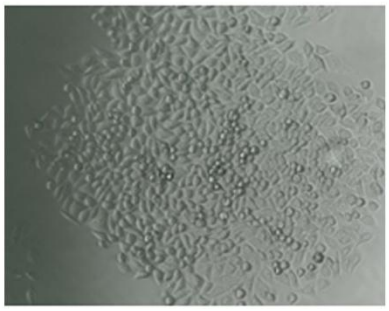

B)

V422-HSV-GFP

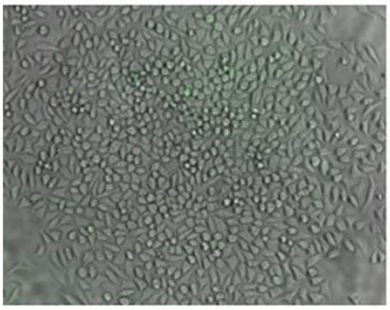

V422-HSV-GFP + HMBA

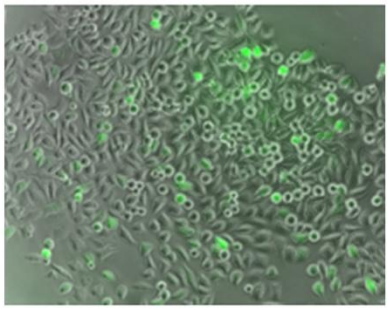

C)

V422-CMV-GFP

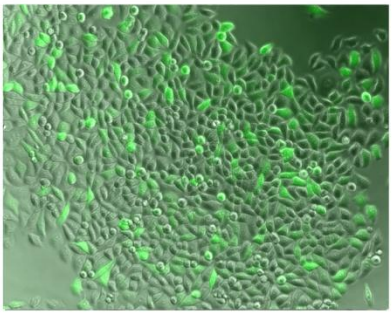

V422-CMV-GFP + HMBA

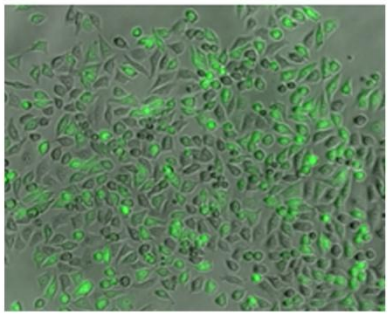

D)

KOS-HSV-GFP

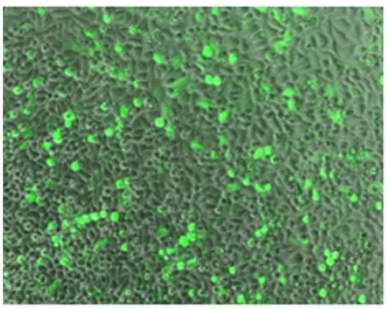

E)

KOS-CMV-GFP

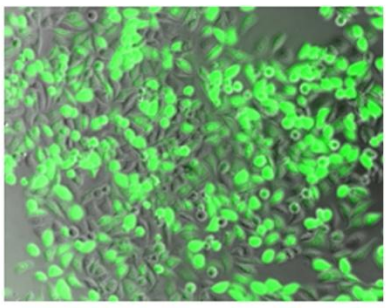

3.3 Characterizing EGFP expression from KOS-HSV/CMV-GFP viruses

The delay of EGFP expression from KOS-(or V422-)-HSV-GFP (compared with that from KOS-CMV-GFP in section 3.2), raised the possibility that the EGFP gene driven by the HSV-IE promoter was not expressed like a typical IE gene in infected HeLa cells. Therefore, the kinetics of accumulation of the viral-EGFP mRNA and protein were characterized and compared to those of HSV-1 IE genes.

3.3.1 The kinetics of EGFP production in infected HeLa cells

3.3.1.1 The kinetics of EGFP mRNA accumulation in infected HeLa cells

In order to determine if the delay of EGFP expression from KOS-HSV-GFP infected HeLa cells is occurring at the mRNA or protein level, mRNA from cells infected with KOS and KOS-derivatives bearing the EGFP gene was isolated and subjected to northern blot analysis.

First of all, RNA from HeLa cells transfected with parental plasmids pUC19-HSV-GFP or pEGFP-C1 was isolated and used as the control for marking the native EGFP mRNA transcribed from the HSV or HCMV IE promoters (Figure 3.3.1). The plasmid transfections in HeLa cells were incubated for 24 hrs, and viral infections (MOI of 5) with KOS-HSV/CMV-GFP in HeLa cells were carried for 6 hrs. The total RNA of each sample was then harvested, and subjected to northern blot analysis with a ^{32}P-labelled DNA probe for EGFP.

The expected 1.3 Kb mRNA labelled by the EGFP probe was the major product from both the pUC19-HSV-GFP and the pEGFP-C1 plasmid-transfected

cells (Figure 3.3.1-indicated by arrow). Although carried with the same conditions of transfection in HeLa cells, the plasmid pEGFP-C1 produced much more EGFP mRNA (1.3 Kb) than the pUC19-HSV-GFP plasmid. This result has also been confirmed by fluorescence microscopy with live HeLa cells transfected with these two plasmids. In addition, two RNAs with larger sizes were produced from the pEGFP-C1 plasmid. This may be due to the circular nature of the plasmid; i.e. RNA polymerase may read though the SV40 poly A signal of the EGFP ORF, and continuously transcribe the plasmid sequence until meeting this signal again. In the case of viral infection, cells infected with either KOS-HSV-GFP or KOS-CMV-GFP produced the expected 1.3 Kb mRNA as their major product. This EGFP mRNA was produced much more from KOS-CMV-GFP virus than the KOS-HSV-GFP one. This result is consistent with the observation of EGFP fluorescence shown in Figure 3.2.1-D&E. Furthermore, one larger RNA was detected from the KOS-HSV-GFP-infected cells. This mRNA is probably not transcribed from the ICP22 promoter, since its accumulation could be abolished by cycloheximide treatment, which is shown in the section 3.3.1.2 (Figure 3.3.4 and 3.3.6). There were also two RNAs with sizes larger than 1.3 Kb produced from KOS-CMV-GFP infected cells. As will be mentioned in section 3.3.1.2, cycloheximide treatment increased the production of the larger of the two minor RNA products, but reduced the production of the other. However, cycloheximide did not abolish the transcription of either RNAs produced from KOS-CMV-GFP (Figure 3.3.6). In summary, as expected, the EGFP mRNA with a size of 1.3 Kb was the major product of both viral infections with KOS-HSV-GFP and KOS-

CMV-GFP, and plasmid transfections with pUC19-HSV-GFP and pEGFP-C1 in HeLa cells (Figure 3.3.1).

Then, I performed a time-course experiment to ask whether the EGFP mRNAs from KOS-HSV-GFP and KOS-CMV-GFP accumulate as a typical IE mRNA of HSV-1. Total RNA was harvested from HeLa cells infected with KOS, KOS-HSV-GFP or KOS-CMV-GFP at an MOI of 5. Samples were harvested at 3, 6, 9, 12, and 15 hpi. PAA was used to block the viral DNA replication, and thus the transcription of true L genes. The samples treated with PAA were harvested at 15 hpi. RNA was resolved using denaturing agarose gel electrophoresis and then was probed with ^{32}P-labelled DNA probes for EGFP and ICP22 sequences (Figure 3.3.2 and 3.3.3).

In HeLa cells, the 1.3 Kb EGFP mRNA from KOS-HSV-GFP could be detected as early as 3 hpi. Moreover, this EGFP mRNA accumulated continuously from 3 to 15 hpi. RNA production was reduced by PAA treatment, shown as the last lane in B. However, PAA treatment did not eliminate the generation of this EGPF mRNA, indicating that the EGFP gene of KOS-HSV-GFP was detectably transcribed before viral DNA replication. The mRNA arising from IE ICP22 gene accumulated with a similar time course. It was also detected as early as 3 hpi from samples infected with KOS or KOS-HSV-GFP (Figure 3.3.2-C), although at 3 hpi ICP22 mRNA was slightly more abundant in cells infected with KOS than in those infected with KOS-HSV-GFP. ICP22 mRNA from KOS and KOS-HSV-GFP infected samples also increased in a comparable fashion over time. Similar to the major EGFP mRNA, PAA decreased ICP22 mRNA production, but it did not

completely inhibit ICP22 mRNA transcription. These northern blot results indicate that the EGFP gene driven by the HSV-IE promoter of KOS-HSV-GFP accumulated with the same time course as IE ICP22 mRNA. The larger RNA mentioned earlier was detected as early as 6 hpi, and it accumulated continuously from 3 to 15 hpi. As was the case for the 1.3 Kb EGFP and ICP22 mRNA, PAA reduced but did not eliminate the accumulation of the larger RNA, detected by the EGFP probe (Figure 3.3.2-B). These results also indicate that the larger RNA was also transcribed before DNA replication.

The kinetics of EGFP and ICP22 mRNA accumulation from KOS-CMV-GFP infection were also measured and compared with KOS infection using northern blot analysis (Figure 3.3.3). As for the KOS-HSV-GFP infection, the 1.3 Kb EGFP mRNA of KOS-CMV-GFP was detected as early as 3 hpi, and this mRNA was produced continuously over time (Figure 3.3.3-B). ICP22 mRNA from KOS and KOS-CMV-GFP could also be seen as early as 3 hpi (Figure 3.3.3-C). The accumulation of ICP22 mRNA produced during KOS infection increased over time. The production of ICP22 mRNA from KOS-CMV-GFP increased from 3 hpi to 9 hpi and then declined slightly during the remainder of the time points examined. This slight decrease may be caused by sample loading differences, since the ribosomal profile shows slightly less RNA in samples at 12 and 15 hpi for KOS-CMV-GFP compared to 9 hpi (Figure 3.3.3-A). The PAA treatment largely reduced, but did not abolish, EGFP and ICP22 mRNA production in KOS and KOS-CMV-GFP infected HeLa cells (Figure 3.3.3-B&C). Therefore, these data suggest that EGFP from either KOS-HSV-GFP or KOS-CMV-GFP

accumulates with a time course similar to the IE ICP22 mRNA. Only the second larger RNA (than 1.3 Kb) mentioned in Figure 3.3.1 was detected by the EGFP probe in the samples from KOS-CMV-GFP infections. As was the case for the larger RNA of KOS-HSV-GFP (Figure 3.3.2-B), this RNA could be detected as early as 6 hpi, and its production accumulated continuously during the incubation time. In addition, PAA reduced the level of this RNA accumulation, but PAA did not abolish its production (Figure 3.3.3-B).

Figure 3.3.1-Identification of the EGFP mRNA transcribed from the HSV and HCMV IE promoters in viral recombinants.

EGFP mRNA expressed from the HSV or HCMV IE promoter was identified in HeLa cells transfected with indicated plasmids or infected with KOS-derived viruses (with an MOI of 5) by northern blot analysis with an EGFP probe (same as the one in southern blot analysis). The transfections and infections were incubated for 24 hours and 6 hours, respectively.

A) Ethidium bromide staining pattern of total RNA profile (displaying ribosomal RNA).

B). The EGFP mRNAs arising from transfected pUC19-HSV-GFP and pEGFP-C1 were used as the positive controls for identifying the EGFP mRNA transcribed from the native promoters of EGFP expression cassette borne in the KOS or V422 derived viruses. KOS infection was used as a negative control. The RNA size ladder is shown on the left side of the blot, and the arrow on the right side points to the predicted EGFP mRNAs driven from the viral IE promoters.

C). The same blot as B. with a shorter exposure time.

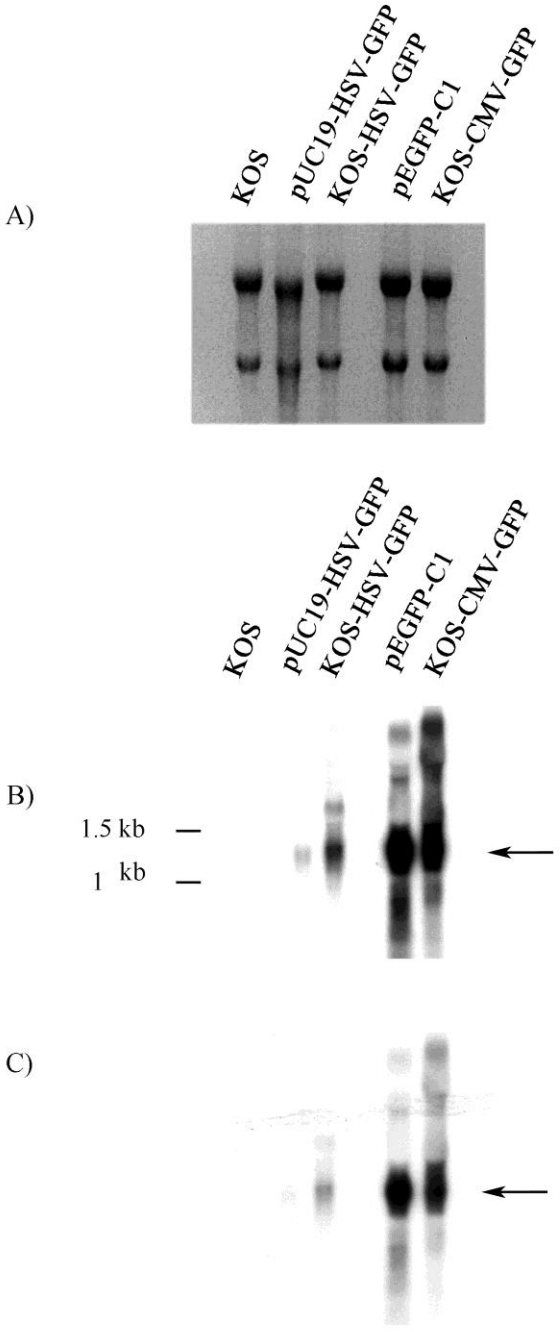
A)
KOS
pUC19-HSV-GFP
KOS-HSV-GFP
pEGFP-C1
KOS-CMV-GFP
B)
KOS
pUC19-HSV-GFP
KOS-HSV-GFP
pEGFP-C1
KOS-CMV-GFP
1.5 kb
1 kb
C)

Figure 3.3.2-The accumulation of the EGFP and ICP22 mRNAs produced in KOS or KOS-HSV-GFP infected HeLa cells.

HeLa cells were infected with KOS or KOS-HSV-GFP at an MOI of 5. RNA of each infection was harvested at indicated times (hpi) and subjected to northern blot analysis. Infections supplied with PAA were harvested at 15hpi. The non-infected cells were used as the mock sample (labelled as M).

A). A) Ethidium bromide staining pattern of total RNA profile (displaying ribosomal RNA).

B). Northern blot analysis with EGFP probe. The 1.3 kb EGFP mRNA is indicated by the arrow.

C). Northern blot analysis with a probe for ICP22.

A)

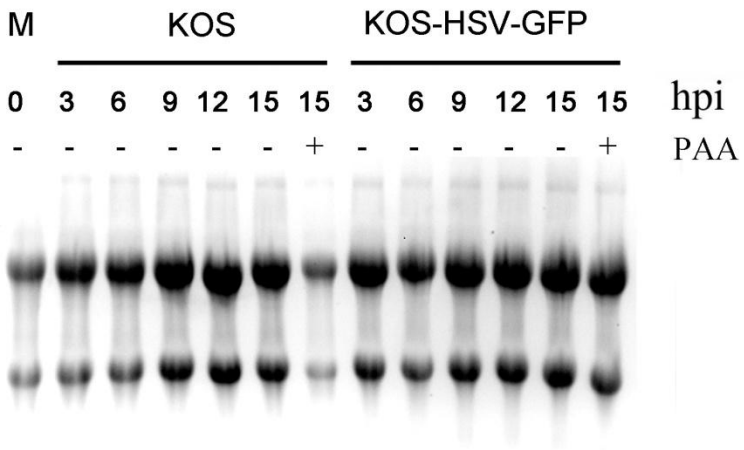
M
KOS
KOS-HSV-GFP
0 3 6 9 12 15 15 3 6 9 12 15 15
hpi
- - - - - - + - - - - - +
PAA

B)

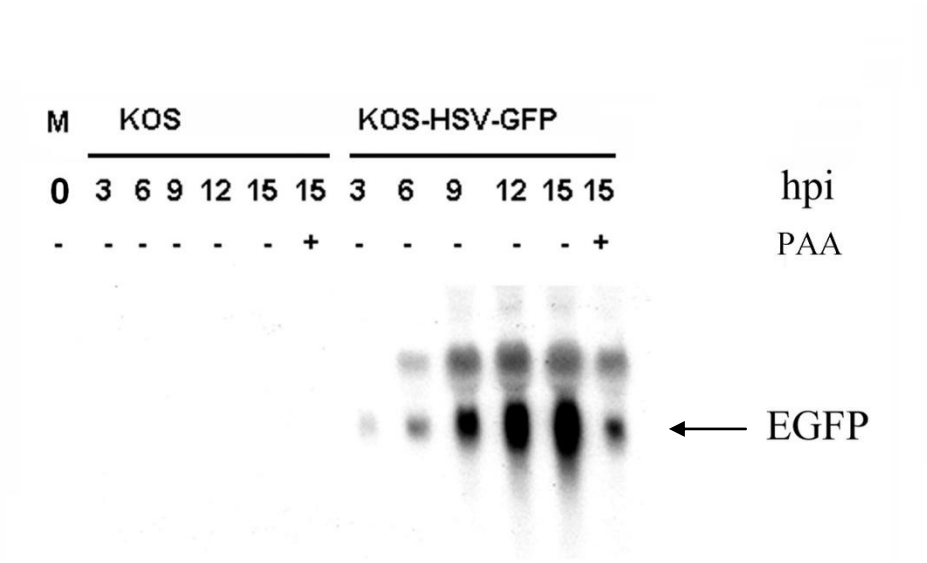
M
KOS
KOS-HSV-GFP
0 3 6 9 12 15 15 3 6 9 12 15 15
hpi
- - - - - - + - - - - - +
PAA
EGFP

C)

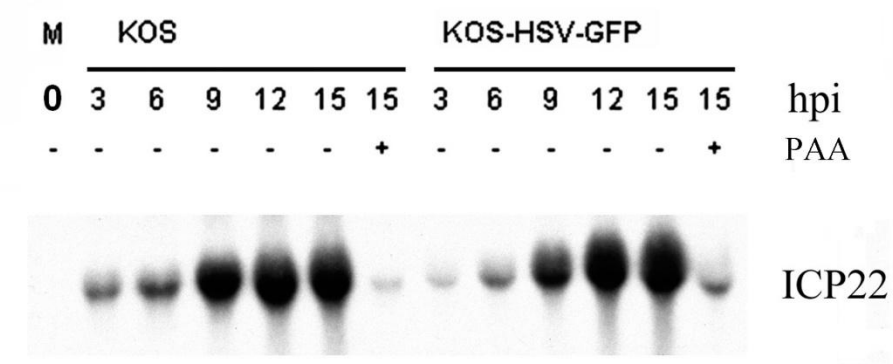
M
KOS
KOS-HSV-GFP
0 3 6 9 12 15 15 3 6 9 12 15 15
hpi
- - - - - - + - - - - - +
PAA
ICP22

Figure 3.3.3- The accumulation of the EGFP and ICP22 mRNAs of KOS and KOS-CMV-GFP in HeLa cells.

HeLa cells were infected with KOS or KOS-CMV-GFP at an MOI of 5. RNA of each infection was harvested at the indicated times (hpi) and subjected to northern blot analysis. Infections carried out in the presence of PAA were harvested at 15hpi. The non-infected cells were used as the mock sample (labelled as M).

A). A) Ethidium bromide staining pattern of total RNA profile (displaying ribosomal RNA).

B). Northern blot analysis with EGFP probe. The 1.3 kb EGFP mRNA is indicated by the arrow.

C). Northern blot analysis with a probe for ICP22.

A)

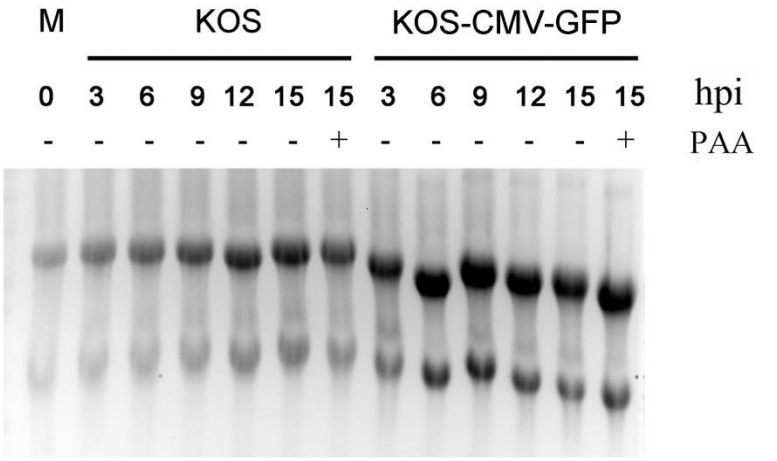
M
KOS
KOS-CMV-GFP
0 3 6 9 12 15 15 3 6 9 12 15 15
hpi
- - - - - - + - - - - - +
PAA

B)

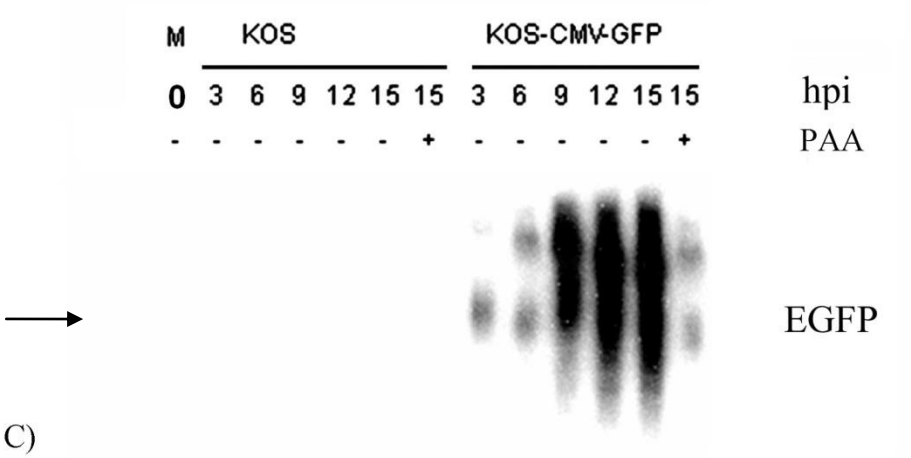
M
KOS
KOS-CMV-GFP
0 3 6 9 12 15 15 3 6 9 12 15 15
hpi
- - - - - - + - - - - - +
PAA
EGFP

C)

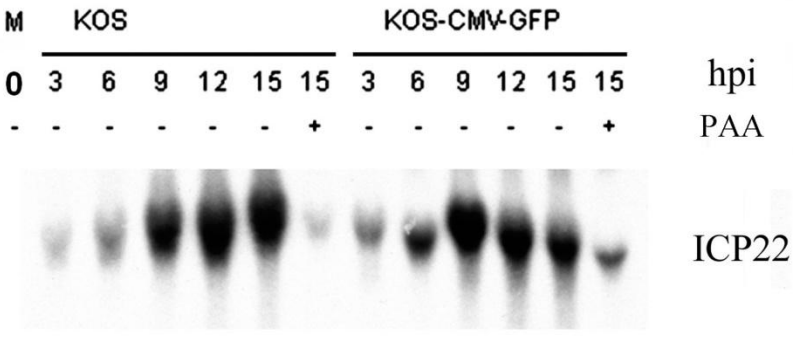
M
KOS
KOS-CMV-GFP
0 3 6 9 12 15 15 3 6 9 12 15 15
hpi
- - - - - - + - - - - - +
PAA
ICP22

3.3.1.2 EGFP transcription occurs during the IE phase of infection

The above data show that the accumulation of 1.3 Kb EGFP mRNAs were reduced but not abolished by the addition of PAA in the infections of KOS-HSV-GFP (Figure 3.3.2-B) and KOS-CMV-GFP (Figure 3.3.3-B). This result eliminates the possibility that the inserted EGFP gene of the KOS-derivatives behaves like a true L gene. As one approach to determine if the EGFP gene of KOS-HSV-GPF was transcribed as an IE gene of HSV-1, the effects of cycloheximide on transcript accumulation were determined. Cycloheximide inhibits protein synthesis through blocking the elongation of host translation machinery in infected cells [277]. Consequently, E or L mRNA cannot be transcribed in the presence of cycloheximide because these genes require IE protein production prior to their expression. Therefore, cycloheximide (300 μg/mL) treatment could be applied to distinguish whether EGFP transcription occurs during the IE phase of infection or during later transcriptional phases. To perform these experiments, total RNA was harvested from infected HeLa cells at 6 hpi, and northern blotting was performed with ^{32}P-labeled ICP22 and EGFP probes (Figure 3.3.4).

EGFP mRNAs were detected in the samples from KOS-GFP viruses, but not the one from KOS or V422. As expected, the EGFP gene downstream of the HCMV promoter was transcribed in the samples from both KOS- and V422-CMV-GFP infections, in the presence and absence of cycloheximide. In the samples of KOS-CMV-GFP infection, cycloheximide treatment enhanced the production of the 1.3 Kb RNA, but interestingly, it reduced the level of the second

larger RNA. The largest RNA shown in the last lane of figure 3.3.1 could not be seen from the blot. This result is consistent with the idea that the larger RNA was transcribed from another promoter, not the HCMV IE promoter. In the case of V422-CMV-GFP infection, the 1.3 Kb RNA was the only product detected in the samples (not the larger RNAs), and its level was increased by cycloheximide treatment. Compared with the wild-type infection, the V422 mutation severely reduced the levels of the 1.3 Kb EGFP mRNA, both in the presence and absence of cycloheximide. The result obtained in the absence of cycloheximide, is expected, since the viral DNA replication of V422-CMV-GFP is restricted in HeLa cells. The VP16 mutation of V422-based viruses causes reduction on the expression of IE genes, and thus the production of E proteins, which are required for viral DNA synthesis; therefore, the viral DNA replication of V422-based viruses was limited in the infected HeLa cells. Furthermore, this consequence reduces the production of newly synthesized EGFP cassettes, which in turn leads to less EGFP mRNA transcription from these DNA templates when compared to the wild-type virus. Surprisingly, the level of EGFP mRNA in the samples from V422-CMV-GFP infection did not reach the level of the wild-type infection, in the presence of cyclohexmide. This result indicates that efficient use of the HCMV promoter requires the activation function of VP16. This is an unexpected result, since the HCMV promoter does not contain the TATGARAT VP16 response element, or it was not activated or repressed by VP16 in a co-transfection experiment (unpublish data from Lucy Bradley). This unexpected result will be discussed in the section of discussion (Chapter 4).

The 1.3 kb EGFP mRNA driven by the HSV IE ICP22 promoter was detected in the wild-type infection, but not in the samples from V422-based infections (in the absence of HMBA), in either the absence or presence of cycloheximide (Figure 3.3.4-B). The larger RNA species mentioned in figure 3.3.1 was also identified from the wild-type infection using the EGFP probe, in the absence of cycloheximide. In contrast to the 1.3 Kb RNA, this larger RNA was abolished by the presence of cycloheximide. This data indicated that the larger RNA product shown in the sample of KOS-HSV-GFP infection was not transcribed from the IE ICP22 promoter (Figure 3.3.4-B).

ICP22 mRNA was used as a positive control for IE mRNA detection in this experiment. ICP22 mRNA was observed in all the wild-type infections, including KOS and KOS-derived GFP viruses (Figure 3.3.4-C). As the case of EGFP mRNA driven by the ICP22 promoter, cycloheximide treatment slightly enhanced the ICP22 mRNA production among all the wild-type infections. This may be due to the absence of ICP4, a repressor of IE promoters [117]. Since ICP4 is an IE protein, its expression was inhibited by cycloheximide in this experiment. As expected, the ICP22 mRNA was not detected in the samples from the V422 and V422-derived infections, in the absence of HMBA. Since the V422-derived viruses express a defective VP16, which functions as a transcription factor of IE genes, the expression of IE genes (eg. ICP22 gene) are reduced in restrictive cells. This in turn leads to reduced productions of E protein, viral DNA and L protein [242]. Some additional, but faster migrating RNA species were also identified with the ICP22 probe in the samples from KOS-CMV-GFP infections (both +/-

cycloheximide), and this RNA could not be detected in either KOS or KOS-HSV-GFP infections. The identity of this RNA species is unknown. In summary, in the presence of cycloheximide, both ICP22 and EGFP mRNA accumulated in the samples from KOS-derived GFP viral infections. Therefore, the above data confirmed that the EGFP mRNA (1.3 Kb) from either KOS-HSV-GFP or KOS-CMV-GFP was transcribed like a typical IE mRNA of HSV-1.

Viral replication of V422 recombinant viruses was shown to be attenuated in HeLa cells, compared to the wild-type infections (Figure 3.2.1). This is an expected consequence. Since compared to the KOS-derived viruses, IE protein expression is reduced by the defective VP16 in V422-derived viruses, this effect leads to reduced production of E and then L proteins and causing an overall reduction in viral gene expression. However, HMBA has been shown to rescue the IE gene expression and the viral replication in the absence of VP16 function [278]. In order to confirm the functional consequences of the VP16 mutation, I asked if HMBA could enhance the transcription of EGFP and ICP22 genes in the V422-derived recombinant viral infections. HeLa cells were infected by V422 and V422-derived GFP viruses at a MOI of 5, in the absence and presence of HMBA (3mM). The infected cells were harvested at 6 hpi, and followed by northern blot analysis with EGFP and ICP22 probes. Infections with KOS and KOS derived viruses were used as a control. The data are shown in figure 3.3.5.

The RNAs labeled by the EGFP probe were only detected in the samples from the recombinant viral infections, not in those from KOS and V422 infections (Figure 3.3.5-B). In the absence of HMBA, the major EGFP mRNA (1.3 Kb) was

detected in the sample from KOS-HSV-GFP infection, but not from V422-HSV-GFP infection. In the presence of HMBA, both RNA species labeled by the EGFP probe were detected in the sample from V422-HSV-GFP infection. Furthermore, the level of the larger RNA was shown to be less than that of the 1.3 Kb mRNA. In contrast to V422-HSV-GFP, the 1.3 Kb RNA were detected in the samples from both V422- and KOS-CMV-GFP infections, in the absence of the HMBA. However, the RNAs with larger sizes could only be detected after the addition of HMBA in the V422-CMV-GFP infection. HMBA also increased the level of the 1.3 Kb RNA in the V422-CMV-GFP infection.

In the absence of HMBA, the ICP22 mRNA could only be detected in the samples from KOS and KOS-derived viral infections (Figure 3.3.5-C). In the case of V422 and V422-derived infections, the ICP22 mRNA was detected after the addition of HMBA. In all samples, there was only one RNA labeled by the ICP22 probe, and the additional band shown in figure 3.3.4-C was not detected in this experiment.

In summary, the above results demonstrate that HMBA enhanced the accumulation of mRNA from the EGFP and ICP22 genes in the V422-derived viral infections. The enhancement of the EGFP mRNA productions in this experiment could either be due to the induction of HSV IE protein synthesis, such as ICP0 and ICP4, or due to the effect of HMBA on the promoter driving EGFP. To distinguish these two possibilities, I asked if HMBA stimulated EGFP mRNA accumulation in the presence of cycloheximide. I performed a similar experiment to the one shown in figure 3.3.5, with the same viruses, MOI and incubation time.

All the V422-related infections were supplied with HMBA (3mM). All the viral infections were performed in the absence and presence of cycloheximide (300μg/mL). The data are shown in figure 3.3.6.

The major EGFP mRNAs (1.3 Kb) were detected only in the samples from the EGFP recombinant viral infections, not from the KOS or V422 infections (Figure 3.3.6-B). In the absence and presence of cycloheximide, the 1.3 Kb RNAs were detected from the samples infected by KOS-derived GFP viruses. In the case of HMBA-treated V422-HSV-GFP and V422-CMV-GFP infections, the 1.3 Kb EGFP mRNAs were not abolished by cycloheximide treatment. In contrast, the larger band shown in the samples from V422- and KOS-HSV-GFP infection was abolished by cycloheximide treatment as shown in figure 3.3.4-B. The same effect of cycloheximide on the larger RNA was also shown in the sample from V422-CMV-GFP infection. Also, cycloheximide greatly reduced (but did not abolish) the level of this RNA in the KOS-CMV-GFP infection. The level of the largest RNA detected in the samples from KOS-CMV-GFP infections was slightly enhanced by cycloheximide treatment. The above data indicate that the enhancement of the transcription of the 1.3 Kb EGFP mRNAs by HMBA (shown in figure 3.3.5) in the samples from V422-derived viral infections were due to activation of the promoters driving EGFP, not to the stimulation of IE proteins. In contrast, the production of other RNA species (sizes larger than 1.3 Kb) labelled by the EGFP probe required the presence of the IE proteins, since their production could be hindered or reduced by cycloheximide. This result was consistent with the idea that these larger RNA species were not transcribed from the native ICP22

or HCMV IE promoter. In the future, additional experiments that exam the effect of HMBA on KOS-derived GFP viruses, and compare with the V422-derived viruses in the presence and absence of the drug, would strength this conclusion.

To confirm that cycloheximide could inhibit the viral protein synthesis, the mRNA of ICP8, an E gene, was detected from the same blot of Figure 3.3.6. In theory, if the IE protein synthesis is blocked by cycloheximide, there would no E mRNAs produced in the infected cells, which require IE proteins to initiate the transcription. The result is shown in Figure 3.3.6-C. In most case, ICP8 mRNA can only be detected from the infections performed in the absence of cycloheximide. However, cycloheximide reduced but did not abolish ICP8 mRNA production during HMBA-treated V422 infections, and this result was not observed in the samples from V422-derived GFP viral infection. This unexpected result has been repeated in 3 individual experiments, and we are unable to explain it at the present time. In contrast, even in the absence of cycloheximide, ICP8 mRNA was not detected in samples from HMBA-treated V422-HSV-GFP infected cells.

In conclusion, the above results from northern blot analysis demonstrate that the EGFP genes driven by either the HCMV or HSV IE promoters from these recombinant viruses were transcribed as a typical IE gene of HSV-1.

Figure 3.3.4- Effects of cycloheximide and the V422 VP16 mutation on accumulation of eGFP mRNA from viral recombinants.

HeLa cells were infected withV422-and KOS-derived viruses in the presence and absence of cycloheximide at an MOI of 5. The non-infected cells were used as the mock sample (labelled as Mock).

A). The ribosomal RNA profile (stained with ethidium bromide).

B). Northern blotting analysis with EGFP probe. V422 and KOS infections were shown as the negative controls for EGFP mRNA detection (indicated by the arrow).

C). Northern analysis with ICP 22 probe. Appearance of ICP22 mRNA (indicated by the arrow) was used as a positive control for cycloheximide treatment.

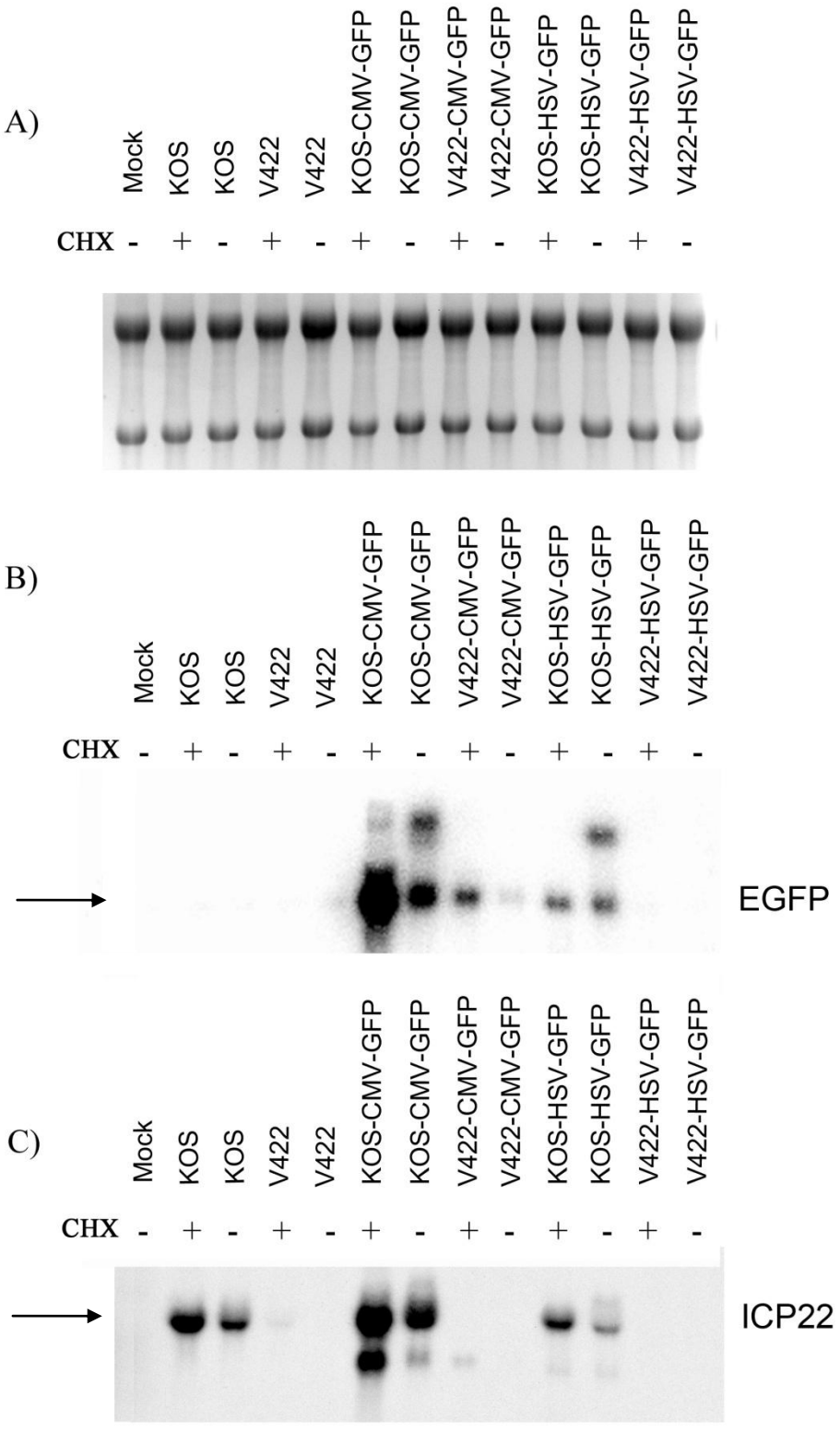
A)
Mock
KOS
KOS
V422
V422
KOS-CMV-GFP
KOS-CMV-GFP
V422-CMV-GFP
V422-CMV-GFP
KOS-HSV-GFP
KOS-HSV-GFP
V422-HSV-GFP
V422-HSV-GFP
CHX - + - + - + - + - + - + - -
B)
Mock
KOS
KOS
V422
V422
KOS-CMV-GFP
KOS-CMV-GFP
V422-CMV-GFP
V422-CMV-GFP
KOS-HSV-GFP
KOS-HSV-GFP
V422-HSV-GFP
V422-HSV-GFP
CHX - + - + - + - + - + - + - -
EGFP
C)
Mock
KOS
KOS
V422
V422
KOS-CMV-GFP
KOS-CMV-GFP
V422-CMV-GFP
V422-CMV-GFP
KOS-HSV-GFP
KOS-HSV-GFP
V422-HSV-GFP
V422-HSV-GFP
CHX - + - + - + - + - + - + - -
ICP22

Figure 3.3.5- Effects of HMBA on mRNA accumulation from recombinant viruses.

HeLa cells were infected with V422 and KOS derived viruses, and HMBA was supplied to the V422 derived viral infections. Infections with KOS-derived viruses were used as a positive control. The non-infected cells were used as the mock sample (labelled as M).

A). The ribosomal RNA profile (stained with ethidium bromide).

B). Northern analysis with EGFP probe.

C). Northern analysis with ICP22 probe. ICP22 mRNA (indicated by the arrow) was detected as a representative for other typical HSV-1 IE genes.

A)

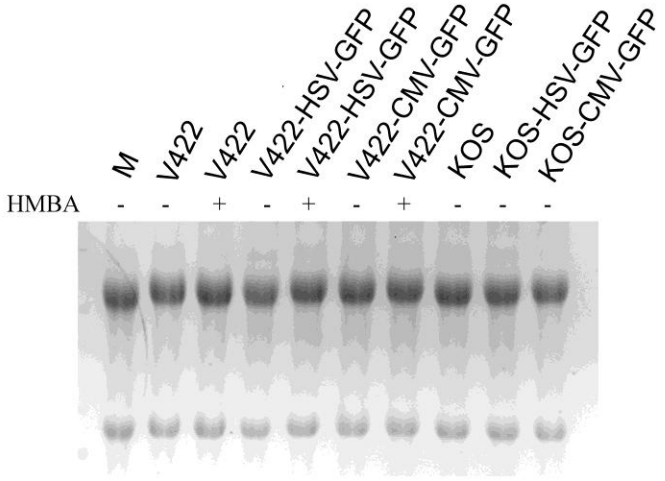
M
V422
V422
V422-HSV-GFP
V422-HSV-GFP
V422-CMV-GFP
V422-CMV-GFP
KOS
KOS-HSV-GFP
KOS-CMV-GFP
HMBA - - + - + - + - - -

B)

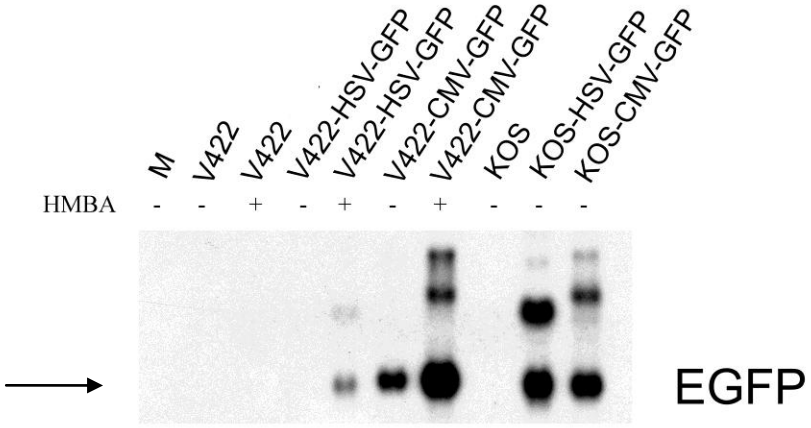
M
V422
V422
V422-HSV-GFP
V422-HSV-GFP
V422-CMV-GFP
V422-CMV-GFP
KOS
KOS-HSV-GFP
KOS-CMV-GFP
HMBA - - + - + - + - - -
EGFP

C)

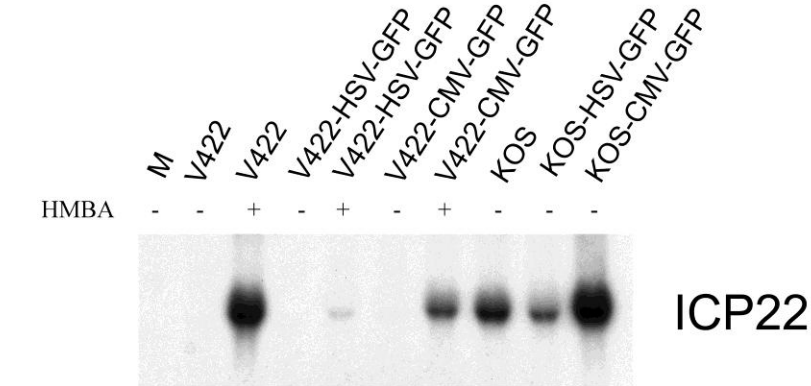
M
V422
V422
V422-HSV-GFP
V422-HSV-GFP
V422-CMV-GFP
V422-CMV-GFP
KOS
KOS-HSV-GFP
KOS-CMV-GFP
HMBA - - + - + - + - - -
ICP22

Figure 3.3.6- HMBA activates mRNA accumulation from viral recombinants in the presence of cycloheximide.

HeLa cells were infected withV422-and KOS-derived viruses in the presence and absence of cycloheximide at an MOI of 5. HMBA (3mM) was supplied to the V422-derived viral infections. The non-infected cells were used as the mock sample (labelled as M).

A). The ribosomal RNA profile (stained with ethidium bromide).

B). Northern blotting analysis with EGFP probe. V422 and KOS infections were shown as the negative controls for EGFP mRNA detection (indicated by the arrow).

C). Northern analysis with ICP8 probe. Appearance of ICP8 mRNA was used as a negative control for cycloheximide treatment.

A)

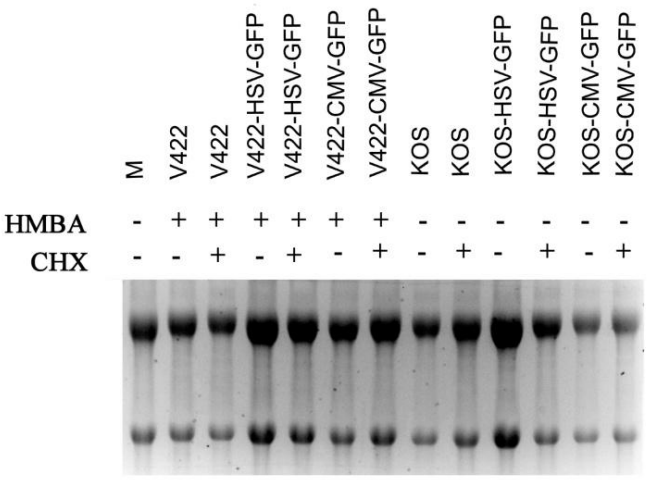
M
V422
V422
V422-HSV-GFP
V422-HSV-GFP
V422-CMV-GFP
V422-CMV-GFP
KOS
KOS
KOS-HSV-GFP
KOS-HSV-GFP
KOS-CMV-GFP
KOS-CMV-GFP
HMBA
CHX

B)

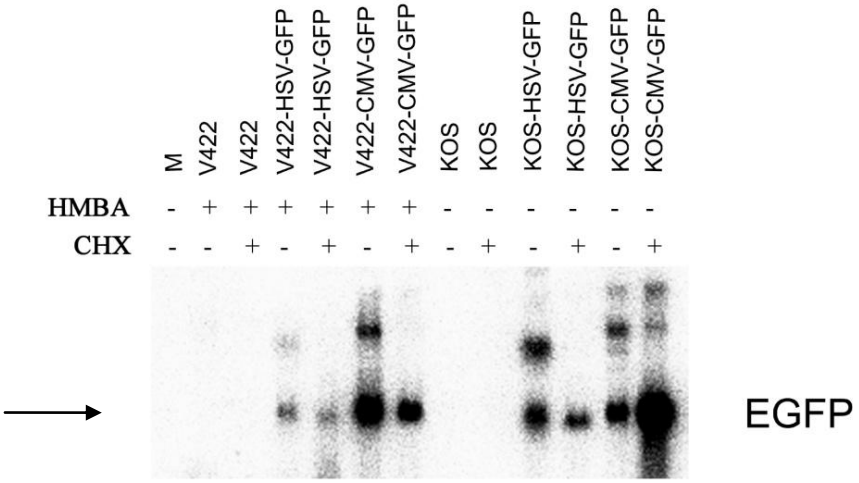
M
V422
V422
V422-HSV-GFP
V422-HSV-GFP
V422-CMV-GFP
V422-CMV-GFP
KOS
KOS
KOS-HSV-GFP
KOS-HSV-GFP
KOS-CMV-GFP
KOS-CMV-GFP
HMBA
CHX
EGFP

C)

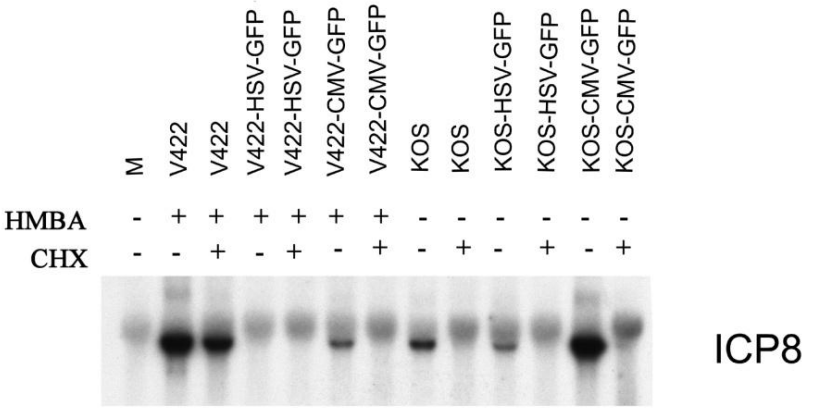
M
V422
V422
V422-HSV-GFP
V422-HSV-GFP
V422-CMV-GFP
V422-CMV-GFP
KOS
KOS
KOS-HSV-GFP
KOS-HSV-GFP
KOS-CMV-GFP
KOS-CMV-GFP
HMBA
CHX
ICP8

3.3.1.3 The kinetics of EGFP protein accumulation in infected HeLa cells

From above results, we confirmed that the delay of EGFP expression in KOS-HSV-GFP infection detected by fluorescence microscopy (section 3.2) is not occurring at the transcriptional level. We decided to look at EGFP expression at the translational level, as well as other viral protein production from the KOS-derived recombinant viruses.

Confluent monolayers of HeLa cells were infected with KOS-HSV/CMV-GFP or KOS viruses at an MOI of 5. The infected cells were harvested at 0 (also for mock infected cells), 3, 6, 9, 12 and 15 hpi. PAA was added to selected wells, and these samples were harvested at 15 hpi. The cell lysates were then analyzed by western blotting with antibodies detecting the HSV-1 IE proteins ICP27 (we did not have the antibody for ICP22), E protein ICP8, leaky L protein VP16, L protein gC, EGFP, and actin. Samples from KOS-HSV-GFP and KOS-CMV-GFP infections in HeLa cells were loaded onto two separate gels while KOS infected samples were loaded on each gel as a control. The two blots were exposed to films for various lengths of time.

In characterizing the new recombinant viruses it was important to examine the temporal regulation of viral protein production. In general, the EGFP and examined viral proteins produced from KOS and KOS-based recombinant viruses increased continuously with time (from 3 to 15 hpi) in the absence of PAA (Figure 3.3.7).

EGFP produced in KOS-HSV-GFP infected cells was detected as early as 9 hpi, and its expression increased from 3 to 15 hpi (Figure 3.3.7-A). Notably, despite being under the control of an HSV IE promoter in the KOS-HSV-GFP virus, EGFP was produced 3 hours later than the IE protein ICP27, which was observed as early as 6 hpi. In contrast, ICP27 from KOS infected cells was observable as early as 3 hpi, which was 3 hours earlier than ICP27 produced from KOS-HSV-GFP. Moreover, at 6 hpi ICP27 expression from KOS was noticeably higher than from KOS-HSV-GFP. Similar to EGFP, expression of ICP27 from both KOS and KOS-HSV-GFP viruses increased constantly during infection from 3 to 15 hpi. The early protein ICP8 was detected as early as 9 hpi in KOS-HSV-GFP infections, which was 3 hours later than from KOS infection. Furthermore, ICP8 protein was noticeably more abundant in KOS infected samples than in KOS-HSV-GFP infected samples at all times examined. ICP8 production also increased over time during wild-type and recombinant virus infections in a similar fashion to ICP27. The leaky late protein VP16 could be observed from 9 hpi onward and its production increased continuously over time in both KOS and KOS-HSV-GFP infections. In contrast, at every examined time, KOS infected samples contained more VP16 than did KOS-HSV-GFP infected samples. The true L protein gC was seen as early as 12 hpi in KOS infected samples and was not detectable in KOS-HSV-GFP infections during the times tested. gC protein production during KOS infection also increased with time similar to the other viral proteins. As expected, PAA greatly reduced the expression of ICP27, ICP8, and VP16 from both KOS and KOS-HSV-GFP viruses. EGFP expression was

also reduced following PAA treatment in KOS-HSV-GFP infections. As a true L protein, gC requires DNA replication for expression. As expected, gC expression was blocked following the PAA treatment (see KOS 15hpi +PAA; Figure 3.3.7-A). The above results suggested that EGFP and the indicated viral genes of KOS-HSV-GFP were expressed later and with less amount of protein than the same genes of KOS.

In section 3.2, the EGFP protein of KOS-CMV-GFP was observed under the fluorescence microscope as early as 4 hpi. As a comparison to KOS-HSV-GFP, the protein samples from KOS-CMV-GFP infected cells were also collected and subjected to western blot analysis (Figure 3.3.7-B). In KOS-CMV-GFP infected HeLa cells, EGFP was detected as early as 3 hpi, which was 3 hours earlier than ICP27 within the same samples. ICP27 production from KOS-CMV-GFP and KOS was comparable over time, and was detected as early as 6 hpi. In regards to early protein production, ICP8 was detected as early as 6 hpi from KOS-CMV-GFP infected samples and appeared to be slightly increased compared to ICP8 production from KOS at the same time post infection. ICP8 protein production also increased continuously with time in KOS and KOS-CMV-GFP infections. VP16 protein produced from KOS and KOS-CMV-GFP viruses was observed as early as 9 hpi; however, the KOS-CMV-GFP virus produced more VP16 than did KOS at all times post infection. The true late protein gC was weakly expressed by 9 hpi in the KOS-CMV-GFP virus, which was 3 hours earlier than gC produced from KOS. Similar to KOS infection, expression of gC from KOS-CMV-GFP was inhibited by PAA treatment. In addition, PAA reduced

the production of EGFP, ICP27, ICP8, and VP16 proteins expressed from both KOS and KOS-CMV-GFP viruses, which was similar to the effect of PAA during KOS-HSV-GFP infections (Figure 3.3.6-B). Based on the above observations, KOS-CMV-GFP behaves like the parental virus-KOS in infected HeLa cells.

In summary, these results demonstrate that the delay of EGFP fluorescence detected from KOS-HSV-GFP in section 3.2 may occur during translation, but not at the transcription level in HeLa cells. On the other hand, the EGFP gene of KOS-CMV-GFP was expressed like a typical IE gene of KOS in HeLa cells.

Figure 3.3.7- Viral gene expression profiles for KOS, KOS-HSV-GFP and KOS-CMV-GFP infected HeLa cells

HeLa cells were infected with the indicated viruses at an MOI of 5. Total protein was harvested at the indicated times (hpi) and subjected to western blot analysis using antibodies against EGFP, ICP27, ICP8, VP16, gC, and actin (loading control). Target proteins were visualized on X-RAY film (FUJI) with the ECL Plus Western Blotting Detection kit (GE Healthcare). Infections carried out in the presence of PAA were harvested at 15 hpi. The non-infected cells were used as the mock sample (labelled as M).

A). Gene expression in KOS-HSV-GFP-infected cells was compared to that in KOS infection.

B). Gene expression in KOS-CMV-GFP-infected cells was compared to that of KOS. The KOS samples in panels A and B are from the same experiment, but different film exposures are presented.

A)

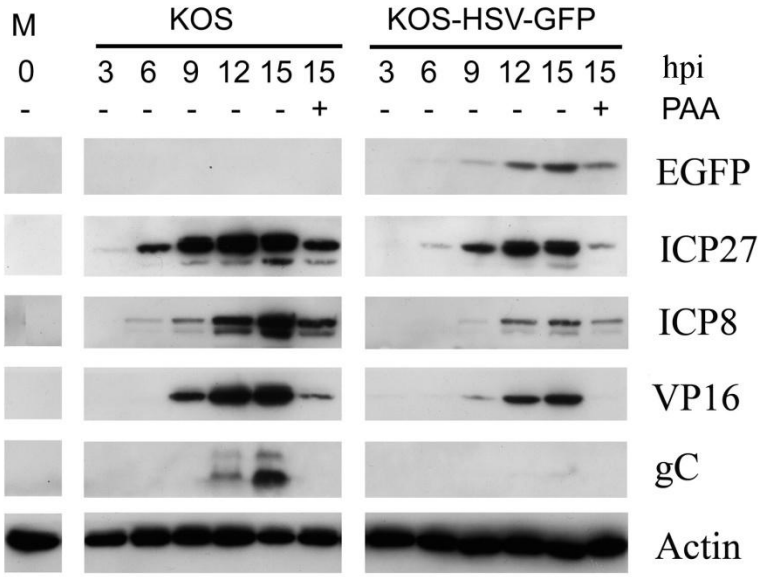
M
KOS
KOS-HSV-GFP
0
3 6 9 12 15 15
3 6 9 12 15 15
hpi
-
- - - - - +
- - - - - +
PAA
EGFP
ICP27
ICP8
VP16
gC
Actin

B)

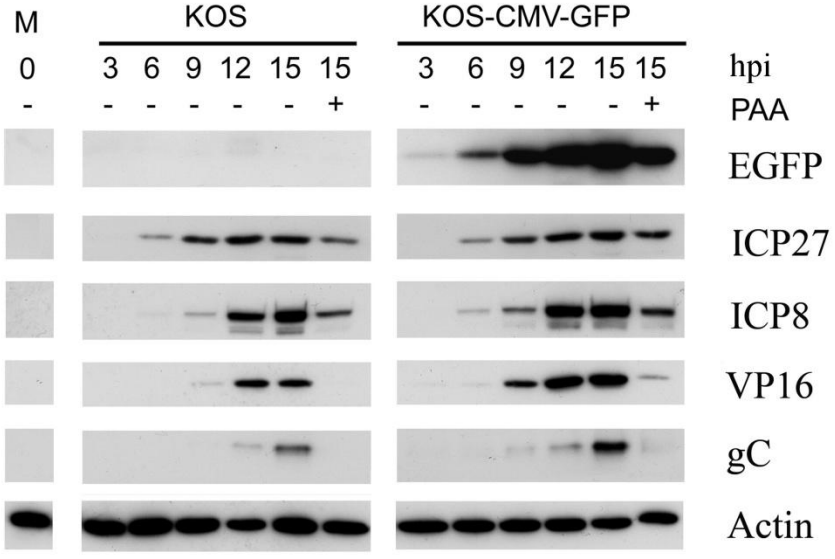
M
KOS
KOS-CMV-GFP
0
3 6 9 12 15 15
3 6 9 12 15 15
hpi
-
- - - - - +
- - - - - +
PAA
EGFP
ICP27
ICP8
VP16
gC
Actin

3.3.2 The kinetics of EGFP production in infected Vero cells

3.3.2.1 The kinetics of EGFP mRNA accumulation in infected Vero cells

To determine if the delay in EGFP production could also be seen in KOS-HSV-GFP infected Vero cells, the kinetics of EGFP accumulation in Vero cells was measured at both the RNA and protein levels. We performed northern blot analyses as in section 3.3.1, with KOS and KOS-HSV-GFP infected Vero cells in the absence of PAA (Figure 3.3.8).

As in HeLa cells, the 1.3 Kb EGFP mRNA was detected as early as 3 hpi in Vero cells infected with KOS-HSV-GFP (Figure 3.3.7-B). The level of this RNA accumulated continuously till 9 hpi, and then it seemed to decline in later infections. However, this reduction may be due to the loading difference of the RNA sample in the lanes (Figure 3.3.8-A). Especially, the amount of RNA loaded in lane "9" of KOS-HSV-GFP panel was shown much more than the lane "12" of the same panel. The larger RNA labeled by the EGFP probe was detected as early as 3 hpi, and its accumulation followed the same pattern as that of the 1.3 Kb RNA. At 15 hpi, the larger RNA could not be detected on the blot.

The ICP22 mRNA was observed as early as 3 hpi in both KOS and KOS-HSV-GFP infections (Figure 3.3.8-C). The accumulation of ICP22 mRNA from KOS-HSV-GFP increased slower than that from KOS, as shown by the lane "6" of both KOS and KOS-HSV-GFP panels. In addition, this observation is consistent with the result shown in Figure 3.3.7-A, which shows the general overall delay in protein production seen in KOS-HSV-GFP-infected HeLa cells.

In contrast, the level of ICP22 mRNA in KOS infected cells increased up to 9 hpi and then dropped in later infections. This trend of ICP22 mRNA production from KOS-infected Vero cells was different than that from KOS-infected HeLa cells, which continuously transcribed the ICP22 mRNA during the examined times (Compare Figure 3.3.2-C to 3.3.7-C). However, it is similar to that seen in ICP22 mRNA production of KOS-CMV-GFP infected HeLa cells (Compare Figure 3.3.3-C to 3.3.7-C). In summary, these observations suggest that the kinetics of EGFP mRNA accumulation has a comparable fashion as that of ICP22 mRNA, in KOS-HSV-GFP-infected Vero cells.

Figure 3.3.8- The accumulation of the EGFP and ICP22 mRNAs of KOS and KOS-CMV-GFP in Vero cells.

Vero cells were infected with KOS, KOS-HSV-GFP and KOS-CMV-GFP at an MOI of 5. Total RNA from each infection was harvested at the indicated times (hpi) and subjected to northern blot analysis with probes for EGFP and ICP22.

A). Ethidium bromide staining pattern (displaying ribosomal RNA).

B). Northern analysis with EGFP probe. EGFP mRNA (1.3 kb) is indicated by the arrow.

C). Northern analysis with ICP22 probe. Non-infected cells were used as the mock sample (labelled as M). ICP22 mRNA (indicated by the arrow) was detected as a representative for other typical HSV-1 IE genes.

A)

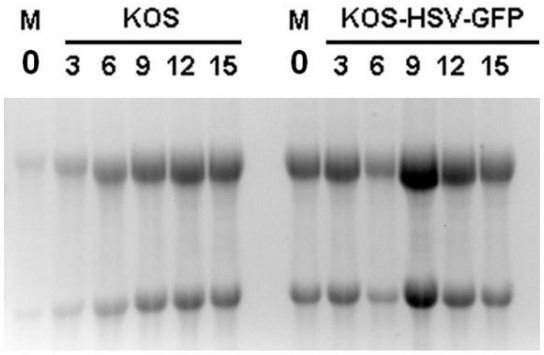
M
KOS
0 3 6 9 12 15
M
KOS-HSV-GFP
0 3 6 9 12 15
hpi

B)

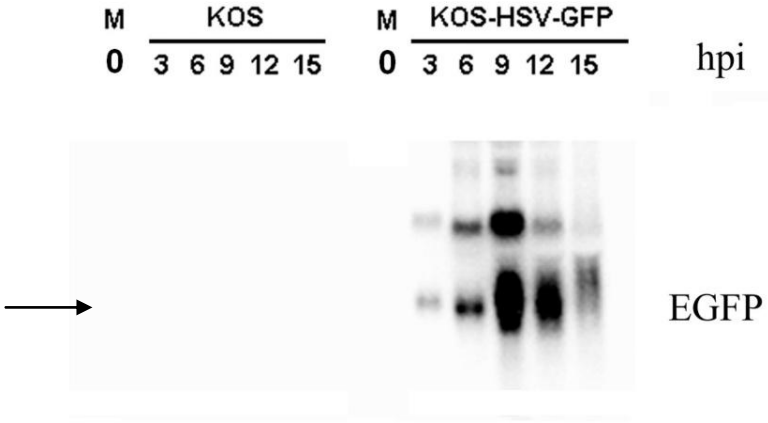
M
KOS
0 3 6 9 12 15
M
KOS-HSV-GFP
0 3 6 9 12 15
hpi
EGFP

C)

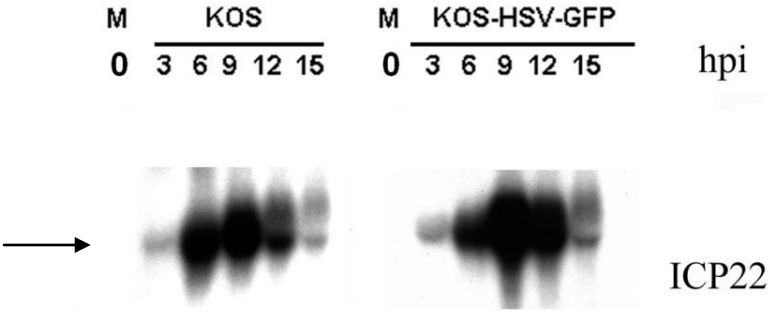
M
KOS
0 3 6 9 12 15
M
KOS-HSV-GFP
0 3 6 9 12 15
hpi
ICP22

3.3.2.2 The kinetics of EGFP protein accumulation in infected Vero cells

To find out whether the delayed viral protein expression of KOS-HSV-GFP was unique to HeLa cells, similar experiments were performed in Vero cells (Figure 3.3.9).

The IE ICP27 protein was detected as early as 3 hpi in KOS-infected Vero cells (Figure 3.3.9-KOS panel). ICP27 was continuously expressed till 12 hpi, and then its protein level was dropped at 15 hpi. The E protein ICP8 was emerged as early as 6 hpi, and its expression followed the same pattern as that of ICP27. VP16 as a leaky L protein was seen as early as 6 hpi, and its accumulation increased along with the examined times. The true L gC protein was detected from 6 hpi, and its accumulation was increased till 12 hpi, then slightly reduced at 15 hpi.

In the KOS-HSV-GFP infected samples, EGFP was detected as early as 6 hpi, and its expression increased over time till 15 hpi (Figure 3.3.9-KOS-HSV-GFP panel). As seen in KOS infections, ICP27 and ICP8 were detected as early as 3 and 6 hpi, and they were expressed constantly over time in KOS-HSV-GFP infected Vero cells. ICP8 produced from KOS infection showed higher protein level than that from KOS-HSV-GFP at all time points. VP16 and gC from KOS-HSV-GFP were produced as early as 9 hpi, and all their protein levels increased constantly along all examined times. In contrast to KOS infection, VP16 and gC proteins from KOS-HSV-GFP-infected Vero cells were seen three hours later than

in a KOS infection, and the levels of VP16 were reduced with KOS-HSV-GFP, especially at the 6 and 9 hour time points.

Compared to the samples from infected-HeLa cells (Figure 3.3.7-A), ICP27 was observed as early as the same times (3 hpi and 6 hpi, respectively) in KOS and KOS-HSV-GFP infected Vero cells (Figure 3.3.9). Interestingly, EGFP was detected as early as 6 hpi in Vero cells infected with KOS-HSV-GFP, which was three hours earlier than in HeLa cells. The largest difference between KOS-HSV-GFP infections in HeLa and Vero cells was that the late protein gC could be detected in Vero cells but not in HeLa cells. Moreover, gC produced during KOS infection appeared slightly earlier than the gC from KOS-HSV-GFP infections (Compare Figure 3.3.7-A to 3.3.9). Therefore, these data suggest that the delay of viral protein expression from KOS-HSV-GFP was also apparent in Vero cells.

Figure 3.3.9-Viral gene expression profiles for KOS and KOS-HSV-GFP infected Vero cells.

Vero cells were infected with KOS or KOS-HSV-GFP at an MOI of 5. Samples were harvested at the indicated times (hpi). Lysates and total protein were analyzed by western blotting with antibodies against the indicated proteins on the figure. The non-infected cells were used as the mock sample (labelled as M). Actin was used as the loading control.

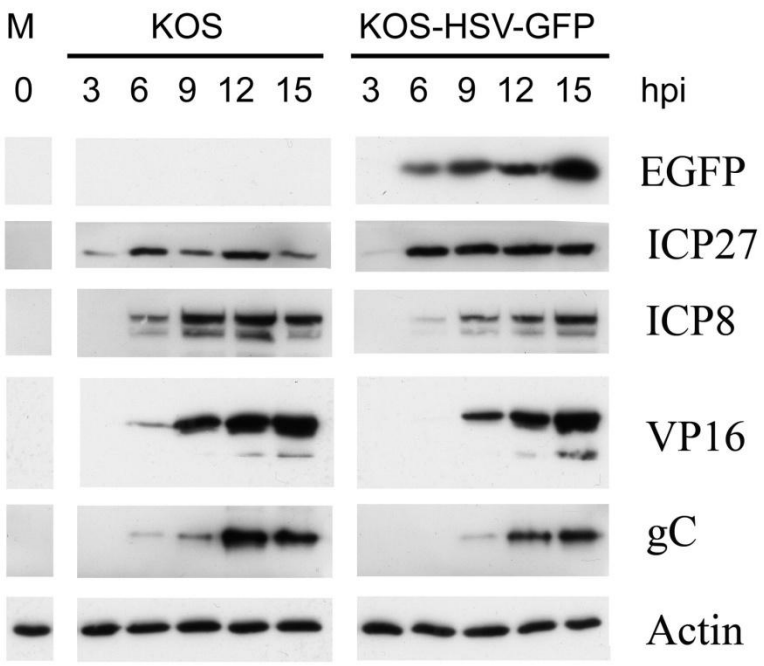
M
KOS
KOS-HSV-GFP
0
3 6 9 12 15
3 6 9 12 15
hpi
EGFP
ICP27
ICP8
VP16
gC
Actin

Chapter 4 Discussion:

4.1 Summary of the results

As mentioned in the introduction, the IE gene expression of HSV-1 is regulated both positively and negatively by viral and cellular proteins. Previous studies have shown that most human cell lines, except the U2OS osteosarcoma cell, are restrictive to the V422 mutant virus of HSV-1, which lacks a functional VP16 protein [249]. This permissive phenotype of U2OS cells to V422 replication is recessive, suggesting that they are missing an inhibitory mechanism present in other cell lines that can be silenced by VP16 during a wild-type infection [264, 265]. My initial objective was to construct reporter HSV-1 recombinant viruses to identify the cellular proteins that repress the viral IE gene expression during V422 infection. In addition, we also wished to screen for additional host factors that promote the IE gene expression during wild-type KOS infection. To this end, four recombinant reporter viruses of HSV-1 were constructed: KOS-CMV-GFP, V422-CMV-GFP, KOS-HSV-GFP and V422-HSV-GFP. In these viruses, the reporter EGFP gene was inserted into the TK locus of the KOS or V422 genome. In the four reporter viruses, the EGFP gene is driven by two different promoters: the HCMV IE promoter and the HSV IE (ICP22) promoter. KOS- and V422-CMV-GFP carry the HCMV IE promoter driving the EGFP gene, and the one in the KOS- and V422-HSV-GFP genome is driven by the HSV IE promoter. Rebecca Minaker constructed the KOS-CMV-GFP virus [272] and I constructed the other three.

After construction of these EGFP recombinant viruses, the desired mutations were confirmed by Southern blot and sequencing analyses (Chapter 3). EGFP fluorescence was also detected in infected HeLa cells. HeLa cells were selected for two main reasons; firstly, they are restrictive to V422 replication, and this phenotype can be overcome by addition of HMBA [265]. Secondly, HeLa cells are more suitable for siRNA transfection than HEL or Vero cells, which are also restrictive to V422 [264, 265]. In HeLa cells, the EGFP of KOS-CMV-GFP and HMBA-treated V422-CMV-GFP is expressed like a typical IE gene temporally (Figure 3.3.7). In contrast, the delayed and reduced EGFP fluorescence was detected in KOS-HSV-GFP infection, relative to KOS-CMV-GFP (Figure 3.3.7).

Following this initial characterization, I performed time course experiments to characterize the kinetics of EGFP expression at both RNA and protein level in KOS-HSV-GFP infected HeLa cells, in comparison with the KOS-CMV-GFP infection (Section 3.3.1). As expected, all four recombinant viruses produced the predicted 1.3 Kb EGFP mRNA. The level of this EGFP mRNA from the HCMV IE promoter was much higher than that from the HSV IE promoter. This observation is consistent with the EGFP expression in HeLa cells transfected with the plasmids carrying these two EGFP cassettes, which showed that the HCMV promoter has a much stronger activity than the HSV one in HeLa cells. KOS-HSV-GFP also produced a larger RNA species, which hybridized to the EGFP probe (figure 3.3.4 and 3.3.6). Since this RNAs could be eliminated by the addition of cycloheximide, it is probably not transcribed from the IE ICP22

promoter of the EGFP cassette. The EGFP expression cassette is inserted downstream of the TK promoter in the same transcriptional direction as the TK gene; thus, it is possible that the larger RNA species is transcribed from the TK promoter, which is induced during the E phase of viral replication. This speculation can be tested in the future through probing the blot in figure 3.3.4 with a TK probe, which has the sequence upstream of the inserted ICP22 promoter (or even a probe of ICP22 promoter).

Also, as expected, the inserted HSV IE (ICP22) promoter driving the EGFP gene in the KOS or V422 genome showed several characteristics of HSV IE promoters. Firstly, it was active in the absence of viral protein synthesis during infection. Secondly, in the presence of the protein synthesis inhibitor-cyclohexmide, EGFP expression from this promoter depended on the transactivation domain of VP16. Finally, this ICP22 promoter can be stimulated by HMBA in the absence of viral protein synthesis and VP16 activation function. Also, as expected, the EGFP expression from KOS-CMV-GFP did not require viral protein synthesis, as well.

However, my results also uncovered two unexpected and interesting findings. First, I obtained evidence that the HCMV promoter is positively regulated by VP16 in my viral recombinants. Second, I found that gene expression from my recombinants bearing the HSV promoter was delayed and reduced relative to other HSV isolates including wild-type virus. Below, I discuss these findings further.

4.2 Evidence that VP16 is required for the activation of the HCMV IE promoter in HSV recombinants

The first unexpected result was that the HCMV IE promoter inserted in the HSV-1 genome requires a functional VP16 for its activity in HeLa cells. Figure 3.3.4-B shows that in the absence of viral protein synthesis, the level of EGFP mRNA arising from V422-CMV-GFP was greatly reduced relative to that from KOS-CMV-GFP. This result was also seen in Vero cells (Appendix, Figure A-3-B). The most significant difference between these two viruses is that V422-CMV-GFP lacks a functional VP16 whereas KOS-CMV-GFP expresses the wild-type VP16. Besides, in the presence of cycloheximide, the viral protein synthesis was blocked, so the newly synthesized viral transcription activators, including ICP4 and ICP0, were absent in the infected cells. Therefore, the transcription of EGFP mRNA was only dependent on the tegument proteins which were carried with the input viral genome, and the only defective tegument protein of V422-CMV-GFP that could cause this reduction on the EGFP mRNA, was VP16. Furthermore, the lack of the ICP22 mRNA from V422-CMV-GFP (Figure 3.3.4-C) demonstrates that the VP16 of this virus is defective in infected cells. In addition, the same experiment was also performed in Vero cells, and the results of EGFP and ICP22 mRNAs were consistent with those shown in Figure 3.3.4 (Appendix, Figure A-3). Therefore, these observations indicate that the HCMV IE promoter is positively regulated by a functional VP16 protein during infection.

However, the effect of VP16 on the HCMV IE promoter shown on figure 3.3.4 was not expected, for two reasons. Firstly, there is no TATGARAT element

in the HCMV IE promoter for VP16-induced complex to recognize and bind to (Figure 3.1.10). Secondly, co-transfection of a vector carrying the VP16 gene with pEGFP-C1 (the plasmid that carries the HCMV-EGFP cassette) did not increase the level of EGFP mRNA relative to the transfection of pEGFP-C1 alone in HeLa cells (unpublished data from Lucy Bradley). Thus, the HCMV IE promoter from the EGFP cassette is apparently regulated by VP16 and its associated protein complexes in the circumstance of viral infection but not following vector transfection in HeLa and Vero cells.

There are several possible explanations for this unexpected result. Firstly, Since the EGFP cassette is inserted inside of the TK ORF, the TK sequence upstream of the HCMV promoter (& downstream of the TK promoter) may contain a TATGARAT element to respond to the VP16 activation. However, preliminary data from Lucy Bradley showed that VP16 did not enhance the HCMV IE promoter activity in HeLa cells transfected with a VP16 vector and the plasmid pTK-green (the parental vector to construct the KOS-CMV-GFP virus), which carries the entire TK ORF inserted with the EGFP gene. Thus, this possibility seems unlikely.

How might VP16 activate the HCMV IE promoter without binding to a nearby TAATGARAT element? One possibility is that VP16 acts in a fashion analogous to pp71, an HCMV tegument protein required for IE promoter activity during HCMV infection. pp71 is the most obvious candidate for a functional counterpart of VP16 in HCMV lifecycle [279]. Previous studies have shown that pp71-null mutants of HCMV are severely impaired for IE expression and

initiation of viral infection at low MOI [280, 281], results which demonstrated the importance of pp71 in activating the HCMV IE promoter during viral infection. However, pp71 was also reported to globally stimulate expression from the entire HCMV genome in addition to the IE genes [279, 282]. It has recently become clear that pp71 exerts its activation on IE promoters through counteracting an intrinsic antiviral defence that is dependent on the cell protein hDaxx [283]. hDaxx is a transcriptional corepressor, and it is a part of the ND10 structure, where the incoming viral genome localizes. The repression by hDaxx of viral gene expression is mediated through modification of histones associated with the viral promoters [283]. In addition, more recent studies showed that other ND10 components, such as PML and hDaxx-associated protein ATRX, are able to repress the IE gene expression of HCMV during lytic infection. In contrast, this repression can be relieved by downregulation of hDaxx, PML and ATRX in cells [283-288]. pp71 has been reported to induce the IE gene expression by disrupting the ATRX-hDaxx complex [285], and promoting hDaxx degradation through an uncommon proteasome-dependent but ubiquitin-independent pathway [287, 289]. Therefore, it seems possible that VP16 may similarly interact with ND10 components directly or indirectly to counteract their repression on the HCMV IE promoter of KOS-CMV-GFP. It will be interesting to see whether downregulation of hDaxx, ATRX and PML could enhance the EGFP expression of V422-CMV-GFP (which has a defective VP16) in the presence of cycloheximide. Preliminary data from Bradley demonstrated that VP16 did not induce the HCMV promoter of pEGFP-C1 in transfection experiment. One possible explanation is that VP16

could be brought close to the HCMV promoter by binding to the TATGARAT elements on the genome next to the insertion site, when the HCMV promoter is inserted within the HSV-1 genome. In contrast, when the HCMV promoter carried by a plasmid, which does not contain any VP16-responding sequence, VP16 cannot reach the HCMV promoter; thus, VP16 cannot enhance the HCMV promoter activity in plasmid transfection experiments.

Another related possibility is that VP16 may globally modify the chromatin structure on the HSV-1 genome, and HCMV IE promoter may only require the active state of associated chromatin structure for its activity, but not other viral transcription activators. Chromatin modification influences the regulation of viral promoter activity and in turn the gene expression, but it is not the only determinant factor for viral gene expression, which also requires certain viral or cellular transcription activators to recruit the host transcription (reviewed in [290, 291]). The HCMV IE promoter is more intrinsicly powerful than HSV-1 ones, which largely depend on the viral transcription activators, including VP16, ICP0 and ICP4. However, all of these promoters may require certain modifications on associated-chromatin in order to allow binding of cellular and viral transcription activators, including the inserted HCMV IE promoter. Therefore, the global effect of VP16 on chromatin modification might induce the HCMV IE promoter, but not the neighbour TK promoter, which requires the additional ICP0 and ICP4 presence. This possibility is also consistent with the speculation that VP16 induces chromatin modification on the entire genome of HSV-1 from a previous publication of our lab [57].

In that paper, Hancock et. al., [57] firstly demonstrated a global effect of VP16 on depleting histones (specifically histone H3) on viral promoters, that was not restricted to the IE promoters. Therefore, it is possible that the histone 3 levels on the HCMV IE promoter would remain low during infection with KOS-CMV-GFP, but increase in the case of V422-CMV-GFP. It will be interesting to determine the histone levels on the HCMV promoter using the CHIP assay with samples from KOS-CMV-GFP and V422-CMV-GFP infections, in the absence and presence of cycloheximide. Secondly Hancock, et. al.,[57] showed that although the histone occupancy remained high at the promoters of V422 genome in U2OS cells, V422 replicated efficiently in this cell type. This result indicates that at least in U2OS cells, viral replication of HSV-1 may be not affected by high histone deposition on the viral genome. Therefore, it also will be interesting to look at the histone level at the HCMV promoter in U2OS cells infected with KOS-CMV-GFP and V422-CMV-GFP. This may help to clarify the connections between viral chromatin modification, viral gene expression and viral replication.

In addition, previous studies from Treizenberg group [47] demonstrated that the activation domain of VP16 is required for recruiting the transcription coactivators, including p300 and CBP histone acetyltransferase or BRM and Brg-1 remodelling enzymes, to the IE promoters of HSV-1. Hancock, et. al.,[57] showed that VP16 enhanced the level of acetylated H3 not only at the IE promoter but also E and L promoters. In addition, it has been reported that in permissive cells, the major IE promoter of HCMV is predominantly associated with histone marks of transcriptional activation, in particular acetylated histone H4 [292].

Therefore, it will be interesting to assay the level of acetylated H3 and H4 level on HCMV IE promoter from both KOS-CMV-GFP and V422-CMV-GFP infections, in the absence of viral protein synthesis. Furthermore, VP16 is reported to selectively bind to the HCF-1 associated with the Set1/Ash2 histone H3K4 methytransferase complex, which induces the active form of chromatin [58]. It also has been reported that during lytic infection, methylated H3 (H3K4me) was found at the promoters of several temporal classes of HSV-1 genes [49]. In contrast, K9 methylation of H3 was demonstrated to be involved in the repression of the major IE promoter of HCMV infection [293]. Thus, it will be interesting to compare the levels of H3K4me/H3K9me at the HCMV promoters from both KOS-CMV-GFP and V422-CMV-GFP in HeLa cells.

It is important to note that some reports suggested that the modifications on viral chromatin structure by VP16 may not correlate to its function on viral gene expression. Firstly, the Triezenberg group [54] showed that the transcriptional coactivators that modify the chromatin structure, including histone acetyltransferases p300, CBP, PCAF, and GCN5 or the BRM and Brg-1 chromatin remodeling complexes, were not required in VP16-mediated induction of IE gene expression. Another paper, authored by the same group, providing a functional VP16 in trans by HSV-2 superinfection, lead to neither an increase in the active chromatin markers on the histones or depletion of these histones on the IE genes (ICP0 and ICP27 promoters, ICP4 and ICP27 ORFs) [294]. Anyhow, these contradictory observations make the research of VP16 very interesting in the future.

Finally, VP16 may induce the viral gene expression through interacting with cellular proteins that influence where the viral genome initially localizes in the nucleus. As a tegument protein, VP16 contributes to the earliest viral activities after infection in the nucleus, either before or after the viral genome enter the nucleus. Initially, VP16 is released into the cytoplasm in host cells along with the nucleocapsid, but the temporal order of viral genome or VP16 entering the nucleus is still unknown. It has shown that after entering the nucleus, viral genomes are restricted at the inner edge of the nucleus, and shortly after, ND10 components migrate to the viral DNAs [180]. The authors also speculated that ND10 proteins are not associated with the viral genomes when the initial IE gene transcriptions occur [180]. Therefore, cellular proteins at the initial location of the viral genome may facilitate the IE gene expression, and VP16 may act as a guide to bring the genome there through direct or indirect interactions with those proteins. Silva et.al., (2008) demonstrated a potential role of A-type lamins in targeting the viral DNA and reducing the heterochromatin on viral promoters during HSV-1 lytic infection [53]. Moreover, their preliminary data showed that the assembly of VP16 activator complex onto IE promoter was dependent on the A-type lamins (unpublished data from Lindsey Silva). Furthermore, they also showed that VP16 is required for targeting the viral genome to the nuclear lamina (unpublished data from Lindsey Silva).

In metazoans, A-type and B-type lamins are the major components of the filamentous meshwork-nuclear lamina, which structurally support the nucleoplasmic surface of the inner nuclear membrane [295, 296]. The nuclear

lamina has been shown to provide a scaffold for the folding of chromosomes inside the nucleus, through binding to specific DNA sequence on the chromosomes [295]. The anchoring of DNA to the nuclear lamina may also occur through associated DNA-binding proteins. For instance, Oct-1 binds to lamin B1 and is present at the nuclear lamina in a lamin B1-dependent manner [297]. Therefore, the targeting of the incoming HSV-1 DNA to nuclear lamina may also occur though the association of Oct-1, since Oct-1 binds to the TATGARAT sequence at the IE promoter of HSV-1. This raises the possibility that the viral genome is captured by free or lamin B1-assoicated Oct-1 proteins, once it is released into the nucleus. Then the viral DNA is tethered at the nuclear lamina through Oct-1 and lamin B1 association. This speculation can be further investigated in lamin B1 silenced cells.

The nuclear lamina is also known to repress gene expression though chromatin modification with its associated proteins. It has been reported that several nuclear lamina associated proteins interact with HDACs, including Lap2β and emerin [298, 299], and hisones in chromatin near the nuclear lamina are normally hypo-acetylated, indicating a high local HDAC activity. Histone methylation is also reported to be involved in gene silencing at the nuclear lamina, including H3K9me2 [300]. In human cells, this modification is possibly mediated through an interaction of the lamina-assoicated protein BAF with the histone methyltransferase G9a [300, 301]. Therefore, VP16 may also counteract the repression of IE gene expression from the lamina-associated proteins, before the

association of ND10 components. The mechanism of VP16 blocking gene repression at nuclear lamina still needs further investigations.

However, since depletion of type A-lamins reduced the VP16 associations with viral genome and HCF-1, the roles of nuclear lamina on viral gene expression should not be limited to repression (unpublished data from Lindsey Silva). Interestingly, silencing of lamin B1 expression in nucleus increases the euchromatin formation at the nuclear lamina, but it does not elevate the transcription due to the promoter proximal stalling of RNA pol II [302]. This observation demonstrates the interactions between lamins and transcription factors that promote the escape from stalling, such as p-TEFb [302]. As mentioned in the introduction, HMBA induces HIV gene transcription through recruiting p-TEFb to promote the elongation of transcription [257]. It is possible that induction of HMBA on V422 replication in restrictive cells is also through the recruitment of p-TEFb. Since HMBA compensates the VP16 function in V422 infections, VP16 may recruit the p-TEFb or other transcription elongation factors to the initiation site of IE genes. In addition, this recruitment may be mediated by the lamin networks. Previous studies showed that disruption of lamin networks by depleting lamin B1 or expressing a truncated lamin A/C also results inactivation of transcriptions for RNA pol II [303, 304]. Together, VP16 activation complex inducing IE gene expression may be mediated by the lamin networks and their associated protein.

Overall, the roles of VP16 in initiating the HSV-1 replication may show in viral genome anchoring, euchromatin activation at the IE promoters, transcription

initiation and elongation of IE genes. The recombinant KOS or V422-derived viruses carrying the HCMV promoter-driving EGFP expression cassette are useful to discover these VP16 functions in HSV life-cycle.

4.3 Abnormal EGFP protein accumulation in KOS-HSV-GFP infections

Another unexpected result from this project is the delayed and reduced EGFP production from KOS-HSV-GFP infections in both HeLa and Vero cells. In addition, the expression of all examined viral proteins in different temporal classes (IE, E, leaky-L and L) from KOS-HSV-GFP was delayed and reduced relative to that from the parental KOS and KOS-CMV-GFP in both cell-lines (Figure 3.3.7 and 3.3.9).

The EGFP expression cassettes are inserted into the TK ORF for both KOS-derived viruses. Since the EGFP gene from KOS-CMV-GFP is expressed as a typical IE protein, the disruption of TK gene should not be the main reason for the abnormal EGFP production profile of KOS-HSV-GFP. Besides, TK gene is reported to be non-essential for viral lytic replication[305], and previous studies have showed that insertion of foreign genes into the TK locus did not affect the viral titer relative to the parental wild-type virus [306, 307]. There are three major differences between the genomic structures of KOS-HSV-GFP and KOS-CMV-GFP, which may most likely cause the different expression patterns of EGFP gene from these two viruses.

Firstly, the promoter driving the EGFP expression cassette differs between the two viruses. Detected by fluorescence microscopy, HeLa cells transfected with the plasmid pEGFP-C1 (carrying the HCMV promoter-driving

EGFP gene) showed enhanced EGFP expression compared to cells transfected with pUC19-HSV-GFP (carrying the ICP22 promoter-driving EGFP gene). This is an expected result, since the HCMV IE promoter has been shown to be active in cellular circumstance [308, 309], and the cells transfected with pUC19-HSV-GFP lack VP16 to enhance transcription from the ICP22 promoter. The preliminary data from Lucy Bradley demonstrate that cotransfection with VP16 vector increases the EGFP expression from pUC19-HSV-GFP up to the level of EGFP from pEGFP-C1 in transfected HeLa cells. Thus, the promoter should not be the reason for different EGFP expressions from KOS-HSV-GFP and KOS-CMV-GFP. Furthermore, although this difference of promoter activity could explain the reduce EGFP expression from KOS-HSV-GFP relative to KOS-CMV-GFP, it does not account for the delayed and reduced expression of other viral genes.

The second major difference between the genomes of KOS-HSV-GFP and KOS-CMV-GFP is that KOS-HSV-GFP carries an extra bacterial artificial chromosome (BAC) sequence located between the gene UL37 and UL38. KOS-HSV-GFP was constructed through BAC recombinneering (Chapter 2), based on cloning of the KOS genome as a BAC in *E. coli* [274]. Compared to the conventional methods for mutagenesis of herpesviruses, such as chemical mutagenesis, site-directed mutagenesis by homologous recombination in eukaryotic cells, BAC recombinneering is especially more efficient and less time consuming, for many herpesviruses (β- and γ-herpesviruses) because of their slow replication rate in vitro (reviewed in [310, 311]). In particular, viral BACs carried by *E. coli* strains can be stored at -80 ℃, and new viral genome DNAs can be

quickly synthesized from the BAC DNAs [311]. To date, mutagenesis using BAC technology has been applied to many human and animal herpesviruses, including HSV, HCMV, pseudorabiesvirus (PRV), EBV, Kaposi's sarcoma herpesvirus (KHSV) and murine gammaherpesvirus 68 (MHV-68) [310]. Some of the previous studies showed that excision of the BAC from the viral genome is necessary for the normal viral activities in vitro and vivo [312-315]. For instance, Adler et. al., showed that although the BAC sequence did not influence the MHV-68 replication in vitro, but the BAC-derived MHV-68 was attenuated in vivo [312]. Excision of the BAC sequence from the viral genome restored the biological properties of the recombinant MHV-68 to wild type level in vivo [312]. In another study, BAC-derived pseudorabiesvirus showed normal viral replication and virulence in animals, but displayed a growth defect in cultured cells [316]. After excision of the BAC sequence, the growth property of the recombinant viruses was comparable to those of the wild type viruses both in vivo and vitro [312-316]. Therefore, the abnormal gene expressions from KOS-HSV-GFP relative to KOS may be due to the existence of BAC sequence in its genome. This speculation need to be tested in the future. In the parental KOS37 BAC, the BAC sequence flanking with a LoxP site on either end, can be readily excised using Cre/LoxP recombination in the cells expressing the Cre enzyme [274]. After excision, the KOS37 virus with a single LoxP site grows very similarly to the wild-type KOS virus, both in vivo and in vitro. However, the authors did not compare the protein expression or the growth curve of KOS37 BAC virus and KOS37 virus in their paper [43]. Therefore, in this case, the BAC sequence could

be removed from the viral genome by growing the KOS-HSV-GFP virus in Cre-Vero cells.

Finally, as described in the section 2.2 (methods and materials), the genome of KOS-HSV-GFP has a sequence deletion and insertion between the 429st and 451st nt of the TK ORF, relative to that of KOS-CMV-GFP. In other words, after homologous recombination, the sequence between the 430th and 450th nt of the TK ORF in the genome of KOS-HSV-GFP was replaced with the EGFP cassette bearing 20 nts of pUC19 sequences at either end. In contrast, the EGFP expression cassette was the only sequence inserted into the TK ORF (between the 422nd and 423rd nt) of KOS-CMV-GFP without any deletion from the TK gene. The sequence deleted from the TK ORF of KOS-HSV-GFP was within the promoter region of UL24 gene [317]. Therefore, this sequence deletion and insertion (pUC19 vector sequence flanking at the EGFP cassette) in KOS-HSV-GFP genome may lead to the abnormal expression of UL24 gene during infection.

UL24 is a 30-kDa protein, expressed with leaky-late kinetics during HSV-1 infection [318]. In the HSV-1 genome, the regulatory and coding sequences of UL24 gene overlap with the ORF of TK gene at its 5' end in a head-to-head orientation [317]. The UL24 gene is conserved among all the three subfamilies (α-, β- and γ-herpesvirus) of *Herpesviridae*, and this conservation suggests an important role for UL24 in the life cycle of these viruses [319]. Indeed UL24 null mutations and mutations in the conserved regions of UL24 cause defects in viral growth, indicating that the UL24 protein is not essential but is important for viral lytic lifecycle in vitro [320]. The detailed function of the UL24 protein in HSV-1

replication is still unknown and under investigation. UL24 has been shown to localize to the nucleus after expression, and it mediates the dispersal of the nucleolar protein nucleolin [321]. Nucleolin is found in the heart of the nucleolus, which is a major site of many nuclear functions, such as rRNA production, and ribosome assembly. As a multi-functional protein, Nucleolin has been implicated in many metabolic processes, including ribosomal biogenesis, cytokinesis, nucleogenesis, cell proliferation and growth (reviewed in [322]). UL24 has been shown to be sufficient to induce the redistribution of nucleolin in the absence viral proteins [321, 323]. Previous study has demonstrated that the UL24 gene of HSV-1 encodes a putative PD-(D/E)XK endonuclease domain [324], and this motif is reported to be important for the ability of UL24 to disperse the nucleolin during infection [325]. Due to these important roles of UL24 in the viral lifecycle, disruption of UL24 expression may relate to the abnormal gene expression profile of KOS-HSV-GFP (Figure 3.3.7 & 3.3.9). Since the EGFP gene is inserted at the promoter region of UL24, the deleted sequence (430^{th}-450^{th} nts of TK ORF) from KOS-HSV-GFP genome may contain important elements for inducing UL24 expression upon infection. This speculation need to be investigated in the future. To test this, firstly, the gene expression profile of UL24 (at both RNA and protein levels) from KOS-HSV-GFP infection needs to be assayed and compared to that from KOS infection. If KOS-HSV-GFP produces abnormal amount of UL24 comparing to KOS (it is likely to be the case, since the productions of all checked viral genes in the three classes-IE, E and L were delayed and reduced in samples from KOS-HSV-GFP relative to KOS, shown in Figure 3.3.7 & 3.3.9), it will be

interesting to assay the expression profile of UL24 from a new KOS-HSV-GFP virus (which does not contain the BAC sequence and have any deletion at the TK ORF), and compare to that from KOS and previously made KOS-HSV-GFP.

4.4 Future directions:

One major reason that I constructed the KOS/V422-HSV-GFP viruses was the concern that the HCMV IE promoter of the EGFP gene from KOS/V422-CMV-GFP would not be regulated by the VP16 protein during infection. If so, then the KOS/V422-CMV-GFP viruses would not be suitable for the original rational of this project, which was to identify the cellular factors that silenced by VP16 during wild-type HSV-1 infection. However, Figure 3.3.4 provides evidence that the HCMV IE promoter was in fact under the control of VP16. This conclusion still needs further testing. If the HCMV IE promoter is confirmed to be induced by VP16, the KOS-HCMV-GFP and V422-CMV-GFP viruses could be very useful in a siRNA screen to identify the host inhibitory factors that are blocked by wild-type VP16 during HSV-1 infection. Also, the KOS-CMV-GFP viruses can be used to identify the host factors that facilitate the viral replication, in a siRNA screen.

As described in last section 4.3, the delayed and reduced gene expression of KOS-HSV-GFP may be caused by sequence deletion in the UL24 promoter region and insertion of BAC sequence between the UL37 and UL38 genes. Thus, in the future, this KOS-HSV-GFP virus will be modified to have a complete UL24 promoter, and the BAC sequence will be deleted from its genome. Then, we are going to perform northern and western blot analysis (as the experiments

described in section 3.3.1) to check whether the viral gene expression of this modified KOS-HSV-GFP, is comparable to that of the parental KOS. If so, this virus and the V422-HSV-GFP with the same modifications can be used in the siRNA screen to identify the cellular factors that regulate the viral IE gene expression during HSV-1 lytic infection.

As mentioned in section 3.2 (results), the Envision plate reader was not sensitive enough to catch the signal of EGFP in KOS-HSV-GFP infected cells even at high MOI. Besides the modifications of this virus mentioned above, the EGFP reporter gene can also be changed. Other reporter genes with stronger signals than EGFP, such as luciferase and β-galactosidase genes, can also be inserted into the KOS/V422 genome to construct more sensitive ones for the plate reader. Also, the siRNA screen can be performed without using a reporter virus. After the siRNA trasnfection and then infection with KOS or V422 virus, the viral activities can be detected by in-cell western technology with an antibody against an IE protein, such as ICP0 or ICP4.

References:

1. Fields BN, Knipe DM, Howley PM: *Fields virology.* 5th edn. Philadelphia: Wolters Kluwer Health/Lippincott Williams & Wilkins; 2007.
2. McGeoch DJ, Dalrymple MA, Davison AJ, Dolan A, Frame MC, McNab D, Perry LJ, Scott JE, Taylor P: **The complete DNA sequence of the long unique region in the genome of herpes simplex virus type 1.** *J Gen Virol* 1988, **69 (Pt 7):**1531-1574.
3. Hayward GS, Jacob RJ, Wadsworth SC, Roizman B: **Anatomy of herpes simplex virus DNA: evidence for four populations of molecules that differ in the relative orientations of their long and short components.** *Proc Natl Acad Sci U S A* 1975, **72:**4243-4247.
4. Schrag JD, Prasad BV, Rixon FJ, Chiu W: **Three-dimensional structure of the HSV1 nucleocapsid.** *Cell* 1989, **56:**651-660.
5. Zhou ZH, Dougherty M, Jakana J, He J, Rixon FJ, Chiu W: **Seeing the herpesvirus capsid at 8.5 A.** *Science* 2000, **288:**877-880.
6. Subak-Sharpe JH, Dargan DJ: **HSV molecular biology: general aspects of herpes simplex virus molecular biology.** *Virus Genes* 1998, **16:**239-251.
7. Campbell ME, Palfreyman JW, Preston CM: **Identification of herpes simplex virus DNA sequences which encode a trans-acting polypeptide responsible for stimulation of immediate early transcription.** *J Mol Biol* 1984, **180:**1-19.
8. Kwong AD, Frenkel N: **The herpes simplex virus virion host shutoff function.** *J Virol* 1989, **63:**4834-4839.
9. Sciortino MT, Suzuki M, Taddeo B, Roizman B: **RNAs extracted from herpes simplex virus 1 virions: apparent selectivity of viral but not cellular RNAs packaged in virions.** *J Virol* 2001, **75:**8105-8116.
10. Sciortino MT, Taddeo B, Poon AP, Mastino A, Roizman B: **Of the three tegument proteins that package mRNA in herpes simplex virions, one (VP22) transports the mRNA to uninfected cells for expression prior to viral infection.** *Proc Natl Acad Sci U S A* 2002, **99:**8318-8323.
11. McKnight JL, Doerr M, Zhang Y: **An 85-kilodalton herpes simplex virus type 1 alpha trans-induction factor (VP16)-VP13/14 fusion protein retains the transactivation and structural properties of the wild-type molecule during virus infection.** *J Virol* 1994, **68:**1750-1757.
12. Elliott G, O'Hare P: **Intercellular trafficking and protein delivery by a herpesvirus structural protein.** *Cell* 1997, **88:**223-233.
13. Grunewald K, Desai P, Winkler DC, Heymann JB, Belnap DM, Baumeister W, Steven AC: **Three-dimensional structure of herpes simplex virus from cryo-electron tomography.** *Science* 2003, **302:**1396-1398.
14. Spear PG, Roizman B: **Buoyant density of herpes simplex virus in solutions of caesium chloride.** *Nature* 1967, **214:**713-714.
15. Spear PG, Eisenberg RJ, Cohen GH: **Three classes of cell surface receptors for alphaherpesvirus entry.** *Virology* 2000, **275:**1-8.

16. Stevens JG, Haarr L, Porter DD, Cook ML, Wagner EK: **Prominence of the herpes simplex virus latency-associated transcript in trigeminal ganglia from seropositive humans.** *J Infect Dis* 1988, **158:**117-123.
17. Taylor TJ, Brockman MA, McNamee EE, Knipe DM: **Herpes simplex virus.** *Front Biosci* 2002, **7:**d752-764.
18. Wittels M, Spear PG: **Penetration of cells by herpes simplex virus does not require a low pH-dependent endocytic pathway.** *Virus Res* 1991, **18:**271-290.
19. Herold BC, Visalli RJ, Susmarski N, Brandt CR, Spear PG: **Glycoprotein C-independent binding of herpes simplex virus to cells requires cell surface heparan sulphate and glycoprotein B.** *J Gen Virol* 1994, **75 (Pt 6):**1211-1222.
20. Laquerre S, Argnani R, Anderson DB, Zucchini S, Manservigi R, Glorioso JC: **Heparan sulfate proteoglycan binding by herpes simplex virus type 1 glycoproteins B and C, which differ in their contributions to virus attachment, penetration, and cell-to-cell spread.** *J Virol* 1998, **72:**6119-6130.
21. Reske A, Pollara G, Krummenacher C, Chain BM, Katz DR: **Understanding HSV-1 entry glycoproteins.** *Rev Med Virol* 2007, **17:**205-215.
22. Krummenacher C, Supekar VM, Whitbeck JC, Lazear E, Connolly SA, Eisenberg RJ, Cohen GH, Wiley DC, Carfi A: **Structure of unliganded HSV gD reveals a mechanism for receptor-mediated activation of virus entry.** *EMBO J* 2005, **24:**4144-4153.
23. Cocchi F, Fusco D, Menotti L, Gianni T, Eisenberg RJ, Cohen GH, Campadelli-Fiume G: **The soluble ectodomain of herpes simplex virus gD contains a membrane-proximal pro-fusion domain and suffices to mediate virus entry.** *Proc Natl Acad Sci U S A* 2004, **101:**7445-7450.
24. Chiang HY, Cohen GH, Eisenberg RJ: **Identification of functional regions of herpes simplex virus glycoprotein gD by using linker-insertion mutagenesis.** *J Virol* 1994, **68:**2529-2543.
25. Cairns TM, Milne RS, Ponce-de-Leon M, Tobin DK, Cohen GH, Eisenberg RJ: **Structure-function analysis of herpes simplex virus type 1 gD and gH-gL: clues from gDgH chimeras.** *J Virol* 2003, **77:**6731-6742.
26. Cai WZ, Person S, DebRoy C, Gu BH: **Functional regions and structural features of the gB glycoprotein of herpes simplex virus type 1. An analysis of linker insertion mutants.** *J Mol Biol* 1988, **201:**575-588.
27. Peng T, Ponce de Leon M, Novotny MJ, Jiang H, Lambris JD, Dubin G, Spear PG, Cohen GH, Eisenberg RJ: **Structural and antigenic analysis of a truncated form of the herpes simplex virus glycoprotein gH-gL complex.** *J Virol* 1998, **72:**6092-6103.
28. Dubin G, Jiang H: **Expression of herpes simplex virus type 1 glycoprotein L (gL) in transfected mammalian cells: evidence that gL**

is not independently anchored to cell membranes. *J Virol* 1995, **69:**4564-4568.
29. Hutchinson L, Browne H, Wargent V, Davis-Poynter N, Primorac S, Goldsmith K, Minson AC, Johnson DC: **A novel herpes simplex virus glycoprotein, gL, forms a complex with glycoprotein H (gH) and affects normal folding and surface expression of gH.** *J Virol* 1992, **66:**2240-2250.
30. Roop C, Hutchinson L, Johnson DC: **A mutant herpes simplex virus type 1 unable to express glycoprotein L cannot enter cells, and its particles lack glycoprotein H.** *J Virol* 1993, **67:**2285-2297.
31. Batterson W, Furlong D, Roizman B: **Molecular genetics of herpes simplex virus. VIII. further characterization of a temperature-sensitive mutant defective in release of viral DNA and in other stages of the viral reproductive cycle.** *J Virol* 1983, **45:**397-407.
32. Knipe DM, Batterson W, Nosal C, Roizman B, Buchan A: **Molecular genetics of herpes simplex virus. VI. Characterization of a temperature-sensitive mutant defective in the expression of all early viral gene products.** *J Virol* 1981, **38:**539-547.
33. Dohner K, Wolfstein A, Prank U, Echeverri C, Dujardin D, Vallee R, Sodeik B: **Function of dynein and dynactin in herpes simplex virus capsid transport.** *Mol Biol Cell* 2002, **13:**2795-2809.
34. Sodeik B, Ebersold MW, Helenius A: **Microtubule-mediated transport of incoming herpes simplex virus 1 capsids to the nucleus.** *J Cell Biol* 1997, **136:**1007-1021.
35. Ojala PM, Sodeik B, Ebersold MW, Kutay U, Helenius A: **Herpes simplex virus type 1 entry into host cells: reconstitution of capsid binding and uncoating at the nuclear pore complex in vitro.** *Mol Cell Biol* 2000, **20:**4922-4931.
36. Jovasevic V, Liang L, Roizman B: **Proteolytic cleavage of VP1-2 is required for release of herpes simplex virus 1 DNA into the nucleus.** *J Virol* 2008, **82:**3311-3319.
37. Wysocka J, Herr W: **The herpes simplex virus VP16-induced complex: the makings of a regulatory switch.** *Trends Biochem Sci* 2003, **28:**294-304.
38. Smiley JR, Elgadi MM, Saffran HA: **Herpes simplex virus vhs protein.** *Methods Enzymol* 2001, **342:**440-451.
39. Cohen GH, Ponce de Leon M, Diggelmann H, Lawrence WC, Vernon SK, Eisenberg RJ: **Structual analysis of the capsid polypeptides of herpes simplex virus type 1 and 2.** *J Virol* 1980, **34:**521-531.
40. Oh J, Fraser NW: **Temporal association of the herpes simplex virus genome with histone proteins during a lytic infection.** *J Virol* 2008, **82:**3530-3537.
41. Pignatti PF, Cassai E: **Analysis of herpes simplex virus nucleoprotein complexes extracted from infected cells.** *J Virol* 1980, **36:**816-828.
42. Poffenberger KL, Roizman B: **A noninverting genome of a viable herpes simplex virus 1: presence of head-to-tail linkages in packaged**

genomes and requirements for circularization after infection. *J Virol* 1985, **53:**587-595.
43. Garber DA, Beverley SM, Coen DM: **Demonstration of circularization of herpes simplex virus DNA following infection using pulsed field gel electrophoresis.** *Virology* 1993, **197:**459-462.
44. Ferenczy MW, DeLuca NA: **Epigenetic modulation of gene expression from quiescent herpes simplex virus genomes.** *J Virol* 2009, **83:**8514-8524.
45. Leinbach SS, Summers WC: **The structure of herpes simplex virus type 1 DNA as probed by micrococcal nuclease digestion.** *J Gen Virol* 1980, **51:**45-59.
46. Muggeridge MI, Fraser NW: **Chromosomal organization of the herpes simplex virus genome during acute infection of the mouse central nervous system.** *J Virol* 1986, **59:**764-767.
47. Herrera FJ, Triezenberg SJ: **VP16-dependent association of chromatin-modifying coactivators and underrepresentation of histones at immediate-early gene promoters during herpes simplex virus infection.** *J Virol* 2004, **78:**9689-9696.
48. Cliffe AR, Knipe DM: **Herpes simplex virus ICP0 promotes both histone removal and acetylation on viral DNA during lytic infection.** *J Virol* 2008, **82:**12030-12038.
49. Huang J, Kent JR, Placek B, Whelan KA, Hollow CM, Zeng PY, Fraser NW, Berger SL: **Trimethylation of histone H3 lysine 4 by Set1 in the lytic infection of human herpes simplex virus 1.** *J Virol* 2006, **80:**5740-5746.
50. Kent JR, Zeng PY, Atanasiu D, Gardner J, Fraser NW, Berger SL: **During lytic infection herpes simplex virus type 1 is associated with histones bearing modifications that correlate with active transcription.** *J Virol* 2004, **78:**10178-10186.
51. Berger SL: **The complex language of chromatin regulation during transcription.** *Nature* 2007, **447:**407-412.
52. Placek BJ, Berger SL: **Chromatin dynamics during herpes simplex virus-1 lytic infection.** *Biochim Biophys Acta* 2010, **1799:**223-227.
53. Silva L, Cliffe A, Chang L, Knipe DM: **Role for A-type lamins in herpesviral DNA targeting and heterochromatin modulation.** *PLoS Pathog* 2008, **4:**e1000071.
54. Kutluay SB, DeVos SL, Klomp JE, Triezenberg SJ: **Transcriptional coactivators are not required for herpes simplex virus type 1 immediate-early gene expression in vitro.** *J Virol* 2009, **83:**3436-3449.
55. van Leeuwen H, Okuwaki M, Hong R, Chakravarti D, Nagata K, O'Hare P: **Herpes simplex virus type 1 tegument protein VP22 interacts with TAF-I proteins and inhibits nucleosome assembly but not regulation of histone acetylation by INHAT.** *J Gen Virol* 2003, **84:**2501-2510.
56. Seo SB, McNamara P, Heo S, Turner A, Lane WS, Chakravarti D: **Regulation of histone acetylation and transcription by INHAT, a**

human cellular complex containing the set oncoprotein. *Cell* 2001, **104:**119-130.
57. Hancock MH, Cliffe AR, Knipe DM, Smiley JR: **Herpes simplex virus VP16, but not ICP0, is required to reduce histone occupancy and enhance histone acetylation on viral genomes in U2OS osteosarcoma cells.** *J Virol* 2010, **84:**1366-1375.
58. Wysocka J, Myers MP, Laherty CD, Eisenman RN, Herr W: **Human Sin3 deacetylase and trithorax-related Set1/Ash2 histone H3-K4 methyltransferase are tethered together selectively by the cell-proliferation factor HCF-1.** *Genes & Development* 2003, **17:**896-911.
59. Hobbs WE, 2nd, DeLuca NA: **Perturbation of cell cycle progression and cellular gene expression as a function of herpes simplex virus ICP0.** *J Virol* 1999, **73:**8245-8255.
60. Lieu PT, Wagner EK: **Two leaky-late HSV-1 promoters differ significantly in structural architecture.** *Virology* 2000, **272:**191-203.
61. Gu H, Liang Y, Mandel G, Roizman B: **Components of the REST/CoREST/histone deacetylase repressor complex are disrupted, modified, and translocated in HSV-1-infected cells.** *Proc Natl Acad Sci U S A* 2005, **102:**7571-7576.
62. Gu H, Roizman B: **Herpes simplex virus-infected cell protein 0 blocks the silencing of viral DNA by dissociating histone deacetylases from the CoREST-REST complex.** *Proc Natl Acad Sci U S A* 2007, **104:**17134-17139.
63. La Boissiere S, Hughes T, O'Hare P: **HCF-dependent nuclear import of VP16.** *EMBO J* 1999, **18:**480-489.
64. Mackem S, Roizman B: **Regulation of herpesvirus macromolecular synthesis: transcription-initiation sites and domains of alpha genes.** *Proc Natl Acad Sci U S A* 1980, **77:**7122-7126.
65. Mackem S, Roizman B: **Structural features of the herpes simplex virus alpha gene 4, 0, and 27 promoter-regulatory sequences which confer alpha regulation on chimeric thymidine kinase genes.** *J Virol* 1982, **44:**939-949.
66. Everett RD: **A detailed mutational analysis of Vmw110, a trans-acting transcriptional activator encoded by herpes simplex virus type 1.** *EMBO J* 1987, **6:**2069-2076.
67. Everett RD: **Analysis of the functional domains of herpes simplex virus type 1 immediate-early polypeptide Vmw110.** *J Mol Biol* 1988, **202:**87-96.
68. Advani SJ, Hagglund R, Weichselbaum RR, Roizman B: **Posttranslational processing of infected cell proteins 0 and 4 of herpes simplex virus 1 is sequential and reflects the subcellular compartment in which the proteins localize.** *J Virol* 2001, **75:**7904-7912.
69. Advani SJ, Weichselbaum RR, Roizman B: **The role of cdc2 in the expression of herpes simplex virus genes.** *Proc Natl Acad Sci U S A* 2000, **97:**10996-11001.

70. Ogle WO, Ng TI, Carter KL, Roizman B: **The UL13 protein kinase and the infected cell type are determinants of posttranslational modification of ICP0.** *Virology* 1997, **235:**406-413.
71. Blaho JA, Mitchell C, Roizman B: **Guanylylation and adenylylation of the alpha regulatory proteins of herpes simplex virus require a viral beta or gamma function.** *J Virol* 1993, **67:**3891-3900.
72. Everett RD, Maul GG: **HSV-1 IE protein Vmw110 causes redistribution of PML.** *EMBO J* 1994, **13:**5062-5069.
73. Kawaguchi Y, Bruni R, Roizman B: **Interaction of herpes simplex virus 1 alpha regulatory protein ICP0 with elongation factor 1delta: ICP0 affects translational machinery.** *J Virol* 1997, **71:**1019-1024.
74. Lopez P, Van Sant C, Roizman B: **Requirements for the nuclear-cytoplasmic translocation of infected-cell protein 0 of herpes simplex virus 1.** *J Virol* 2001, **75:**3832-3840.
75. Van Sant C, Lopez P, Advani SJ, Roizman B: **Role of cyclin D3 in the biology of herpes simplex virus 1 ICPO.** *J Virol* 2001, **75:**1888-1898.
76. Van Sant C, Hagglund R, Lopez P, Roizman B: **The infected cell protein 0 of herpes simplex virus 1 dynamically interacts with proteasomes, binds and activates the cdc34 E2 ubiquitin-conjugating enzyme, and possesses in vitro E3 ubiquitin ligase activity.** *Proc Natl Acad Sci U S A* 2001, **98:**8815-8820.
77. Everett RD: **ICP0 induces the accumulation of colocalizing conjugated ubiquitin.** *J Virol* 2000, **74:**9994-10005.
78. Parkinson J, Everett RD: **Alphaherpesvirus proteins related to herpes simplex virus type 1 ICP0 induce the formation of colocalizing, conjugated ubiquitin.** *J Virol* 2001, **75:**5357-5362.
79. Everett RD, Freemont P, Saitoh H, Dasso M, Orr A, Kathoria M, Parkinson J: **The disruption of ND10 during herpes simplex virus infection correlates with the Vmw110- and proteasome-dependent loss of several PML isoforms.** *J Virol* 1998, **72:**6581-6591.
80. Everett RD, Meredith M, Orr A, Cross A, Kathoria M, Parkinson J: **A novel ubiquitin-specific protease is dynamically associated with the PML nuclear domain and binds to a herpesvirus regulatory protein.** *EMBO J* 1997, **16:**1519-1530.
81. Stadler M, Chelbi-Alix MK, Koken MH, Venturini L, Lee C, Saib A, Quignon F, Pelicano L, Guillemin MC, Schindler C, et al.: **Transcriptional induction of the PML growth suppressor gene by interferons is mediated through an ISRE and a GAS element.** *Oncogene* 1995, **11:**2565-2573.
82. Guldner HH, Szostecki C, Grotzinger T, Will H: **IFN enhance expression of Sp100, an autoantigen in primary biliary cirrhosis.** *J Immunol* 1992, **149:**4067-4073.
83. Grotzinger T, Jensen K, Will H: **The interferon (IFN)-stimulated gene Sp100 promoter contains an IFN-gamma activation site and an imperfect IFN-stimulated response element which mediate type I IFN inducibility.** *J Biol Chem* 1996, **271:**25253-25260.

84. Negorev D, Maul GG: **Cellular proteins localized at and interacting within ND10/PML nuclear bodies/PODs suggest functions of a nuclear depot.** *Oncogene* 2001, **20:**7234-7242.
85. Hollenbach AD, McPherson CJ, Mientjes EJ, Iyengar R, Grosveld G: **Daxx and histone deacetylase II associate with chromatin through an interaction with core histones and the chromatin-associated protein Dek.** *J Cell Sci* 2002, **115:**3319-3330.
86. Luciani JJ, Depetris D, Usson Y, Metzler-Guillemain C, Mignon-Ravix C, Mitchell MJ, Megarbane A, Sarda P, Sirma H, Moncla A, et al: **PML nuclear bodies are highly organised DNA-protein structures with a function in heterochromatin remodelling at the G2 phase.** *J Cell Sci* 2006, **119:**2518-2531.
87. Zhang R, Poustovoitov MV, Ye X, Santos HA, Chen W, Daganzo SM, Erzberger JP, Serebriiskii IG, Canutescu AA, Dunbrack RL, et al: **Formation of MacroH2A-containing senescence-associated heterochromatin foci and senescence driven by ASF1a and HIRA.** *Dev Cell* 2005, **8:**19-30.
88. Zhong S, Hu P, Ye TZ, Stan R, Ellis NA, Pandolfi PP: **A role for PML and the nuclear body in genomic stability.** *Oncogene* 1999, **18:**7941-7947.
89. Eskiw CH, Dellaire G, Bazett-Jones DP: **Chromatin contributes to structural integrity of promyelocytic leukemia bodies through a SUMO-1-independent mechanism.** *J Biol Chem* 2004, **279:**9577-9585.
90. Ching RW, Dellaire G, Eskiw CH, Bazett-Jones DP: **PML bodies: a meeting place for genomic loci?** *J Cell Sci* 2005, **118:**847-854.
91. Everett RD, Rechter S, Papior P, Tavalai N, Stamminger T, Orr A: **PML contributes to a cellular mechanism of repression of herpes simplex virus type 1 infection that is inactivated by ICP0.** *J Virol* 2006, **80:**7995-8005.
92. Everett RD, Parada C, Gripon P, Sirma H, Orr A: **Replication of ICP0-null mutant herpes simplex virus type 1 is restricted by both PML and Sp100.** *J Virol* 2008, **82:**2661-2672.
93. Lukashchuk V, Everett RD: **Regulation of ICP0-null mutant herpes simplex virus type 1 infection by ND10 components ATRX and hDaxx** *J Virol* 2010, **84:**4026-4040.
94. Wilkinson KD: **Roles of ubiquitinylation in proteolysis and cellular regulation.** *Annu Rev Nutr* 1995, **15:**161-189.
95. Everett RD, Earnshaw WC, Findlay J, Lomonte P: **Specific destruction of kinetochore protein CENP-C and disruption of cell division by herpes simplex virus immediate-early protein Vmw110.** *EMBO J* 1999, **18:**1526-1538.
96. Lomonte P, Sullivan KF, Everett RD: **Degradation of nucleosome-associated centromeric histone H3-like protein CENP-A induced by herpes simplex virus type 1 protein ICP0.** *J Biol Chem* 2001, **276:**5829-5835.

97. Paladino P, Collins SE, Mossman KL: **Cellular localization of the herpes simplex virus ICP0 protein dictates its ability to block IRF3-mediated innate immune responses.** *PLoS One*, **5:**e10428.
98. Lomonte P, Thomas J, Texier P, Caron C, Khochbin S, Epstein AL: **Functional interaction between class II histone deacetylases and ICP0 of herpes simplex virus type 1.** *J Virol* 2004, **78:**6744-6757.
99. Kawaguchi Y, Tanaka M, Yokoymama A, Matsuda G, Kato K, Kagawa H, Hirai K, Roizman B: **Herpes simplex virus 1 alpha regulatory protein ICP0 functionally interacts with cellular transcription factor BMAL1.** *Proc Natl Acad Sci U S A* 2001, **98:**1877-1882.
100. Kalamvoki M, Roizman B: **Circadian CLOCK histone acetyl transferase localizes at ND10 nuclear bodies and enables herpes simplex virus gene expression.** *Proc Natl Acad Sci U S A* 2010, **107:**17721-17726.
101. Kawaguchi Y, Van Sant C, Roizman B: **Eukaryotic elongation factor 1delta is hyperphosphorylated by the protein kinase encoded by the U(L)13 gene of herpes simplex virus 1.** *J Virol* 1998, **72:**1731-1736.
102. Kawaguchi Y, Kato K, Tanaka M, Kanamori M, Nishiyama Y, Yamanashi Y: **Conserved protein kinases encoded by herpesviruses and cellular protein kinase cdc2 target the same phosphorylation site in eukaryotic elongation factor 1delta.** *J Virol* 2003, **77:**2359-2368.
103. Kalamvoki M, Roizman B: **Interwoven roles of cyclin D3 and cdk4 recruited by ICP0 and ICP4 in the expression of herpes simplex virus genes.** *J Virol* 2010, **84:**9709-9717.
104. Gelman IH, Silverstein S: **Co-ordinate regulation of herpes simplex virus gene expression is mediated by the functional interaction of two immediate early gene products.** *J Mol Biol* 1986, **191:**395-409.
105. Everett RD: **Trans activation of transcription by herpes virus products: requirement for two HSV-1 immediate-early polypeptides for maximum activity.** *EMBO J* 1984, **3:**3135-3141.
106. Liu M, Rakowski B, Gershburg E, Weisend CM, Lucas O, Schmidt EE, Halford WP: **ICP0 antagonizes ICP4-dependent silencing of the herpes simplex virus ICP0 gene.** *PLoS One* 2010, **5:**e8837.
107. Harris RA, Everett RD, Zhu XX, Silverstein S, Preston CM: **Herpes simplex virus type 1 immediate-early protein Vmw110 reactivates latent herpes simplex virus type 2 in an in vitro latency system.** *J Virol* 1989, **63:**3513-3515.
108. Stow EC, Stow ND: **Complementation of a herpes simplex virus type 1 Vmw110 deletion mutant by human cytomegalovirus.** *J Gen Virol* 1989, **70 (Pt 3):**695-704.
109. Preston CM, Nicholl MJ: **Repression of gene expression upon infection of cells with herpes simplex virus type 1 mutants impaired for immediate-early protein synthesis.** *J Virol* 1997, **71:**7807-7813.
110. Samaniego LA, Neiderhiser L, DeLuca NA: **Persistence and expression of the herpes simplex virus genome in the absence of immediate-early proteins.** *J Virol* 1998, **72:**3307-3320.

111. Preston CM: **Reactivation of expression from quiescent herpes simplex virus type 1 genomes in the absence of immediate-early protein ICP0.** *J Virol* 2007, **81:**11781-11789.
112. Courtney RJ, Benyesh-Melnick M: **Isolation and characterization of a large molecular-weight polypeptide of herpes simplex virus type 1.** *Virology* 1974, **62:**539-551.
113. Meisterernst M, Roy AL, Lieu HM, Roeder RG: **Activation of class II gene transcription by regulatory factors is potentiated by a novel activity.** *Cell* 1991, **66:**981-993.
114. Shepard AA, Tolentino P, DeLuca NA: **trans-dominant inhibition of herpes simplex virus transcriptional regulatory protein ICP4 by heterodimer formation.** *J Virol* 1990, **64:**3916-3926.
115. Everett RD, Sourvinos G, Leiper C, Clements JB, Orr A: **Formation of nuclear foci of the herpes simplex virus type 1 regulatory protein ICP4 at early times of infection: localization, dynamics, recruitment of ICP27, and evidence for the de novo induction of ND10-like complexes.** *J Virol* 2004, **78:**1903-1917.
116. Carrozza MJ, DeLuca NA: **Interaction of the viral activator protein ICP4 with TFIID through TAF250.** *Mol Cell Biol* 1996, **16:**3085-3093.
117. Gu B, Kuddus R, DeLuca NA: **Repression of activator-mediated transcription by herpes simplex virus ICP4 via a mechanism involving interactions with the basal transcription factors TATA-binding protein and TFIIB.** *Mol Cell Biol* 1995, **15:**3618-3626.
118. Smith CA, Bates P, Rivera-Gonzalez R, Gu B, DeLuca NA: **ICP4, the major transcriptional regulatory protein of herpes simplex virus type 1, forms a tripartite complex with TATA-binding protein and TFIIB.** *J Virol* 1993, **67:**4676-4687.
119. Sampath P, Deluca NA: **Binding of ICP4, TATA-binding protein, and RNA polymerase II to herpes simplex virus type 1 immediate-early, early, and late promoters in virus-infected cells.** *J Virol* 2008, **82:**2339-2349.
120. Kuddus RH, DeLuca NA: **DNA-dependent oligomerization of herpes simplex virus type 1 regulatory protein ICP4.** *J Virol* 2007, **81:**9230-9237.
121. DeLuca NA, Schaffer PA: **Activities of herpes simplex virus type 1 (HSV-1) ICP4 genes specifying nonsense peptides.** *Nucleic Acids Res* 1987, **15:**4491-4511.
122. DeLuca NA, Schaffer PA: **Physical and functional domains of the herpes simplex virus transcriptional regulatory protein ICP4.** *J Virol* 1988, **62:**732-743.
123. Gu B, DeLuca N: **Requirements for activation of the herpes simplex virus glycoprotein C promoter in vitro by the viral regulatory protein ICP4.** *J Virol* 1994, **68:**7953-7965.
124. Shepard AA, Imbalzano AN, DeLuca NA: **Separation of primary structural components conferring autoregulation, transactivation, and**

DNA-binding properties to the herpes simplex virus transcriptional regulatory protein ICP4. *J Virol* 1989, **63:**3714-3728.
125. Shepard AA, DeLuca NA: **Intragenic complementation among partial peptides of herpes simplex virus regulatory protein ICP4.** *J Virol* 1989, **63:**1203-1211.
126. DeLuca NA, Schaffer PA: **Activation of immediate-early, early, and late promoters by temperature-sensitive and wild-type forms of herpes simplex virus type 1 protein ICP4.** *Mol Cell Biol* 1985, **5:**1997-2008.
127. O'Hare P, Hayward GS: **Comparison of upstream sequence requirements for positive and negative regulation of a herpes simplex virus immediate-early gene by three virus-encoded trans-acting factors.** *J Virol* 1987, **61:**190-199.
128. Roberts MS, Boundy A, O'Hare P, Pizzorno MC, Ciufo DM, Hayward GS: **Direct correlation between a negative autoregulatory response element at the cap site of the herpes simplex virus type 1 IE175 (alpha 4) promoter and a specific binding site for the IE175 (ICP4) protein.** *J Virol* 1988, **62:**4307-4320.
129. Smiley JR, Johnson DC, Pizer LI, Everett RD: **The ICP4 binding sites in the herpes simplex virus type 1 glycoprotein D (gD) promoter are not essential for efficient gD transcription during virus infection.** *J Virol* 1992, **66:**623-631.
130. Imbalzano AN, Coen DM, DeLuca NA: **Herpes simplex virus transactivator ICP4 operationally substitutes for the cellular transcription factor Sp1 for efficient expression of the viral thymidine kinase gene.** *J Virol* 1991, **65:**565-574.
131. Mavromara-Nazos P, Silver S, Hubenthal-Voss J, McKnight JL, Roizman B: **Regulation of herpes simplex virus 1 genes: alpha gene sequence requirements for transient induction of indicator genes regulated by beta or late (gamma 2) promoters.** *Virology* 1986, **149:**152-164.
132. Shapira M, Homa FL, Glorioso JC, Levine M: **Regulation of the herpes simplex virus type 1 late (gamma 2) glycoprotein C gene: sequences between base pairs -34 to +29 control transient expression and responsiveness to transactivation by the products of the immediate early (alpha) 4 and 0 genes.** *Nucleic Acids Res* 1987, **15:**3097-3111.
133. Grondin B, DeLuca N: **Herpes simplex virus type 1 ICP4 promotes transcription preinitiation complex formation by enhancing the binding of TFIID to DNA.** *J Virol* 2000, **74:**11504-11510.
134. O'Hare P, Hayward GS: **Three trans-acting regulatory proteins of herpes simplex virus modulate immediate-early gene expression in a pathway involving positive and negative feedback regulation.** *J Virol* 1985, **56:**723-733.
135. Gu B, Rivera-Gonzalez R, Smith CA, DeLuca NA: **Herpes simplex virus infected cell polypeptide 4 preferentially represses Sp1-activated over basal transcription from its own promoter.** *Proc Natl Acad Sci U S A* 1993, **90:**9528-9532.

136. Rivera-Gonzalez R, Imbalzano AN, Gu B, Deluca NA: **The role of ICP4 repressor activity in temporal expression of the IE-3 and latency-associated transcript promoters during HSV-1 infection.** *Virology* 1994, **202:**550-564.
137. Stelz G, Rucker E, Rosorius O, Meyer G, Stauber RH, Spatz M, Eibl MM, Hauber J: **Identification of two nuclear import signals in the alpha-gene product ICP22 of herpes simplex virus 1.** *Virology* 2002, **295:**360-370.
138. Purves FC, Ogle WO, Roizman B: **Processing of the herpes simplex virus regulatory protein alpha 22 mediated by the UL13 protein kinase determines the accumulation of a subset of alpha and gamma mRNAs and proteins in infected cells.** *Proc Natl Acad Sci U S A* 1993, **90:**6701-6705.
139. Prod'hon C, Machuca I, Berthomme H, Epstein A, Jacquemont B: **Characterization of regulatory functions of the HSV-1 immediate-early protein ICP22.** *Virology* 1996, **226:**393-402.
140. Cress WD, Triezenberg SJ: **Critical structural elements of the VP16 transcriptional activation domain.** *Science* 1991, **251:**87-90.
141. Jahedi S, Markovitz NS, Filatov F, Roizman B: **Colocalization of the herpes simplex virus 1 UL4 protein with infected cell protein 22 in small, dense nuclear structures formed prior to onset of DNA synthesis.** *J Virol* 1999, **73:**5132-5138.
142. Leopardi R, Ward PL, Ogle WO, Roizman B: **Association of herpes simplex virus regulatory protein ICP22 with transcriptional complexes containing EAP, ICP4, RNA polymerase II, and viral DNA requires posttranslational modification by the U(L)13 proteinkinase.** *J Virol* 1997, **71:**1133-1139.
143. Dai-Ju JQ, Li L, Johnson LA, Sandri-Goldin RM: **ICP27 interacts with the C-terminal domain of RNA polymerase II and facilitates its recruitment to herpes simplex virus 1 transcription sites, where it undergoes proteasomal degradation during infection.** *J Virol* 2006, **80:**3567-3581.
144. Fraser KA, Rice SA: **Herpes simplex virus type 1 infection leads to loss of serine-2 phosphorylation on the carboxyl-terminal domain of RNA polymerase II.** *J Virol* 2005, **79:**11323-11334.
145. Fraser KA, Rice SA: **Herpes simplex virus immediate-early protein ICP22 triggers loss of serine 2-phosphorylated RNA polymerase II.** *J Virol* 2007, **81:**5091-5101.
146. Long MC, Leong V, Schaffer PA, Spencer CA, Rice SA: **ICP22 and the UL13 protein kinase are both required for herpes simplex virus-induced modification of the large subunit of RNA polymerase II.** *J Virol* 1999, **73:**5593-5604.
147. Bastian TW, Livingston CM, Weller SK, Rice SA: **Herpes simplex virus type 1 immediate-early protein ICP22 is required for VICE domain formation during productive viral infection.** *J Virol* 2010, **84:**2384-2394.

148. Sears AE, Halliburton IW, Meignier B, Silver S, Roizman B: **Herpes simplex virus 1 mutant deleted in the alpha 22 gene: growth and gene expression in permissive and restrictive cells and establishment of latency in mice.** *J Virol* 1985, **55:**338-346.
149. Ogle WO, Roizman B: **Functional anatomy of herpes simplex virus 1 overlapping genes encoding infected-cell protein 22 and US1.5 protein.** *J Virol* 1999, **73:**4305-4315.
150. Poon AP, Ogle WO, Roizman B: **Posttranslational processing of infected cell protein 22 mediated by viral protein kinases is sensitive to amino acid substitutions at distant sites and can be cell-type specific.** *J Virol* 2000, **74:**11210-11214.
151. Advani SJ, Brandimarti R, Weichselbaum RR, Roizman B: **The disappearance of cyclins A and B and the increase in activity of the G(2)/M-phase cellular kinase cdc2 in herpes simplex virus 1-infected cells require expression of the alpha22/U(S)1.5 and U(L)13 viral genes.** *J Virol* 2000, **74:**8-15.
152. Advani SJ, Weichselbaum RR, Roizman B: **cdc2 cyclin-dependent kinase binds and phosphorylates herpes simplex virus 1 U(L)42 DNA synthesis processivity factor.** *J Virol* 2001, **75:**10326-10333.
153. Advani SJ, Weichselbaum RR, Roizman B: **Herpes simplex virus 1 activates cdc2 to recruit topoisomerase II alpha for post-DNA synthesis expression of late genes.** *Proc Natl Acad Sci U S A* 2003, **100:**4825-4830.
154. Smith RW, Malik P, Clements JB: **The herpes simplex virus ICP27 protein: a multifunctional post-transcriptional regulator of gene expression.** *Biochem Soc Trans* 2005, **33:**499-501.
155. Mears WE, Rice SA: **The herpes simplex virus immediate-early protein ICP27 shuttles between nucleus and cytoplasm.** *Virology* 1998, **242:**128-137.
156. Phelan A, Clements JB: **Herpes simplex virus type 1 immediate early protein IE63 shuttles between nuclear compartments and the cytoplasm.** *J Gen Virol* 1997, **78 (Pt 12):**3327-3331.
157. Soliman TM, Sandri-Goldin RM, Silverstein SJ: **Shuttling of the herpes simplex virus type 1 regulatory protein ICP27 between the nucleus and cytoplasm mediates the expression of late proteins.** *J Virol* 1997, **71:**9188-9197.
158. McCarthy AM, McMahan L, Schaffer PA: **Herpes simplex virus type 1 ICP27 deletion mutants exhibit altered patterns of transcription and are DNA deficient.** *J Virol* 1989, **63:**18-27.
159. Lopez C: **Genetics of natural resistance to herpesvirus infections in mice.** *Nature* 1975, **258:**152-153.
160. Rice SA, Knipe DM: **Genetic evidence for two distinct transactivation functions of the herpes simplex virus alpha protein ICP27.** *J Virol* 1990, **64:**1704-1715.

161. Uprichard SL, Knipe DM: **Herpes simplex ICP27 mutant viruses exhibit reduced expression of specific DNA replication genes.** *J Virol* 1996, **70:**1969-1980.
162. Jean S, LeVan KM, Song B, Levine M, Knipe DM: **Herpes simplex virus 1 ICP27 is required for transcription of two viral late (gamma 2) genes in infected cells.** *Virology* 2001, **283:**273-284.
163. McGregor F, Phelan A, Dunlop J, Clements JB: **Regulation of herpes simplex virus poly (A) site usage and the action of immediate-early protein IE63 in the early-late switch.** *J Virol* 1996, **70:**1931-1940.
164. McLauchlan J, Phelan A, Loney C, Sandri-Goldin RM, Clements JB: **Herpes simplex virus IE63 acts at the posttranscriptional level to stimulate viral mRNA 3' processing.** *J Virol* 1992, **66:**6939-6945.
165. McLauchlan J, Simpson S, Clements JB: **Herpes simplex virus induces a processing factor that stimulates poly(A) site usage.** *Cell* 1989, **59:**1093-1105.
166. Sandri-Goldin RM, Mendoza GE: **A herpesvirus regulatory protein appears to act post-transcriptionally by affecting mRNA processing.** *Genes Dev* 1992, **6:**848-863.
167. Zhou C, Knipe DM: **Association of herpes simplex virus type 1 ICP8 and ICP27 proteins with cellular RNA polymerase II holoenzyme.** *J Virol* 2002, **76:**5893-5904.
168. Li L, Johnson LA, Dai-Ju JQ, Sandri-Goldin RM: **Hsc70 focus formation at the periphery of HSV-1 transcription sites requires ICP27.** *PLoS One* 2008, **3:**e1491.
169. Johnson LA, Li L, Sandri-Goldin RM: **The cellular RNA export receptor TAP/NXF1 is required for ICP27-mediated export of herpes simplex virus 1 RNA, but the TREX complex adaptor protein Aly/REF appears to be dispensable.** *J Virol* 2009, **83:**6335-6346.
170. Chen IH, Sciabica KS, Sandri-Goldin RM: **ICP27 interacts with the RNA export factor Aly/REF to direct herpes simplex virus type 1 intronless mRNAs to the TAP export pathway.** *J Virol* 2002, **76:**12877-12889.
171. Stutz F, Bachi A, Doerks T, Braun IC, Seraphin B, Wilm M, Bork P, Izaurralde E: **REF, an evolutionary conserved family of hnRNP-like proteins, interacts with TAP/Mex67p and participates in mRNA nuclear export.** *RNA* 2000, **6:**638-650.
172. Le Hir H, Izaurralde E, Maquat LE, Moore MJ: **The spliceosome deposits multiple proteins 20-24 nucleotides upstream of mRNA exon-exon junctions.** *EMBO J* 2000, **19:**6860-6869.
173. Le Hir H, Gatfield D, Izaurralde E, Moore MJ: **The exon-exon junction complex provides a binding platform for factors involved in mRNA export and nonsense-mediated mRNA decay.** *EMBO J* 2001, **20:**4987-4997.
174. Zhou Z, Luo MJ, Straesser K, Katahira J, Hurt E, Reed R: **The protein Aly links pre-messenger-RNA splicing to nuclear export in metazoans.** *Nature* 2000, **407:**401-405.

175. Rodrigues JP, Rode M, Gatfield D, Blencowe BJ, Carmo-Fonseca M, Izaurralde E: **REF proteins mediate the export of spliced and unspliced mRNAs from the nucleus.** *Proc Natl Acad Sci U S A* 2001, **98:**1030-1035.
176. Phelan A, Carmo-Fonseca M, McLaughlan J, Lamond AI, Clements JB: **A herpes simplex virus type 1 immediate-early gene product, IE63, regulates small nuclear ribonucleoprotein distribution.** *Proc Natl Acad Sci U S A* 1993, **90:**9056-9060.
177. Bryant HE, Wadd SE, Lamond AI, Silverstein SJ, Clements JB: **Herpes simplex virus IE63 (ICP27) protein interacts with spliceosome-associated protein 145 and inhibits splicing prior to the first catalytic step.** *J Virol* 2001, **75:**4376-4385.
178. Hargett D, McLean T, Bachenheimer SL: **Herpes simplex virus ICP27 activation of stress kinases JNK and p38.** *J Virol* 2005, **79:**8348-8360.
179. Johnson KE, Song B, Knipe DM: **Role for herpes simplex virus 1 ICP27 in the inhibition of type I interferon signaling.** *Virology* 2008, **374:**487-494.
180. Everett RD, Murray J: **ND10 components relocate to sites associated with herpes simplex virus type 1 nucleoprotein complexes during virus infection.** *J Virol* 2005, **79:**5078-5089.
181. Sourvinos G, Everett RD: **Visualization of parental HSV-1 genomes and replication compartments in association with ND10 in live infected cells.** *EMBO J* 2002, **21:**4989-4997.
182. Lukonis CJ, Burkham J, Weller SK: **Herpes simplex virus type 1 prereplicative sites are a heterogeneous population: only a subset are likely to be precursors to replication compartments.** *J Virol* 1997, **71:**4771-4781.
183. Uprichard SL, Knipe DM: **Assembly of herpes simplex virus replication proteins at two distinct intranuclear sites.** *Virology* 1997, **229:**113-125.
184. Lilley CE, Carson CT, Muotri AR, Gage FH, Weitzman MD: **DNA repair proteins affect the lifecycle of herpes simplex virus 1.** *Proc Natl Acad Sci U S A* 2005, **102:**5844-5849.
185. Wilcock D, Lane DP: **Localization of p53, retinoblastoma and host replication proteins at sites of viral replication in herpes-infected cells.** *Nature* 1991, **349:**429-431.
186. Honess RW, Roizman B: **Regulation of herpesvirus macromolecular synthesis. I. Cascade regulation of the synthesis of three groups of viral proteins.** *J Virol* 1974, **14:**8-19.
187. Boehmer PE, Lehman IR: **Herpes simplex virus DNA replication.** *Annu Rev Biochem* 1997, **66:**347-384.
188. Frenkel N, Locker H, Batterson W, Hayward GS, Roizman B: **Anatomy of herpes simplex virus DNA. VI. Defective DNA originates from the S component.** *J Virol* 1976, **20:**527-531.
189. Locker H, Frenkel N, Halliburton I: **Structure and expression of class II defective herpes simplex virus genomes encoding infected cell polypeptide number 8.** *J Virol* 1982, **43:**574-593.

190. Polvino-Bodnar M, Orberg PK, Schaffer PA: **Herpes simplex virus type 1 oriL is not required for virus replication or for the establishment and reactivation of latent infection in mice.** *J Virol* 1987, **61:**3528-3535.
191. Balliet JW, Schaffer PA: **Point mutations in herpes simplex virus type 1 oriL, but not in oriS, reduce pathogenesis during acute infection of mice and impair reactivation from latency.** *J Virol* 2006, **80:**440-450.
192. Igarashi K, Fawl R, Roller RJ, Roizman B: **Construction and properties of a recombinant herpes simplex virus 1 lacking both S-component origins of DNA synthesis.** *J Virol* 1993, **67:**2123-2132.
193. Baines JD, Roizman B: **The UL11 gene of herpes simplex virus 1 encodes a function that facilitates nucleocapsid envelopment and egress from cells.** *J Virol* 1992, **66:**5168-5174.
194. Rice SA, Long MC, Lam V, Spencer CA: **RNA polymerase II is aberrantly phosphorylated and localized to viral replication compartments following herpes simplex virus infection.** *J Virol* 1994, **68:**988-1001.
195. Knipe DM, Senechek D, Rice SA, Smith JL: **Stages in the nuclear association of the herpes simplex virus transcriptional activator protein ICP4.** *J Virol* 1987, **61:**276-284.
196. Randall RE, Dinwoodie N: **Intranuclear localization of herpes simplex virus immediate-early and delayed-early proteins: evidence that ICP 4 is associated with progeny virus DNA.** *J Gen Virol* 1986, **67 (Pt 10):**2163-2177.
197. Olesky M, McNamee EE, Zhou C, Taylor TJ, Knipe DM: **Evidence for a direct interaction between HSV-1 ICP27 and ICP8 proteins.** *Virology* 2005, **331:**94-105.
198. McNamee EE, Taylor TJ, Knipe DM: **A dominant-negative herpesvirus protein inhibits intranuclear targeting of viral proteins: effects on DNA replication and late gene expression.** *J Virol* 2000, **74:**10122-10131.
199. Zabierowski S, DeLuca NA: **Differential cellular requirements for activation of herpes simplex virus type 1 early (tk) and late (gC) promoters by ICP4.** *J Virol* 2004, **78:**6162-6170.
200. Church GA, Wilson DW: **Study of herpes simplex virus maturation during a synchronous wave of assembly.** *J Virol* 1997, **71:**3603-3612.
201. de Bruyn Kops A, Uprichard SL, Chen M, Knipe DM: **Comparison of the intranuclear distributions of herpes simplex virus proteins involved in various viral functions.** *Virology* 1998, **252:**162-178.
202. Nalwanga D, Rempel S, Roizman B, Baines JD: **The UL 16 gene product of herpes simplex virus 1 is a virion protein that colocalizes with intranuclear capsid proteins.** *Virology* 1996, **226:**236-242.
203. Ward PL, Barker DE, Roizman B: **A novel herpes simplex virus 1 gene, UL43.5, maps antisense to the UL43 gene and encodes a protein which colocalizes in nuclear structures with capsid proteins.** *J Virol* 1996, **70:**2684-2690.

204. Walters JN, Sexton GL, McCaffery JM, Desai P: **Mutation of single hydrophobic residue I27, L35, F39, L58, L65, L67, or L71 in the N terminus of VP5 abolishes interaction with the scaffold protein and prevents closure of herpes simplex virus type 1 capsid shells.** *J Virol* 2003, **77:**4043-4059.
205. Newcomb WW, Homa FL, Thomsen DR, Booy FP, Trus BL, Steven AC, Spencer JV, Brown JC: **Assembly of the herpes simplex virus capsid: characterization of intermediates observed during cell-free capsid formation.** *J Mol Biol* 1996, **263:**432-446.
206. Trus BL, Booy FP, Newcomb WW, Brown JC, Homa FL, Thomsen DR, Steven AC: **The herpes simplex virus procapsid: structure, conformational changes upon maturation, and roles of the triplex proteins VP19c and VP23 in assembly.** *J Mol Biol* 1996, **263:**447-462.
207. Newcomb WW, Trus BL, Booy FP, Steven AC, Wall JS, Brown JC: **Structure of the herpes simplex virus capsid. Molecular composition of the pentons and the triplexes.** *J Mol Biol* 1993, **232:**499-511.
208. Newcomb WW, Homa FL, Thomsen DR, Trus BL, Cheng N, Steven A, Booy F, Brown JC: **Assembly of the herpes simplex virus procapsid from purified components and identification of small complexes containing the major capsid and scaffolding proteins.** *J Virol* 1999, **73:**4239-4250.
209. Deiss LP, Chou J, Frenkel N: **Functional domains within the a sequence involved in the cleavage-packaging of herpes simplex virus DNA.** *J Virol* 1986, **59:**605-618.
210. Newcomb WW, Juhas RM, Thomsen DR, Homa FL, Burch AD, Weller SK, Brown JC: **The UL6 gene product forms the portal for entry of DNA into the herpes simplex virus capsid.** *J Virol* 2001, **75:**10923-10932.
211. Beard PM, Taus NS, Baines JD: **DNA cleavage and packaging proteins encoded by genes U(L)28, U(L)15, and U(L)33 of herpes simplex virus type 1 form a complex in infected cells.** *J Virol* 2002, **76:**4785-4791.
212. McNab AR, Desai P, Person S, Roof LL, Thomsen DR, Newcomb WW, Brown JC, Homa FL: **The product of the herpes simplex virus type 1 UL25 gene is required for encapsidation but not for cleavage of replicated viral DNA.** *J Virol* 1998, **72:**1060-1070.
213. Simpson-Holley M, Baines J, Roller R, Knipe DM: **Herpes simplex virus 1 U(L)31 and U(L)34 gene products promote the late maturation of viral replication compartments to the nuclear periphery.** *J Virol* 2004, **78:**5591-5600.
214. Simpson-Holley M, Colgrove RC, Nalepa G, Harper JW, Knipe DM: **Identification and functional evaluation of cellular and viral factors involved in the alteration of nuclear architecture during herpes simplex virus 1 infection.** *J Virol* 2005, **79:**12840-12851.
215. Wisner TW, Wright CC, Kato A, Kawaguchi Y, Mou F, Baines JD, Roller RJ, Johnson DC: **Herpesvirus gB-induced fusion between the virion**

envelope and outer nuclear membrane during virus egress is regulated by the viral US3 kinase. *J Virol* 2009, **83:**3115-3126.
216. Epstein MA: **Observations on the mode of release of herpes virus from infected HeLa cells.** *J Cell Biol* 1962, **12:**589-597.
217. Skepper JN, Whiteley A, Browne H, Minson A: **Herpes simplex virus nucleocapsids mature to progeny virions by an envelopment --> deenvelopment --> reenvelopment pathway.** *J Virol* 2001, **75:**5697-5702.
218. Whiteley A, Bruun B, Minson T, Browne H: **Effects of targeting herpes simplex virus type 1 gD to the endoplasmic reticulum and trans-Golgi network.** *J Virol* 1999, **73:**9515-9520.
219. Kristie TM, Pomerantz JL, Twomey TC, Parent SA, Sharp PA: **The cellular C1 factor of the herpes simplex virus enhancer complex is a family of polypeptides.** *J Biol Chem* 1995, **270:**4387-4394.
220. Lefstin JA, Thomas JR, Yamamoto KR: **Influence of a steroid receptor DNA-binding domain on transcriptional regulatory functions.** *Genes Dev* 1994, **8:**2842-2856.
221. Reilly PT, Herr W: **Spontaneous reversion of tsBN67 cell proliferation and cytokinesis defects in the absence of HCF-1 function.** *Exp Cell Res* 2002, **277:**119-130.
222. Kakizawa T, Miyamoto T, Ichikawa K, Kaneko A, Suzuki S, Hara M, Nagasawa T, Takeda T, Mori J, Kumagai M, Hashizume K: **Functional interaction between Oct-1 and retinoid X receptor.** *J Biol Chem* 1999, **274:**19103-19108.
223. Cleary MA, Herr W: **Mechanisms for flexibility in DNA sequence recognition and VP16-induced complex formation by the Oct-1 POU domain.** *Mol Cell Biol* 1995, **15:**2090-2100.
224. O'Hare P, Goding CR, Haigh A: **Direct combinatorial interaction between a herpes simplex virus regulatory protein and a cellular octamer-binding factor mediates specific induction of virus immediate-early gene expression.** *EMBO J* 1988, **7:**4231-4238.
225. Walker S, Hayes S, O'Hare P: **Site-specific conformational alteration of the Oct-1 POU domain-DNA complex as the basis for differential recognition by Vmw65 (VP16).** *Cell* 1994, **79:**841-852.
226. Herr W, Sturm RA, Clerc RG, Corcoran LM, Baltimore D, Sharp PA, Ingraham HA, Rosenfeld MG, Finney M, Ruvkun G, et al.: **The POU domain: a large conserved region in the mammalian pit-1, oct-1, oct-2, and Caenorhabditis elegans unc-86 gene products.** *Genes Dev* 1988, **2:**1513-1516.
227. Lai JS, Cleary MA, Herr W: **A single amino acid exchange transfers VP16-induced positive control from the Oct-1 to the Oct-2 homeo domain.** *Genes Dev* 1992, **6:**2058-2065.
228. Stern S, Tanaka M, Herr W: **The Oct-1 homoeodomain directs formation of a multiprotein-DNA complex with the HSV transactivator VP16.** *Nature* 1989, **341:**624-630.

229. Xiao H, Lis JT, Greenblatt J, Friesen JD: **The upstream activator CTF/NF1 and RNA polymerase II share a common element involved in transcriptional activation.** *Nucleic Acids Res* 1994, **22:**1966-1973.
230. Kobayashi N, Horn PJ, Sullivan SM, Triezenberg SJ, Boyer TG, Berk AJ: **DA-complex assembly activity required for VP16C transcriptional activation.** *Mol Cell Biol* 1998, **18:**4023-4031.
231. Klemm RD, Goodrich JA, Zhou S, Tjian R: **Molecular cloning and expression of the 32-kDa subunit of human TFIID reveals interactions with VP16 and TFIIB that mediate transcriptional activation.** *Proc Natl Acad Sci U S A* 1995, **92:**5788-5792.
232. Kurosu T, Peterlin BM: **VP16 and ubiquitin; binding of P-TEFb via its activation domain and ubiquitin facilitates elongation of transcription of target genes.** *Curr Biol* 2004, **14:**1112-1116.
233. Peng J, Zhu Y, Milton JT, Price DH: **Identification of multiple cyclin subunits of human P-TEFb.** *Genes Dev* 1998, **12:**755-762.
234. Peterlin BM, Price DH: **Controlling the elongation phase of transcription with P-TEFb.** *Mol Cell* 2006, **23:**297-305.
235. Yamauchi Y, Kiriyama K, Kubota N, Kimura H, Usukura J, Nishiyama Y: **The UL14 tegument protein of herpes simplex virus type 1 is required for efficient nuclear transport of the alpha transinducing factor VP16 and viral capsids.** *J Virol* 2008, **82:**1094-1106.
236. Zhang Y, Sirko DA, McKnight JL: **Role of herpes simplex virus type 1 UL46 and UL47 in alpha TIF-mediated transcriptional induction: characterization of three viral deletion mutants.** *J Virol* 1991, **65:**829-841.
237. Zhang Y, McKnight JL: **Herpes simplex virus type 1 UL46 and UL47 deletion mutants lack VP11 and VP12 or VP13 and VP14, respectively, and exhibit altered viral thymidine kinase expression.** *J Virol* 1993, **67:**1482-1492.
238. Perez-Parada J, Saffran HA, Smiley JR: **RNA degradation induced by the herpes simplex virus vhs protein proceeds 5' to 3' in vitro.** *J Virol* 2004, **78:**13391-13394.
239. Fenwick ML, Clark J: **Early and delayed shut-off of host protein synthesis in cells infected with herpes simplex virus.** *J Gen Virol* 1982, **61 (Pt l):**121-125.
240. Fenwick ML, Everett RD: **Transfer of UL41, the gene controlling virion-associated host cell shutoff, between different strains of herpes simplex virus.** *J Gen Virol* 1990, **71 (Pt 2):**411-418.
241. Fenwick ML, Owen SA: **On the control of immediate early (alpha) mRNA survival in cells infected with herpes simplex virus.** *J Gen Virol* 1988, **69 (Pt 11):**2869-2877.
242. Lam Q, Smibert CA, Koop KE, Lavery C, Capone JP, Weinheimer SP, Smiley JR: **Herpes simplex virus VP16 rescues viral mRNA from destruction by the virion host shutoff function.** *EMBO J* 1996, **15:**2575-2581.

243. Smibert CA, Popova B, Xiao P, Capone JP, Smiley JR: **Herpes simplex virus VP16 forms a complex with the virion host shutoff protein vhs.** *J Virol* 1994, **68:**2339-2346.
244. Taddeo B, Sciortino MT, Zhang W, Roizman B: **Interaction of herpes simplex virus RNase with VP16 and VP22 is required for the accumulation of the protein but not for accumulation of mRNA.** *Proc Natl Acad Sci U S A* 2007, **104:**12163-12168.
245. Weinheimer SP, Boyd BA, Durham SK, Resnick JL, O'Boyle DR, 2nd: **Deletion of the VP16 open reading frame of herpes simplex virus type 1.** *J Virol* 1992, **66:**258-269.
246. Mossman KL, Sherburne R, Lavery C, Duncan J, Smiley JR: **Evidence that herpes simplex virus VP16 is required for viral egress downstream of the initial envelopment event.** *J Virol* 2000, **74:**6287-6299.
247. Kelly BJ, Fraefel C, Cunningham AL, Diefenbach RJ: **Functional roles of the tegument proteins of herpes simplex virus type 1.** *Virus Res* 2009, **145:**173-186.
248. Ace CI, McKee TA, Ryan JM, Cameron JM, Preston CM: **Construction and characterization of a herpes simplex virus type 1 mutant unable to transinduce immediate-early gene expression.** *J Virol* 1989, **63:**2260-2269.
249. Smiley JR, Duncan J: **Truncation of the C-terminal acidic transcriptional activation domain of herpes simplex virus VP16 produces a phenotype similar to that of the in1814 linker insertion mutation.** *J Virol* 1997, **71:**6191-6193.
250. Miller WH, Jr., Maerz WJ, Kurie J, Moy D, Baselga J, Lucas DA, Grippo JF, Masui H, Dmitrovsky E: **All-trans-retinoic acid and hexamethylene bisacetamide (HMBA) regulate TGF-alpha and Hst-1/kFGF expression in differentiation sensitive but not in resistant human teratocarcinomas.** *Differentiation* 1994, **55:**145-152.
251. Siegel DS, Zhang X, Feinman R, Teitz T, Zelenetz A, Richon VM, Rifkind RA, Marks PA, Michaeli J: **Hexamethylene bisacetamide induces programmed cell death (apoptosis) and down-regulates BCL-2 expression in human myeloma cells.** *Proc Natl Acad Sci U S A* 1998, **95:**162-166.
252. Rifkind RA, Richon VM, Marks PA: **Induced differentiation, the cell cycle, and the treatment of cancer.** *Pharmacol Ther* 1996, **69:**97-102.
253. Blondeau JM, Aoki FY: **In vitro reactivation of latent herpes simplex virus by the demethylating compound hexamethylene-bis-acetamide.** *J Virol Methods* 1992, **40:**323-329.
254. Kondo Y, Yura Y, Iga H, Yanagawa T, Yoshida H, Furumoto N, Sato M: **Effect of hexamethylene bisacetamide and cyclosporin A on recovery of herpes simplex virus type 2 from the in vitro model of latency in a human neuroblastoma cell line.** *Cancer Res* 1990, **50:**7852-7857.
255. Kitagawa R, Takahashi Y, Takahashi M, Imazu H, Yasuda M, Sadanari H, Tanaka J: **Hexamethylene bisacetamide can convert nonpermissive**

human cells to a permissive state for expressing the major immediate-early genes of human cytomegalovirus by up-regulating NF-kappaB activity. *Virology* 2009, **383:**195-206.
256. Boshart M, Weber F, Jahn G, Dorsch-Hasler K, Fleckenstein B, Schaffner W: **A very strong enhancer is located upstream of an immediate early gene of human cytomegalovirus.** *Cell* 1985, **41:**521-530.
257. Contreras X, Barboric M, Lenasi T, Peterlin BM: **HMBA releases P-TEFb from HEXIM1 and 7SK snRNA via PI3K/Akt and activates HIV transcription.** *PLoS Pathog* 2007, **3:**1459-1469.
258. Antoni BA, Rabson AB, Kinter A, Bodkin M, Poli G: **NF-kappa B-dependent and -independent pathways of HIV activation in a chronically infected T cell line.** *Virology* 1994, **202:**684-694.
259. Barboric M, Kohoutek J, Price JP, Blazek D, Price DH, Peterlin BM: **Interplay between 7SK snRNA and oppositely charged regions in HEXIM1 direct the inhibition of P-TEFb.** *EMBO J* 2005, **24:**4291-4303.
260. Shim EY, Walker AK, Shi Y, Blackwell TK: **CDK-9/cyclin T (P-TEFb) is required in two postinitiation pathways for transcription in the C. elegans embryo.** *Genes Dev* 2002, **16:**2135-2146.
261. Everett RD, Boutell C, Orr A: **Phenotype of a herpes simplex virus type 1 mutant that fails to express immediate-early regulatory protein ICP0.** *J Virol* 2004, **78:**1763-1774.
262. Jamieson DR, Robinson LH, Daksis JI, Nicholl MJ, Preston CM: **Quiescent viral genomes in human fibroblasts after infection with herpes simplex virus type 1 Vmw65 mutants.** *J Gen Virol* 1995, **76 (Pt 6):**1417-1431.
263. Yao F, Schaffer PA: **An activity specified by the osteosarcoma line U2OS can substitute functionally for ICP0, a major regulatory protein of herpes simplex virus type 1.** *J Virol* 1995, **69:**6249-6258.
264. Hancock MH, Corcoran JA, Smiley JR: **Herpes simplex virus regulatory proteins VP16 and ICP0 counteract an innate intranuclear barrier to viral gene expression.** *Virology* 2006, **352:**237-252.
265. Hancock MH, Mossman KL, Smiley JR: **Cell fusion-induced activation of interferon-stimulated genes is not required for restriction of a herpes simplex virus VP16/ICP0 mutant in heterokarya formed between permissive and restrictive cells.** *J Virol* 2009, **83:**8976-8979.
266. Hancock MH: **The roles of HSV-1 VP16 and ICP0 in modulating cellular innate antiviral responses** University of Alberta, Medical Microbiology and Immunology; 2010.
267. Whitehead KA, Langer R, Anderson DG: **Knocking down barriers: advances in siRNA delivery.** *Nat Rev Drug Discov* 2009, **8:**129-138.
268. Kok KH, Lei T, Jin DY: **siRNA and shRNA screens advance key understanding of host factors required for HIV-1 replication.** *Retrovirology* 2009, **6:**78.
269. Randall G, Panis M, Cooper JD, Tellinghuisen TL, Sukhodolets KE, Pfeffer S, Landthaler M, Landgraf P, Kan S, Lindenbach BD, et al:

Cellular cofactors affecting hepatitis C virus infection and replication. *Proc Natl Acad Sci U S A* 2007, **104:**12884-12889.

270. Krishnan MN, Ng A, Sukumaran B, Gilfoy FD, Uchil PD, Sultana H, Brass AL, Adametz R, Tsui M, Qian F, et al: **RNA interference screen for human genes associated with West Nile virus infection.** *Nature* 2008, **455:**242-245.
271. Warming S, Costantino N, Court DL, Jenkins NA, Copeland NG: **Simple and highly efficient BAC recombineering using galK selection.** *Nucleic Acids Res* 2005, **33:**e36.
272. Minaker RL, Mossman KL, Smiley JR: **Functional inaccessibility of quiescent herpes simplex virus genomes.** *Virol J* 2005, **2:**85.
273. Epstein AL: **HSV-1-based amplicon vectors: design and applications.** *Gene Ther* 2005, **12 Suppl 1:**S154-158.
274. Gierasch WW, Zimmerman DL, Ward SL, Vanheyningen TK, Romine JD, Leib DA: **Construction and characterization of bacterial artificial chromosomes containing HSV-1 strains 17 and KOS.** *J Virol Methods* 2006, **135:**197-206.
275. Zahariadis G, Wagner MJ, Doepker RC, Maciejko JM, Crider CM, Jerome KR, Smiley JR: **Cell-type-specific tyrosine phosphorylation of the herpes simplex virus tegument protein VP11/12 encoded by gene UL46.** *J Virol* 2008, **82:**6098-6108.
276. Cheung P, Panning B, Smiley JR: **Herpes simplex virus immediate-early proteins ICP0 and ICP4 activate the endogenous human alpha-globin gene in nonerythroid cells.** *J Virol* 1997, **71:**1784-1793.
277. Obrig TG, Culp WJ, McKeehan WL, Hardesty B: **The mechanism by which cycloheximide and related glutarimide antibiotics inhibit peptide synthesis on reticulocyte ribosomes.** *J Biol Chem* 1971, **246:**174-181.
278. McFarlane M, Daksis JI, Preston CM: **Hexamethylene bisacetamide stimulates herpes simplex virus immediate early gene expression in the absence of trans-induction by Vmw65.** *J Gen Virol* 1992, **73 (Pt 2):**285-292.
279. Homer EG, Rinaldi A, Nicholl MJ, Preston CM: **Activation of Herpesvirus Gene Expression by the Human Cytomegalovirus Protein pp71.** *J Virol* 1999, **73:**8512-8518.
280. Bresnahan WA, Shenk TE: **UL82 virion protein activates expression of immediate early viral genes in human cytomegalovirus-infected cells.** *Proc Natl Acad Sci U S A* 2000, **97:**14506-14511.
281. Cantrell SR, Bresnahan WA: **Interaction between the human cytomegalovirus UL82 gene product (pp71) and hDaxx regulates immediate-early gene expression and viral replication.** *J Virol* 2005, **79:**7792-7802.
282. Baldick CJ, Jr., Marchini A, Patterson CE, Shenk T: **Human cytomegalovirus tegument protein pp71 (ppUL82) enhances the infectivity of viral DNA and accelerates the infectious cycle.** *J Virol* 1997, **71:**4400-4408.

283. Woodhall DL, Groves IJ, Reeves MB, Wilkinson G, Sinclair JH: **Human Daxx-mediated repression of human cytomegalovirus gene expression correlates with a repressive chromatin structure around the major immediate early promoter.** *J Biol Chem* 2006, **281:**37652-37660.
284. Cantrell SR, Bresnahan WA: **Human cytomegalovirus (HCMV) UL82 gene product (pp71) relieves hDaxx-mediated repression of HCMV replication.** *J Virol* 2006, **80:**6188-6191.
285. Lukashchuk V, McFarlane S, Everett RD, Preston CM: **Human cytomegalovirus protein pp71 displaces the chromatin-associated factor ATRX from nuclear domain 10 at early stages of infection.** *J Virol* 2008, **82:**12543-12554.
286. Preston CM, Nicholl MJ: **Role of the cellular protein hDaxx in human cytomegalovirus immediate-early gene expression.** *J Gen Virol* 2006, **87:**1113-1121.
287. Saffert RT, Kalejta RF: **Inactivating a cellular intrinsic immune defense mediated by Daxx is the mechanism through which the human cytomegalovirus pp71 protein stimulates viral immediate-early gene expression.** *J Virol* 2006, **80:**3863-3871.
288. Tavalai N, Papior P, Rechter S, Leis M, Stamminger T: **Evidence for a role of the cellular ND10 protein PML in mediating intrinsic immunity against human cytomegalovirus infections.** *J Virol* 2006, **80:**8006-8018.
289. Hwang J, Kalejta RF: **Proteasome-dependent, ubiquitin-independent degradation of Daxx by the viral pp71 protein in human cytomegalovirus-infected cells.** *Virology* 2007, **367:**334-338.
290. Kutluay SB, Triezenberg SJ: **Role of chromatin during herpesvirus infections.** *Biochim Biophys Acta* 2009, **1790:**456-466.
291. Kouzarides T: **Chromatin modifications and their function.** *Cell* 2007, **128:**693-705.
292. Murphy JC, Fischle W, Verdin E, Sinclair JH: **Control of cytomegalovirus lytic gene expression by histone acetylation.** *EMBO J* 2002, **21:**1112-1120.
293. Ioudinkova E, Arcangeletti MC, Rynditch A, De Conto F, Motta F, Covan S, Pinardi F, Razin SV, Chezzi C: **Control of human cytomegalovirus gene expression by differential histone modifications during lytic and latent infection of a monocytic cell line.** *Gene* 2006, **384:**120-128.
294. Kutluay SB, Triezenberg SJ: **Regulation of histone deposition on the herpes simplex virus type 1 genome during lytic infection.** *J Virol* 2009, **83:**5835-5845.
295. Kind J, van Steensel B: **Genome-nuclear lamina interactions and gene regulation.** *Curr Opin Cell Biol* 2010, **22:**320-325.
296. Prokocimer M, Davidovich M, Nissim-Rafinia M, Wiesel-Motiuk N, Bar DZ, Barkan R, Meshorer E, Gruenbaum Y: **Nuclear lamins: key regulators of nuclear structure and activities.** *J Cell Mol Med* 2009, **13:**1059-1085.

297. Malhas AN, Lee CF, Vaux DJ: **Lamin B1 controls oxidative stress responses via Oct-1.** *J Cell Biol* 2009, **184:**45-55.
298. Holaska JM, Wilson KL: **An emerin "proteome": purification of distinct emerin-containing complexes from HeLa cells suggests molecular basis for diverse roles including gene regulation, mRNA splicing, signaling, mechanosensing, and nuclear architecture.** *Biochemistry* 2007, **46:**8897-8908.
299. Somech R, Shaklai S, Geller O, Amariglio N, Simon AJ, Rechavi G, Gal-Yam EN: **The nuclear-envelope protein and transcriptional repressor LAP2beta interacts with HDAC3 at the nuclear periphery, and induces histone H4 deacetylation.** *J Cell Sci* 2005, **118:**4017-4025.
300. Yokochi T, Poduch K, Ryba T, Lu J, Hiratani I, Tachibana M, Shinkai Y, Gilbert DM: **G9a selectively represses a class of late-replicating genes at the nuclear periphery.** *Proc Natl Acad Sci U S A* 2009, **106:**19363-19368.
301. Montes de Oca R, Shoemaker CJ, Gucek M, Cole RN, Wilson KL: **Barrier-to-autointegration factor proteome reveals chromatin-regulatory partners.** *PLoS One* 2009, **4:**e7050.
302. Shimi T, Pfleghaar K, Kojima S, Pack CG, Solovei I, Goldman AE, Adam SA, Shumaker DK, Kinjo M, Cremer T, Goldman RD: **The A- and B-type nuclear lamin networks: microdomains involved in chromatin organization and transcription.** *Genes Dev* 2008, **22:**3409-3421.
303. Pendas AM, Zhou Z, Cadinanos J, Freije JM, Wang J, Hultenby K, Astudillo A, Wernerson A, Rodriguez F, Tryggvason K, Lopez-Otin C: **Defective prelamin A processing and muscular and adipocyte alterations in Zmpste24 metalloproteinase-deficient mice.** *Nat Genet* 2002, **31:**94-99.
304. Spann TP, Goldman AE, Wang C, Huang S, Goldman RD: **Alteration of nuclear lamin organization inhibits RNA polymerase II-dependent transcription.** *J Cell Biol* 2002, **156:**603-608.
305. Dubbs D, Kit S: **Mutant Strains of Herpes Simplex Deficient in Thymidine Kinase-Inducing Activity.** *Virology* 1964, **22:**493-502.
306. Post LE, Mackem S, Roizman B: **Regulation of alpha genes of herpes simplex virus: expression of chimeric genes produced by fusion of thymidine kinase with alpha gene promoters.** *Cell* 1981, **24:**555-565.
307. Panning B, Smiley JR: **Regulation of cellular genes transduced by herpes simplex virus.** *J Virol* 1989, **63:**1929-1937.
308. Boshart M, Weber F, Jahn G, Dorsch-Häsler K, Fleckenstein B, Schaffner W: **A very strong enhancer is located upstream of an immediate early gene of human cytomegalovirus.** *Cell* 1985, **41:**521-530.
309. Foecking MK, Hofstetter H: **Powerful and versatile enhancer-promoter unit for mammalian expression vectors.** *Gene* 1986, **45:**101-105.
310. Adler H, Messerle M, Koszinowski UH: **Cloning of herpesviral genomes as bacterial artificial chromosomes.** *Rev Med Virol* 2003, **13:**111-121.
311. Warden C, Tang Q, Zhu H: **Herpesvirus BACs: past, present, and future.** *J Biomed Biotechnol* 2010, **2011:**124595.

312. Adler H, Messerle M, Koszinowski UH: **Virus reconstituted from infectious bacterial artificial chromosome (BAC)-cloned murine gammaherpesvirus 68 acquires wild-type properties in vivo only after excision of BAC vector sequences.** *J Virol* 2001, **75:**5692-5696.
313. Smith GA, Enquist LW: **A self-recombining bacterial artificial chromosome and its application for analysis of herpesvirus pathogenesis.** *Proceedings of the National Academy of Sciences of the United States of America* 2000, **97:**4873-4878.
314. Wagner M, Jonjic S, Koszinowski UH, Messerle M: **Systematic excision of vector sequences from the BAC-cloned herpesvirus genome during virus reconstitution.** *J Virol* 1999, **73:**7056-7060.
315. Yu D, Smith GA, Enquist LW, Shenk T: **Construction of a self-excisable bacterial artificial chromosome containing the human cytomegalovirus genome and mutagenesis of the diploid TRL/IRL13 gene.** *J Virol* 2002, **76:**2316-2328.
316. Smith GA, Enquist LW: **Construction and Transposon Mutagenesis in Escherichia coli of a Full-Length Infectious Clone of Pseudorabies Virus, an Alphaherpesvirus.** *J Virol* 1999, **73:**6405-6414.
317. Cook WJ, Coen DM: **Temporal Regulation of Herpes Simplex Virus Type 1 UL24 mRNA Expression via Differential Polyadenylation.** *Virology* 1996, **218:**204-213.
318. Pearson A, Coen DM: **Identification, Localization, and Regulation of Expression of the UL24 Protein of Herpes Simplex Virus Type 1.** *J Virol* 2002, **76:**10821-10828.
319. McGeoch DJ, Cook S, Dolan A, Jamieson FE, Telford EAR: **Molecular Phylogeny and Evolutionary Timescale for the Family of Mammalian Herpesviruses.** *Journal of Molecular Biology* 1995, **247:**443-458.
320. Jacobson JG, Martin SL, Coen DM: **A conserved open reading frame that overlaps the herpes simplex virus thymidine kinase gene is important for viral growth in cell culture.** *J Virol* 1989, **63:**1839-1843.
321. Lymberopoulos MH, Pearson A: **Involvement of UL24 in herpes-simplex-virus-1-induced dispersal of nucleolin.** *Virology* 2007, **363:**397-409.
322. Tuteja R, Tuteja N: **Nucleolin: a multifunctional major nucleolar phosphoprotein.** *Crit Rev Biochem Mol Biol* 1998, **33:**407-436.
323. Bertrand L, Pearson A: **The conserved N-terminal domain of herpes simplex virus 1 UL24 protein is sufficient to induce the spatial redistribution of nucleolin.** *J Gen Virol* 2008, **89:**1142-1151.
324. Knizewski L, Kinch L, Grishin NV, Rychlewski L, Ginalski K: **Human herpesvirus 1 UL24 gene encodes a potential PD-(D/E)XK endonuclease.** *J Virol* 2006, **80:**2575-2577.
325. Bertrand L, Leiva-Torres GA, Hyjazie H, Pearson A: **Conserved Residues in the UL24 Protein of Herpes Simplex Virus 1 Are Important for Dispersal of the Nucleolar Protein Nucleolin.** *J Virol* 2010, **84:**109-118.

Appendix:

Figure A-1: The EGFP sequence alignment of plasmid pUC19-HSV-GFP and pEGFP-C1

The start and stop codons are showed as bolded and underlined letters. There are 78 additional nts in the EGFP ORF of pEGFP-C1, which are labelled by italic letters. Other differences between these two sequences are due to unclear sequenced results (shown as “N” in the sequences).

```
PUC19-HSV-GFP     ATGGTGAGCNAGGGCGANGAGCTGTTCANCGGGGTGGTGCCCNTCCTGGTCGAGNTGGAC 60
pEGFP-C1          ATGGTGAGCAAGGGCGAGGAGCTGTTCACCGGGGTGGTGCCCATCCTGGTCGAGCTGGAC 60
                  ********* ******* ********** ************* *********** *****

PUC19-HSV-GFP     GGCGACGTAAACGGCCACAANTTNAGCGTNTCNGGCGAGGNNNNNNGCGATGCCANNNN- 119
pEGFP-C1          GGCGACGTAAACGGCCACAAGTTCAGCGTGTCCGGCGAGGGCGAGGGCGATGCCACCTAC 120
                  ******************* ** ***** ** *******      *********

PUC19-HSV-GFP     GGCAAGCTGACCCNGNAGTTCATNTGCACCACCGGCAAGCTGCCCGTGCCCTGGCCCACC 179
pEGFP-C1          GGCAAGCTGACCCTGAAGTTCATCTGCACCACCGGCAAGCTGCCCGTGCCCTGGCCCACC 180
                  ************* * ******* ************************************

PUC19-HSV-GFP     CTCGTGACCNCCNTGACNTACGGCGTGCAGTGCTTCAGCCGCTACCCCGACCACATGAAG 239
pEGFP-C1          CTCGTGACCACCCTGACCTACGGCGTGCAGTGCTTCAGCCGCTACCCCGACCACATGAAG 240
                  ********* ** **** ****************************************

PUC19-HSV-GFP     CAGCACGACTTCTTCAAGTCCGCCATGCCCGAAGGCTACGTCCAGGAGCGCACCATCTTC 299
pEGFP-C1          CAGCACGACTTCTTCAAGTCCGCCATGCCCGAAGGCTACGTCCAGGAGCGCACCATCTTC 300
                  ************************************************************

PUC19-HSV-GFP     TTCAAGGACGACGGCAACTACAAGACCCGCGCCGAGGTGAAGTTCGAGGGCGACACCCTG 359
pEGFP-C1          TTCAAGGACGACGGCAACTACAAGACCCGCGCCGAGGTGAAGTTCGAGGGCGACACCCTG 360
                  ************************************************************

PUC19-HSV-GFP     GTGAACCGCATCGAGCTGAAGGGCATCGACTTCAAGGAGGACGGCAACATCCTGGGGCAC 419
pEGFP-C1          GTGAACCGCATCGAGCTGAAGGGCATCGACTTCAAGGAGGACGGCAACATCCTGGGGCAC 420
                  ************************************************************

PUC19-HSV-GFP     AAGCTGGAGTACAACTACAACAGCCACAACGTCTATATCATGGCCGACAAGCAGAAGAAC 479
pEGFP-C1          AAGCTGGAGTACAACTACAACAGCCACAACGTCTATATCATGGCCGACAAGCAGAAGAAC 480
                  ************************************************************

PUC19-HSV-GFP     GGCATCAAGGTGAACTTCAAGATCCGCCACAACATCGAGGACGGCAGCGTGCAGCTCGCC 539
pEGFP-C1          GGCATCAAGGTGAACTTCAAGATCCGCCACAACATCGAGGACGGCAGCGTGCAGCTCGCC 540
                  ************************************************************

PUC19-HSV-GFP     GACCACTACCAGCAGAACACCCCCATCGGCGACGGCCCCGTGCTGCTGCCCGACAACCAC 599
pEGFP-C1          GACCACTACCAGCAGAACACCCCCATCGGCGACGGCCCCGTGCTGCTGCCCGACAACCAC 600
                  ************************************************************

PUC19-HSV-GFP     TACCTGAGCACCCAGTCCGCCCTGAGCAAAGACCCCAACGAGAAGCGCGATCACATGGTC 659
pEGFP-C1          TACCTGAGCACCCAGTCCGCCCTGAGCAAAGACCCCAACGAGAAGCGCGATCACATGGTC 660
                  ************************************************************

PUC19-HSV-GFP     CTGCTGGAGTTCGTGACCGCCGCCGGGATCACTCTCGGCATGGACGAGCTGTACAAGTAA 718
pEGFP-C1          CTGCTGGAGTTCGTGACCGCCGCCGGGATCACTCTCGGCATGGACGANCTGTACAAGTCC 720
                  ********************************************** **********

PUC19-HSV-GFP     ------------------------------------------------------------ 726
pEGFP-C1          GGACTCAGATCTCGAGCTCAAGCTTCGAATTCTGCAGTCGACGGTACCGCGGGCCCGGGA 780

PUC19-HSV-GFP     ------------------
pEGFP-C1          TCCACCGGATCTAGATAA 803
```

Figure A-2: Inserted direction of EGFP in the recombinant viruses

The directions of EGFP insertion in the recombinant viruses were examined by sequencing with a reverse primer JRS171, which binds to the 3' end of TK gene. This is demonstrated in A). B) and C) show the sequences of KOS-HSV-GFP/V422-HSV-GFP and KOS-CMV-GFP/V422-CMV-GFP. The 3' ends of EGFP gene and TK gene are labelled as bolded letters and normal letters, respectively.

A)

5’-Promoter of TK EGFP gene

←JRS171

B) KOS-HSV-GFP/V422-HSV-GFP sequences:

TGTGCCGGGCAAGGTCGGCGGGATGAGGGCCACGAACGCCAGCACGG
CCTGGGGGGTCATGCTGCCCATAAGGTATCGCGCGGCCGGGTAGCACA
GGAGGGCGGCGATGGGATGGCGGTCGAAGATGAGGGTGAGGGCCGG
GGGCGGGGCATGTCC (TK gene)

ATGATTACGCCAAGCTTGCATGCCTGCTATTGTCTTCCCAATCCTC
CCCCTTGCTGTCCTGCCCCACCCCACCCCCCAGAATAGAATGACA
CCTACTCAGACAATGCGATGCAATTTCCTCATTTTATTAGGAAAGG
ACAGTGGGAGTGGCACCTTCCAGGGTCAAGGAAGGCACGGGGGA
GGGGCAAACAACAGATGGCTGGCAACTAGAAGGCACAGTCGAGG
CTGATCAGCGAGCTCTAGGGCCGCTTTACTTGTACAGCTCGTCCA
TGCCGAGAGTGATCCCGGCGGCGGTCACGAACTCCAGCAGGACC
ATGTGATCGCGCTTCTCGTTGGGGTATTTGCTCAGGGCGGACTGG
(EGFP gene)

C) KOS-CMV-GFP/V422-CMV-GFP sequences:

TGTGCCGGGCAAGGTCGGCGGGATGAGGGCCACGAACGCCAGCACGG
CCTGGGGGGTCATGCTGCCCATAAGGTATCGCGCGGCCGGGTAGCACA
GGAGGGCGGCGATGGGATGGCGGTCGAAGATGGGGGGGAGGGCCGG
GGGCGGGGCATGTGC (TK gene)

GCGTTAAGATACATTGATGAGTTTGGACAAACCACAACTAGAATG
CAGTGAAAAAAATGCTTTATTTGTGAAATTTGTGATGCTATTGCTT
TATTTGTAACCATTATAAGCTGCAATAAACAAGTTAACAACAACAA
TTGCATTCATTTTATGTTTCAGGTTCAGGGGGAGGTGTGGGAGGT
TTTTTAAAGCAAGTAAAACCTCTACAAATGTGGTATGGCTGATTAT
GATCAGTTATCTAGATCCGGTGGATCCCGGGCCCGCGGTACCGTC
GACTGCAGAATTCGAAGCTTGA (EGFP gene)

Figure A-3: Effects of cycloheximide and the V422 VP16 mutation on accumulation of eGFP mRNA from viral recombinants.

Vero cells were infected withV422-and KOS-derived viruses in the presence and absence of cycloheximide at an MOI of 5. The non-infected cells were used as the mock sample (labelled as Mock).
A). The total RNA profile (stained with ethidium bromide)
B). Northern blotting analysis with EGFP probe. V422 and KOS infections were shown as the negative controls for EGFP mRNA detection (indicated by the arrow).
C). Northern analysis with ICP 22 probe. Appearance of ICP22 mRNA (indicated by the arrow) was used as a positive control for cycloheximide treatment.

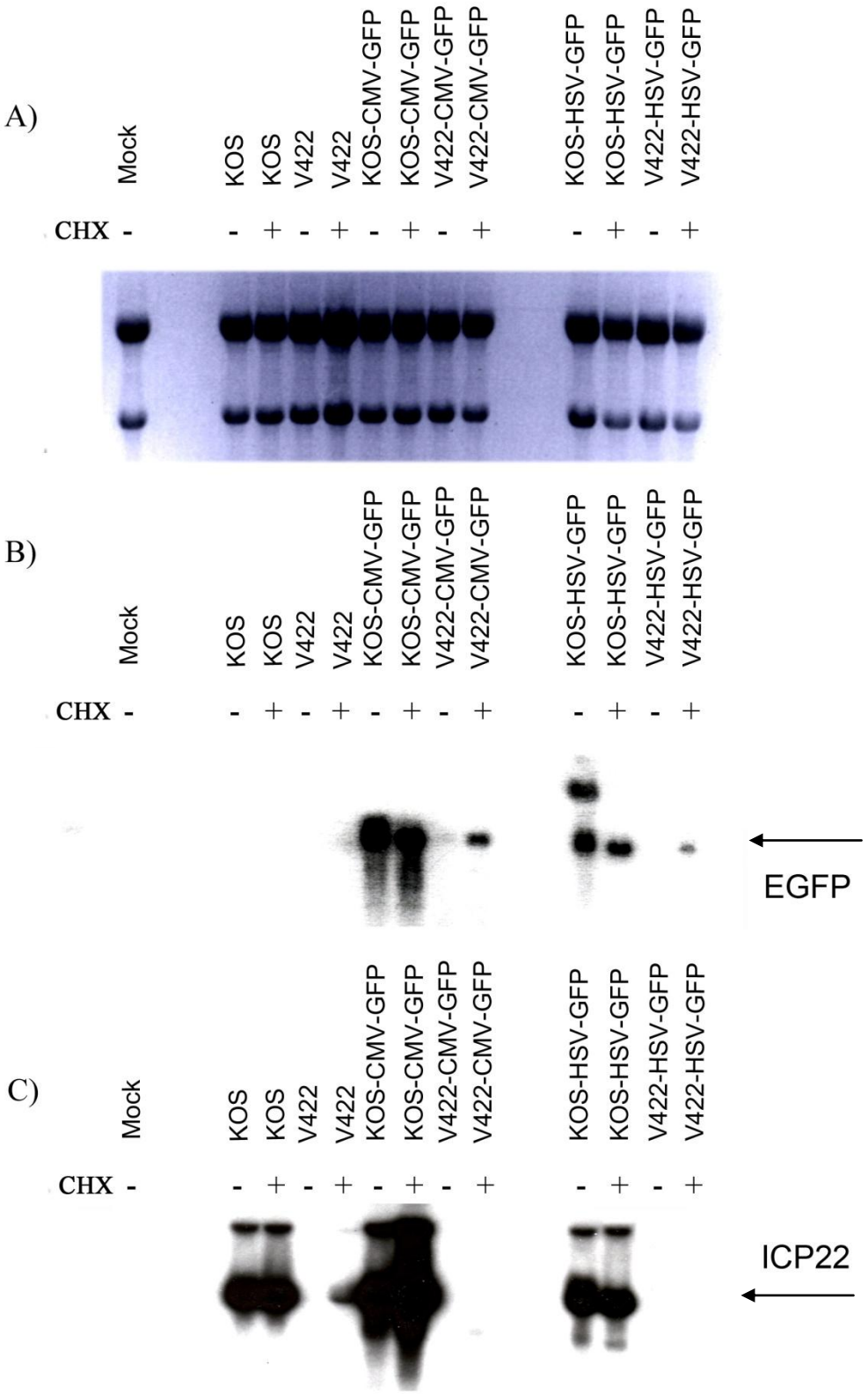
A)
Mock
KOS
KOS
V422
V422
KOS-CMV-GFP
KOS-CMV-GFP
V422-CMV-GFP
V422-CMV-GFP
KOS-HSV-GFP
KOS-HSV-GFP
V422-HSV-GFP
V422-HSV-GFP
CHX - - + - + - + - + - + - +
B)
Mock
KOS
KOS
V422
V422
KOS-CMV-GFP
KOS-CMV-GFP
V422-CMV-GFP
V422-CMV-GFP
KOS-HSV-GFP
KOS-HSV-GFP
V422-HSV-GFP
V422-HSV-GFP
CHX - - + - + - + - + - + - +
EGFP
C)
Mock
KOS
KOS
V422
V422
KOS-CMV-GFP
KOS-CMV-GFP
V422-CMV-GFP
V422-CMV-GFP
KOS-HSV-GFP
KOS-HSV-GFP
V422-HSV-GFP
V422-HSV-GFP
CHX - - + - + - + - + - + - +
ICP22